Utilizing 'Power-to-Gas' Technology for Storing Energy and to Optimize the Synergy between Environmental Obligations and Economical Requirements

by

Kamal Al Rafea

A thesis

presented to the University of Waterloo

in fulfillment of the

thesis requirement for the degree of

Doctor of Philosophy

in

Chemical Engineering

Waterloo, Ontario, Canada, 2017

Examining Committee Membership

The following served on the Examining Committee for this thesis. The decision of the Examining Committee is by majority vote.

External Examiner   NAME: Hossam Gabbar

                                                                    Title: Professor

 Supervisor(s)   NAME: Ali Elkamel

                                                                    Title: Professor

Internal Member   NAME: Xianshe Feng

                                                                    Title: University Research Chair & Professor

Internal-external Member   NAME: Fatih Erenay

                                                                     Title: Assistant Professor

Other Member   NAME: Evgueniy Entchev

                                                                     Title: PhD, Senior Scientist, Canmet-Energy

Author Declaration

This thesis consists of materials all of which I authored. This is a true copy of the thesis, including any required final revisions, as accepted by my examiners.

I understand that my thesis may be made electronically available to the public.

ABSTRACT

This work develops a generalized modeling framework using several approaches for assessing the feasibility of storing energy in order to demonstrate the economic and environmental benefits of managing the existing power generation sources in Ontario. Optimizing the costs and emissions while maintaining energy demand is the main and general target for this study. The purpose of this research is to provide the energy systems management and decision makers an effective tool for assessing the optimum way of utilizing an existing energy sources in Ontario. The major contributions from this research are: to assess the feasibility of integrating renewable energy sources into Ontario power grid in terms of cost and emissions; and optimizing energy storage capacity in natural gas network within the power-to-gas concept. Power to Gas as an energy storage is a novel technology that is considered to be a viable solution for the curtailed off-peak surplus power generated from intermittent renewable energy sources, particularly wind and solar. The unique technology of 'power-to-gas' represents a promising system in managing storing energy when addressing the current challenges of demand satisfaction, grid-flexibility, related emissions and costs.

In the first part of the research, the integration of intermittent renewable energy sources of wind and solar into a larger scale fossil-fueled combined cycle power plant (CCPP) utilizing hydrogen as an energy vector is explored in order to meet the needed load following energy profile at minimum costs and lower emissions. GAMS is used to model energy hub costs to approach the problem using mathematical programming while power cost and emission credits represent the model outputs. The cost-emissions models will aid in sizing of the key components within the hub and optimizing its operation. Two different types of modeling are used, Mixed Complementary Problem (MCP) and Mixed-Integer Linear Programming (MILP) in simulating the configuration of the proposed energy systems, while monetizing health impacts associated with exposure to conventional energy sources emissions.

In order to bring attention to the risks that associate with utilizing NG-fueled energy sources such as combined cycle power plant CCPP, the third part of the research is developed to assess the monetary value of the risks of the expected pollutants on human mortality and morbidity. The pollutants of carbon monoxide (CO), nitrogen dioxide (NO_2), fine particles ($PM_{2.5}$), and sulfur dioxide (SO_2) from a sample of natural gas NG, were chosen based on their emission rates and

their severity on the health impacts. To lessen the health impact from natural gas fuel, hydrogen-enriched natural gas (HENG) fuel was examined to fuel the combined cycle power plant. The Health Canada's Air Quality Benefits Assessment Tool, AQBAT was used for monetizing the impacts of pollutants on health by taking into account a range of morbidity and mortality outcomes as well as their dollar value, when the natural gas and the hydrogen enriched natural gas fuels were used.

The final part of this research is designed to measure the feasibility of new decentralized power system as a critical mechanism in meeting energy demand and as a step forward towards an energy sustainable future. Decentralized power systems are characterized by generating power near the demand area, it can operate by interactions with the local grid, in which it feeds surplus power generated to it, or it can behave as a stand-alone isolated energy system. The development of community power requires the consideration of several sustainability criteria in order to meet the minimum requirements that satisfy communities' demands and maximize energy generation benefits. These criteria include cost effectiveness, risks to the environment and humans, scaling, efficiency, and resilience. The existing natural gas distribution system is utilized to store and to distribute hydrogen produced via electrolysis with and without the consideration of additional hydrogen storage while considering two recovery pathways: 'power-to-gas-to-power' and 'power-to-gas-to-end users' to satisfy power and end-users demands. The multi-objective and multi-period mixed integer linear programming model is employed to minimize the cost of generating electricity and storage, the cost of health impacts associated with emissions, and the cost of power losses from renewable intermittent energy sources. The proposed model is designed to evaluate the optimal operation and sizing of the energy producers and the energy storage system, as well as the interactions between them.

The cost of generating electricity is found to depend on the operational hours of energy sources and on the estimated cost of electricity varied from $0.092 to $0.11 per kWh. Blending hydrogen with natural gas to fuel combined cycle power plant could save on human's health and environment, at hydrogen concentration of 2.3%, it could save CAD$1.15 for every MWh produced when meeting power demand. Storing the surplus electricity from wind and solar during off-peak periods by producing hydrogen through electrolysis process and storing it within the natural gas pipeline network saved 10% of the cost of electricity that generated to meet the power-demand.

Acknowledgement

Table of Contents

List of Tables

List of Figures

List of Acronyms

Acronyms	Their Meaning	Acronyms	Their Meaning
CCPP	Combined Cycle Power Plant	COE	Cost of Energy
GAMS	General Algebraic Modelling System	GHG	Green House Gas
MCP	Mixed Complementary Problem	RE	Renewable Energy
MILP	Mixed-Integer Linear Programming	OPA	Ontario Power Authority
AQBAT	Air Quality Benefits Assessment Tool	AEL	Alkaline Electrolyzer
FIT	Feed-in-Tariff	CTG	Combustion Turbine Generator
IEA	International Energy Agency	DLN	Dry Low NO_x
UHNG	Underground Hydrogen-Natural Gas	SCR	Selective Catalytic Reduction
OMA	Ontario Medical Association	LLC	Land Lease Cost
NRC	National Research Council	AEP	Annual Energy Produced
WTP	Willing-to-Pay		
LCOE	Levelized Cost of Electricity	MVC	Monetary Value of Carbon
TPHD	Toronto Public Health Department	MAC	Marginal Abatement Cost
HENG	Hydrogen Enriched Natural Gas	AQHI	Air Quality Health Index
HOMER	Hybrid Optimization Model for Electric Renewables	IPA	Impact Pathway Approach
PtGtU	Power-to-Gas-to-Users	COI	Cost of Illness
PtGtP	Power-to-Gas-to-Power	BOD	Burden of Disease
NREL	National Renewable Energy Lab	QALY	Quality-Adjusted Life Year
CHFCA	Canadian Hydrogen and Fuel Cell Association	OME	Ontario Ministry of the Environment
GTI	Gas Technology Institute	ERF	Exposure Response Function
CNG	Compressed Natural Gas	CRF	Concentration Response Function
HHV	High Heating Value	VSL	Value of Statistical Life
LHV	Low Heating Value	MIP	Mixed Integer Program
IEC	International Electro-technical Commission	LBN	Lawrence Berkeley National
SBG	Base-Load Generation		
IESO	Independent Electricity System Operator		
WT	Wind Turbine		
PV	Photo Voltaic		
PCS	Power Conditioning System		
HRSG	Heat Recovery Steam Generator		

Chapter One

1. Introduction

This research focuses on demonstrating the benefits of adopting new hybrid energy concepts such as energy hub and new systems such as 'power-to-gas' technology in terms of economic and environmental aspects while meeting energy demand. Integrating these technologies into the existing energy system in Ontario represents a critical step towards sustaining the future of energy.

The scope of this research is limited to fiscal assessment including capital costs, O&M costs, and fuels costs (including generating hydrogen costs); and environmental effects including health impacts due to mortality and morbidity impacts.

The area of south west of Ontario is considered to be the specified area for this research due to its wind and solar potential. This location is connected to the major electrical and natural gas distribution system assets plus its potential for minimizing the transportation costs of energy.

The operation of the proposed energy systems is balanced in this research to achieve two main viable targets that are: economics and minimized environmental-health impacts; therefore, the decision makers are considered to be the most relevant recipients particularly in managing energy while reducing environmental impacts without interrupting any new investment in energy facilities. The established bi-objective function in the optimization model to balance the analysis of economic versus environmental-impacts represents the most and unique contribution to the energy system management field.

This research presents the need to store un-expensive surplus power during off-peaks and then to be recovered and distributed at on-peaks in order to strengthen power networks and maintain load levels.

This research contributes to the energy systems management's field by: achieving results of more reality and significance due to utilizing an hourly input parameters rather than average monthly or seasonally; accomplishing feasible targets due to incorporate the laws of thermodynamics, economics, statistical environmental-health impacts studies and fundamentals of process design; utilizing AQBAT as a Canadian tool that was designed for measuring health impacts from traffic-emissions to measure health impacts from combined cycle power plant emissions; applying practical cost-assessment to incorporate environmental-health impacts cost within generating

electricity cost in order to present the importance of integrating power-to-gas system into existing Ontario power; examining the benefits of utilizing hydrogen as an energy carrier in storing and transforming energy in terms of economic and environmental-health impacts; and analyzing different concepts of storing surplus energy during off-peak periods and reuse it in on-peak periods in terms of optimum cost-environmental objectives.

Chapter two illustrates the research background, describes in details the approach that used in designing the energy hub concept, review the literature, and explore the new and unique concepts that can support the current research. It includes: quantifying health impacts associated with emissions from CCPP, comparing energy hub concept with power-to-gas technology, investigates the technical challenges of storing hydrogen in natural gas pipelines, explores storing electrical energy, and describes the modelling-optimization tools that are used in this research.

Chapter three focuses on integrating of wind and solar as emissions-free and intermittent renewable sources into conventional natural gas fueled combined cycle power plant as dispatchable power generation source. The main idea is to investigate the feasibility of utilizing the curtailed power from wind and solar during off-peak periods to be used in electrolysis process for generating hydrogen economically. A similar approach is presented in chapter four with some modifications, the renewable energy sources of wind and solar are used only for generating power to feed the electrolysis process while the natural gas fueled combined cycle power plant is utilized to meet the power demand. More hydrogen could be produced and its optimum concentration in hydrogen enrich natural gas fuel is examined.

Chapter five performs a cost-analysis for estimating hidden costs of generating electricity from conventional fossil-fueled sources such as combined cycle power plants. Presenting these invisible costs will give warnings to the governments and decision makers to be more aware when considering the conventional energy sources in meeting power demand; their environmental-health impacts associated with emissions are serious concerns.

Chapter six examines the potential benefits of utilizing decentralized energy system to provide communities with renewable energy, and it is also considered to be a significant step towards a sustainable energy future. The locally sited, decentralized, and based on renewable energy technologies can either be grid-connected or stand-alone energy system. This approach has received increasing attention in Ontario due to the adoption of the Green Energy and Green

Economy Act, which includes a Feed-In-Tariff policy. The optimization-model considers the sizing of the electrolyzers farm to maximize the capacity factor of the units during their operation.

Comparing the results of all four studies is performed and presented in chapter seven while discussing the major outcomes and the conclusions. Recommendations are presented as well for future work. The flow of current research is summarized in Figure (1.1).
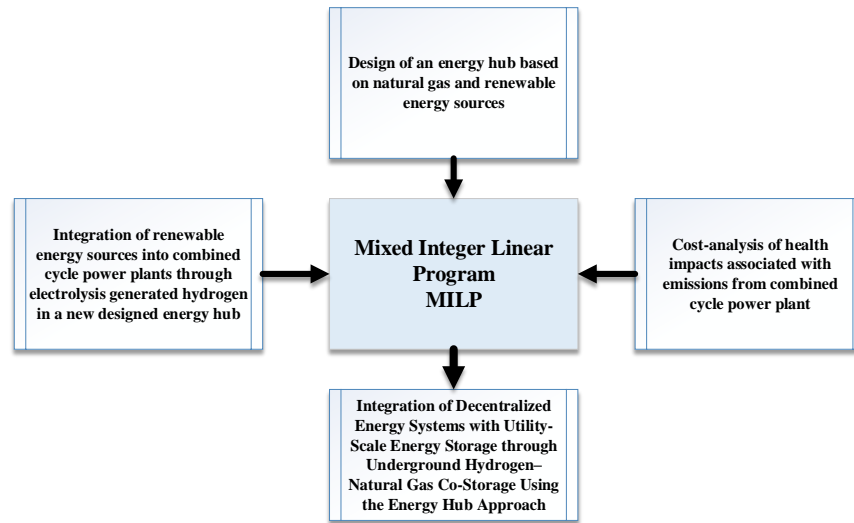
Figure (1.1): Research Flow

1.1 Problem Statement

There are continuing efforts to increase the capacity of renewable energy generators such as wind and solar in the energy supply mix in order to combat the increase in carbon emissions and to rely on more sustainable energy sources. Ontario's feed-in-tariff (FIT) is a green energy investment program that provides a guaranteed pricing structure of electricity produced from renewable sources. The program incorporates standardized rules, prices and contracts with the purpose of unlocking private cash flows into the renewable energy infrastructure (Ontario Feed-In Tariff, 2011) and (Ministry of Energy, 2011). The FIT program has contracted 8,623 MW of renewable non-hydro energy projects as of 2015 (IESO, 2015), which is expected to increase to 12,000 MW by 2020 (Weis, et al., 2013).

Renewable energy resources, particularly wind and solar, are inherently intermittent, which results in difficulties in making them dis-patchable. The maximum capacity of production from solar photovoltaics and wind turbine generators is determined by the weather conditions. Moreover, curtailing production during periods of surplus baseload generation is economically unfavorable due to the fixed FIT contracts with renewable energy generators. The reduced flexibility in production poses a concern for grid operators and hinders the penetration of these resources into the energy supply mix.

Exploring the approach of utilizing electrolysis process in generating hydrogen as an energy carrier in storing the surplus power from renewable sources during their available and off-peak periods in order to be recovered during on-peak periods for long terms is critical to continue in adopting/integrating more of renewable sources into existing grid.

The utilization of hydrogen as an energy storage medium for managing the intermittent supply of solar and wind power in Ontario is still at the conceptual stage and is the main focus of this research.

1.2 Research Motivation

By establishing adaptive energy ecosystems, where gas pipelines and electricity transmission are integrated for bi-directional energy flows and seasonal storage, the provincial energy market will achieve improved system operability, greater system efficiency, and an overall reduction in emissions. There is an expected significant reduction in greenhouse gases, as CO_2 free wind and solar power will be effectively used and emission reductions for Ontario validated. This will ultimately result in improved consumer economics through more efficient use of energy sources. The use of hydrogen blends in the natural gas combustion process has shown to have air emission reduction benefits. Since much of the infrastructure already exists, there is only a low/modest capital investment required.

The use of energy storage technologies as a buffer between renewable energy sources and the load is a promising solution to address the surplus generation and renewable intermittency problem. They respond to dispatches of electric generators and demand side management, and function as a capture technology for intermittent renewable energy from which output can be regulated.

Ontario has all the key conditions and industrial expertise to deliver on this transformative convergence of infrastructure for a smart-energy-grid. This includes the technical requirement to manage unique power grid conditions that have coincident surplus baseload with increasing supplies of off-peak intermittent renewables. The province also contains the unique geological infrastructure for underground storage, and Enbridge and Union Gas already maintains over 276 billion cubic feet of underground storage as two of Canada's largest gas distributors.

Repurposing existing gas grid assets for new services such as energy storage for intermittent power has the potential to provide significant value to ratepayer benefits for both electricity and gas consumers. A report by International Energy Agency (IEA) estimates that the new worldwide installations of energy storage capacity will increase 100-fold between 2011 and 2021 to 12,350MW, or a $25 billion market (IEA, 2014). Further, it estimates that 50% of this market will be for long duration or grid-scale energy storage like power-to-gas. Establishing a domestic market in Ontario for renewable gas technology adoption will provide advantage to local technology developers and system integrators.

The importance of this research is to exhibit the possibilities for different energy sources to operate in a synergistic manner in order to meet the market electricity demand at reasonable prices while minimizing emissions impacts on the environment and health.

The successful integration of multiple decentralized energy technologies such as wind and solar photovoltaics energy converters is highly dependent on the consideration of energy storage and distribution technologies in the design planning of the energy system. Utilizing the underground hydrogen-natural gas (UHNG) system to store electrolytic hydrogen produced using power outputs of wind and solar energy during off-peak demand represents a unique path to overcome the intermittent nature of these resources. The proposed UHNG system adds flexibility to the power generation and distribution system, and allows for the lowering of overall emissions due to the reduced consumption of natural gas and the higher consumption of the non-GHG emitting hydrogen.

Unlike other energy storage options, there are different pathways by which energy can be recovered from the UHNG. There are various configurations and tradeoffs that can be achieved in the proposed energy system, which requires the application of optimization tools in order to determine the optimal set of decision variables in the system. These variables include number of

energy producers (i.e. gas turbines, solar photovoltaics, wind turbines and electrolyzers), energy flows between energy producers and UHNG, energy flows within the UHNG system, energy flows between energy producers and end users, and energy flows between UHNG and end users. Exogenous parameters such as hourly power demand, hydrogen demand, fuel prices, and techno-economic data are all considered in this research.

The distinctive features of this research can be summarized as follows:

- A simulation model for an energy hub is developed to measure the availability of wind and solar as the chosen renewable sources when they stand alone for satisfying eletcrolyzers power demand in order to produce required hydrogen in different scenarios,

- The resulted health damages due to the emissions from natural gas fueled power plants is quantified and monetized to assess the extra hidden costs of generating power demand,

- A multi-objective and multi-period MILP model is used to minimize total cost of power production and storage, cost of health impact of emissions, and power curtailment from intermittent renewable energy sources,

- The model considers the development of potential power-to-gas that incorporate the existing natural gas storage and distribution system to manage the off-peak surplus of intermittent renewables, for which multiple recovery pathways are considered (i.e. power-to-gas-to-users and power-to-gas-to-power),

- The multi-objective component considers various criteria that pertain to the aspirations of users/communities, which include cost effectiveness, accessibility and reliability, and reduction in environmental/health costs (i.e. consideration of multiple pollutants and their associated environmental and health impact costs),

- The model considers the interactions with the local grid based on the currently available FIT policy, and

- The model considers capacity expansion decisions to allow for the future planning of community power portfolios.

Chapter Two

2. Background

This chapter intends to provide background for monetizing environmental-health impacts associated with Combined Cycle Power Plants (CCPPs) emissions; new energy systems including energy hub and power-to-gas while discussing the main challenges; modelling and optimization tools used; and the critical need for electrical energy storage system. It includes a brief summary of similar published articles and their relations to this research.

2.1 Quantifying Health Impacts Associated with CCPP's Emissions

Among Canada's industrial sectors, the electricity generation sector has made a significant contribution to the country's air pollution, emitting more than its fair share of NO_x and SO_x emissions, consequently contributing to smog, acid rain, and the formation of fine PM_x (USA-EPA, 2016). As the CCPPs burn natural gas (NG), a relatively clean fossil fuel, their emissions' rates are low compared to other fossil fuels. Low levels of air pollution emissions accompanied by a limited amount of wasted heat due to high operating efficiency are the most significant advantages of utilizing the CCPPs in generating heat and electricity (Kehlhofer, et al., 2009). Combusting NG produces low levels of sulfur, mercury, and particulates. Burning NG also produces NO_x, which is a precursor to smog, but the gas occurs at lower levels than when burning gasoline and diesel (C2ES, 2013). Although NG-fueled CCPPs emit limited levels of Green House Gases (GHGs) and criteria air pollutants compared to other fossil fuel-powered plants, the considerable accumulated levels of these emissions cannot be ignored (European Commission, 2016). The NG-fueled CCPPs as the proposed sources for meeting power-peak demand have noticeable environmental-health impacts due to their emitted air pollutants including NO_x, PM_x, CO, and SO_x in addition to the GHGs such as CO_2. Air pollution impacts humans' health and thus imposes significant financial and social costs on the society in terms of: increased health care costs, missed days of work, and reduced worker productivity. It is estimated that air pollution costs society and the economy billions of dollars every year (Environment Canada, 2013). The full social costs of air pollution could include not just damage human-health and lost human-productivity, but are even higher to include the indirect losses such as health care expenses required to reduce pain, reduce suffering, and preventing death. Air pollution is linked in varying degrees with a

variety of health-impacts including asthma, cancers and cardiovascular diseases. In Canada, the researchers from Toronto Public Health Department and from Ontario Medical Association (OMA) all prove that air pollution complications can associate with premature death, increased hospital admissions, increased emergency room visits, and higher absenteeism rates from work (Environment Canada, 2013). Reductions in these emissions translate into public health benefits, as these pollutants have been linked with problems such as asthma, bronchitis, lung cancer, and heart disease for hundreds of thousands of people (California Environmental Protection Agency, 2012). Serious health issues like asthma, bronchitis, lung cancer, and heart disease have been declared by the California Environmental Protection Agency (CEPA) to be the direct expected impacts due to exposure to the aforementioned air pollutants; therefore emission abatement requires urgent action and will translate into public health benefits (California Environmental Protection Agency, 2012). Although NG-fuelled CCPPs emit relatively low levels of air pollution, their accumulated emission impacts can influence the air quality in local and regional areas. Rising concentrations of hazardous air pollutants should be managed before they can negatively affect humans and the environment (EPA, 2015b). Long-term exposure to certain levels of the criteria air pollutants can cause serious and unexpected health outcomes, including respiratory symptoms and cardiac disease, and may lead to certain cancers. It has been found that the residents living within 800 meters of NG operating facilities are at greater risk of health impacts from air pollution than those living farther from the sites (McKenzie, et al., 2012).

When electricity generation costs do not adequately reflect all associated social/environmental cost, the monetary value assigned to benefits or adverse effects, referred to as damages, are "hidden" in the sense that government and other decision makers, such as electric utility managers, may not recognize the full economic and social costs of their actions on the public. When market failures like this occur, there is a case for government interventions in the form of regulations, taxes, fees, tradable permits or other instruments that will motivate such recognition (NRC, 2009). The external costs of electricity are the costs of damages imposed on society and the environment by an electricity generation chain, but not accounted for in the market price of electricity (Molnar, et al., 2008). Evaluating the environmental impacts of the energy sector should be expressed in terms of external or additional cost per energy unit. These costs are called "External" because their effects are 'outside' of the normal pricing system. 'Externalities' are also defined as benefits or costs, generated as a byproduct of an economic activity, that do not accrue to the parties involved

in the activity (El-Guindy, 2013). Utilizing the true cost of electricity could affect regulations in two ways: one is in planning and permitting for new investments, and the second is through the operation of existing facilities.

There are two main methods for estimating the true costs of electricity generation: (1) The damage function approach which establishes the relationship between emissions and impacts and then monetizes the accrued damages; and (2) The abatement cost approach which uses the cost of reducing pollution given current regulations as an estimate of damages from pollution. The damage function approach is far superior to the abatement cost approach, but is more data and methodologically intensive (Burtraw & Krupnick, 2012).

Estimating the economic and social costs associated with external effects is a multistep process. USA's National Research Council (NRC) delivered a methodology based on the "damage function approach" which starts with an estimation of pollutants' impacts using mathematical models and then estimates the pollutants' resultant ambient concentrations and ensuing exposures (National Academy of Sciences, 2009). The exposures are then associated with consequent impacts to certain levels. These impacts then can be monetized as estimated damages. Studying people's preferences for reducing the health and social damages represents one of the ways that researchers can approach assigning monetary values to energy-related adverse emission impacts. Monetizing these damages is similar to the methodology of the price that people are willing-to-pay (WTP) for commercial products. Based on the outcomes of external-cost studies, there should be more focus on evaluated damages related to PM_X, SO_2, and NO_x as the criteria air pollutants emissions (Committee on Health and Environmental, 2010). The research associated with these studies has monetized the impacts of air criteria pollutants on health, crops, construction materials, recreation, and visibility. Health damage, including premature mortality and morbidity, represents the largest area of interest in monetizing health damages. This level of interest in monetization is likely due to the vast variety, direct impact, and high cost of morbidity, while premature mortality represents the largest health-damage category. Burtraw et al (Burtraw, et al., 2012) provided a review of methodologies for calculating the actual cost of generating electricity from conventional energy technologies in the United States. The infrastructure has been built to support the integration of renewable energy facilities through a desired policy network for the 21st century (REN21). Their work also aims to explore new methodologies for developing new approaches in estimating the true costs of generating electricity by adopting such technical-analysis at various levels of detail

and rigor. The expected results of the desired analysis as well as the discussions with stakeholders are critical in providing guidance to decision-makers. Another study by Biegler (Biegler, 2009) estimated the external costs of utilizing coal and NG to fuel power plants; the researcher calculated health damages due to expose to PM_{10}, SO_2, and NO_X; examined the results, and then adjusted for local application in different population densities. Using this methodology, the health-related damage costs were estimated to be CAD\$0.70 per MWh for a typical NG-fired power plant. Roth and Ambs (Roth & Ambs, 2004) calculated the levelized cost of electricity (LCOE), including the external costs when generating electricity from conventional fuels. Their analysis includes fuel cycle costs incorporated by the ''externalities'' approach which increases the likelihood of adopting renewable power resources from a societal perspective. The methodologies of externalities include calculating all related damage costs caused by air pollution, energy security, and transmission, and from distribution facilities. The monetized health impacts expressed as ranges of values are explored in the literature and commonly represent the expense of maintaining the impact of air pollution emissions (Roth & Ambs, 2004). Another investigation of the impacts of air pollutants on public health is performed by Chen, X. et al (Chen, et al., 2016), this study employed a spatial Durbin model to investigate the impacts of air pollutants on public health in 116 cities of China during time period from 2006 to 2012; they utilized a survey data from mortality and respiratory diseases to investigate public health impacts as well as using a statistical data of emissions for specified air pollutants such as SO_3 and soot in order to discover how they can be connected. Air pollution impact was investigated by the Toronto Public Health Department (TPHD), it is found that in Toronto alone there were 6,000 hospitalizations and 1,700 premature deaths each year that are directly related to air pollution impacts. The study showed that these cases would not have happened if individuals had not been exposed to the chronic levels of air pollution experienced in Toronto at different time periods (Toronto Public Health, 2004).

2.2 'Energy Hub' Concept versus 'Power-to-Gas' Technology

To investigate the feasibility of the economic liability of power-to-gas as the proposed technology for storing surplus power, the energy hub concept is used in this approach (Bucher, et al., 2015). The energy hub represents a modelling frame work used to describe such a proposed configuration in order to perform specific analysis; whereas power-to-gas is an established technology used for storing surplus power generated by renewable sources during off-peak periods and to be used during on-peak periods. The surplus power can be stored as hydrogen when electrolysis process is used or as methane when methanation process is used.

As a tool, energy hub is utilized in this research to model two different configurations as mentioned in the first and second published papers. Both papers have proposed the concept of integrating renewable energy sources into power grid while storing the surplus power by generating hydrogen and to be injected into natural gas network; the 2nd paper investigates the concept of utilizing the hydrogen enriched natural gas (HENG) to fuel combined cycle power plant for minimizing environmental emissions.

Energy hubs can be defined as new concepts of energy systems in which the energy sources can be integrated and interconnected; whereas their multiple energy carriers can be converted, conditioned, and stored (Geidl, et al., 2007). Energy carriers such as electricity, natural gas (NG), and hydrogen are critical in commercial, industrial and residential use. Harmonized such hybrid energy systems have increasingly received better attention in the last two decades due to their related environmental-health benefits versus the controversial, conventional fossil-fueled power plants (Giannakoudis, et al., 2010). Energy hub concept did not get enough research as most of the simulation literature in the past has focused only on power generation systems that have independent energy carriers such as electricity and natural gas. Just few researches have considered multi-generation power systems in their studies (Geidl, et al., 2007), (Favre-Perrod, et al., 2005) and (Geidl & Andersson, 2005). Improving the grid-performance, increasing the grid-flexibility, and increasing the grid-reliability by eliminating the intermittency issues of wind and solar are the major advantages of adopting energy hub concept. The surplus electricity generated by wind and solar can be converted into hydrogen through electrolyzers to be stored or sold to local markets. Such scenario will contribute to the development of hydrogen economy.

The flexibility that the energy hub can added to the existing grid is another advantage, through the input units the system depletes energy of different kinds such as electricity and heat; whereas the system could produce electricity, heat, and by-products such as hydrogen or methane as the outputs (Geidl, et al., 2007). Significant advantages can be achieved when using the energy hub concept compared to the other existing conventional energy systems. The main advantages include: reliability in power supply due to overcome the issue of intermittent nature of wind and solar; increase in the system performance due to use energy management when balancing supply and demand; utilization of various kinds of energy sources when renewable sources as well as fossil-fueled sources are combined in the hub; and improvement in the efficiency due to minimize the energy waste (Geidl, et al., 2007). The combination of two main objectives of maximizing energy efficiency and minimizing overall energy-generation cost is the critical requirements for the effective power generation and delivery system.

Utilizing of an energy system combines fossil-fueled such as NG-fueled CCPP with renewable sources such as wind and solar will reduce air pollution emissions while meeting power demand at different on/off peak levels. The techno-economic studies of PV/wind/CCPP power systems that carried out using HOMER (Hybrid Optimization Model for Electric Renewables) software showed that these systems will be a potential replacement for fossil-fueled power plants when meeting the required load in terms of health and climate damages that could be avoided (Li & Yu, 2016) and (Shaahid, et al., 2014). A detailed study from Europe concludes that reducing the dependence on conventional power plants by integrating cleaner renewable energy systems will improve the air quality and thus lead to significant improvements in human health and boost productivity (HCWH Europe and HEAL, 2010). It is estimated that the European Union could save up to €80 billion a year in the form of avoided illnesses and losses in productivity when improvements in air quality are applied through reductions in PM_x, NO_x, and SO_2 emissions from power generation plants.

The term "Power-to-Gas" is used to describe the process of converting electrical energy into a gaseous form, making storage and transportation via the existing natural gas infrastructure possible, bridging the power grid with the natural gas grid (see Figure 2.1). It is a novel concept which emerged from Germany in the last 15 years. In the first step of the Power-to-Gas process, the surplus electricity from renewable sources such as wind and solar is used in electrolysis to generate hydrogen, the generated hydrogen is then injected into natural gas pipeline network to form Hydrogen Enriched Natural Gas (HENG) fuel. The HENG fuel can be transported directly

to customers where it can be used as a gas-blend. Large-scale electrolysis technology is critical for the true convergence of the natural gas and power grids. Electrolysis-based hydrogen storage technology brings with it unsurpassed energy storage capacity, timescale, and dynamic responsiveness for grid stabilization.
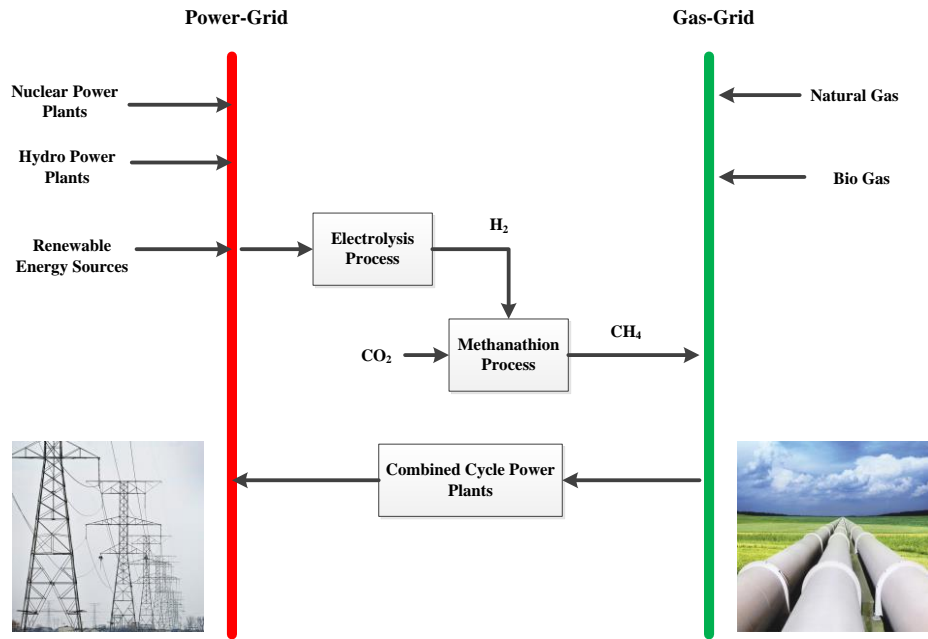
Figure (2.1): 'Power-to-Gas' bridges the power-grid into gas-grid

Informational and control systems for power and gas grids can be networked to manage this energy flow from power to gas, and then from gas back to power when, and where, these energy conversions are most beneficial to the provincial power grids. In power-to-gas process, the electrolytic-generated hydrogen is directly injected into the natural gas network as an additive; the resulting mixture, hydrogen enriched natural gas (HENG) can be used as fuel, as long as its composition meets end-use appliances' requirements and do not threaten the structural integrity of network components. This direct hydrogen injection is appropriate where the renewable produced hydrogen volumes are typically less than 10% by volume, and this process is preferred due to technology simplicity and higher system efficiencies (> 85% conversion efficiencies). In addition to the environmental benefits of using HENG fuel and large-scale energy storage, such bidirectional conversion between key energy vectors is expected to improve the utilization of assets in both energy networks and to increase supply reliability through supply redundancy. The

challenge is two-fold. While initial market penetration of HENG fuel can occur today, achieving the maximum system integration, renewable penetration levels, and consumer economics will require predictive system operability modeling to asses, and plan, how the energy systems (gas and electricity) can be optimized for geography, time, and energy supply/demand mixes. Coincident with these efforts, industry and technology developers can use the early research activities and results to define the techno-economic benefits of adaptive and integrated energy infrastructure that span both electricity and natural gas grids. HENG-fuelled CCPP power plants represents such creative and successful process to enhance the performance and to reduce the GHG emissions of mentioned power plants to minimum levels. HENG fuel has the potential of reducing NO_x emissions without the limitations found in other NO_x control methods (Melaina, et al., 2013). As a volumetric mixture, HENG can be in the range of zero to 20% hydrogen which is compatible with existing natural gas transmission and distribution infrastructure. Integrating sustainable, zero-emissions and non-dis-patchable resources such as wind turbines and photovoltaic solar into Ontario power grid by producing hydrogen represents the main advantage for health and the environment (Goldstein & MacDougall, 2012). This plan would offer cleaner, flexible and secure energy supply while utilizing local energy resources.

For Power-to-Gas to be a province-wide, utility-scale storage solution with defined system-wide benefits, the above interfaces must be modeled to reflect a fully engineered, functional and seamlessly operation. The resulting modeling and research will be valuable for industry to plan the future electricity-gas grid interfaces and to drive industry-uptake and operational-buy-in that achieves the desired system benefits. It's a market potentially worth billions of dollars, and it is working with "leading utilities worldwide" on demonstration projects, setting the stage for commercial projects. The power-to-gas approach allows it to "convert multi-megawatts of renewable electricity to hydrogen and then use it in multiple applications." Those applications include commingling the hydrogen with existing natural gas, with it flowing to end-users to generate electricity or heat (Bentein, 2014).

The challenge is preparing for the hydrogen economy by defining the conditions under which the existing natural gas system can be used for HENG fuel; whereas the aim is to encourage and facilitate a transition to the hydrogen economy on a shorter timeframe by providing a transition stage by using the existing gas infra-structure to convey a HENG fuel.

The underground hydrogen storage with natural gas (UHNG) is an innovative technology, the underground stored hydrogen can be recovered and send to the market while get benefits of utilizing the existing natural gas distribution system. The stored HENG fuel can be retrieved and directed towards two different pathways:

(1) Power-to-Gas-to-Users (PtGtU): the HENG is distributed to end users to be used instead of pure natural gas; and

(2) Power-to-Gas-to-Power (PtGtP): the HENG fuel is sent to combine cycle power plant (CCPP) for generating electricity, which can be exported to the power grid or to satisfy local demand.

The selected pathways for the hydrogen usage represent a near term use of hydrogen, and represent a transitioning step to a longer term hydrogen based economy where hydrogen can become a critical emissions free mobility fuel.

The technical issues of integration the intermittent renewable energy sources such as wind and solar can be solved by incorporating the power-to-gas technology into NG-pipeline network. There is no doubt that exploring a solution for scaling/sizing energy storage is critical as an inquiry for achieving better integration of renewable energy sources in the future. Other energy storage technologies such as flywheels, batteries, pumped-water-hydro and other facilities have their advantages, but none of them has an ability to store seasonal surplus energy at the terawatt scale other than power-to-gas technology. Power-to-Gas is a unique innovation that simply uses surplus renewable electricity to generate renewable hydrogen to be stored/injected in natural gas pipelines or can be used in transportation. Existing NG-pipelines can store hundreds of terawatt hours of energy as hydrogen for different periods of time. Power-to-Gas can bridge the power, natural gas and transport networks together towards unique options as an energy storage, see Figure (2.2) (Hydrogenics , 2013).
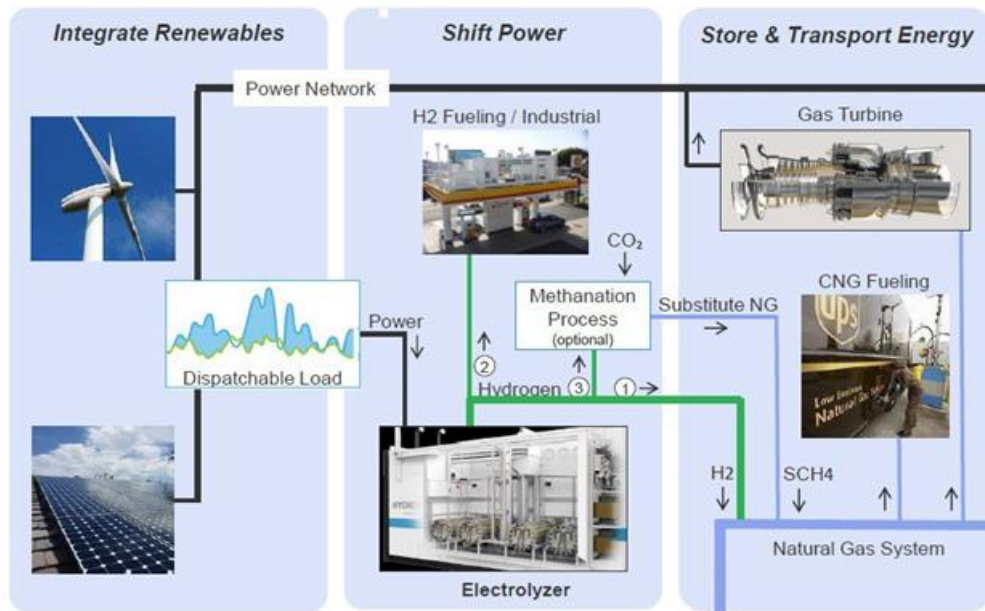
Figure (2.2): Power-to-Gas representation

In Germany and neighboring countries there are 30 power-to-gas plants at different levels of commercial-power generation. The related technologies being employed to create this innovative technology is rapid in the space. Power-to-gas begins with simple electrolysis process, using electricity to separate water into its components hydrogen and oxygen. Produced Oxygen can be sold or used in different industrial/commercial applications and the hydrogen can be deployed in other energy-related applications. Hydrogen can be mixed with natural gas in NG-pipelines grid; whereas further research is needed to determine what concentrations of hydrogen can be supported. Originally there was thought that maximum hydrogen concentration is 5% that could be used, but based on many technical parameters of pipeline engineering and downstream end-users, ratio can reach up to 12% has been achieved. Cast iron and steel NG-pipes have limited ability to contain hydrogen due to their embrittlement impacts by hydrogen. Higher hydrogen concentrations can be achieved by using plastic NG-pipes effectively, but end-users should be informed to ensure their appliances are not impacted by higher hydrogen ratios (Dodge, 2014).

Historically pipelines is a one-way flow of electrical energy from intermittent renewables, but using the power-to-gas solution enables Ontario's pipeline infrastructure to integrate the electricity grid for bi-directional energy flows to absorb and potential store surplus power; or use the natural gas distribution system to move the energy to another location where it can then be used for

generating electricity or heat. The only new infrastructure required in the system is the electrolyzer. With this addition the vast natural gas infrastructure can offer the electricity system a very large, distributed, energy storage network that can also transport energy from one area of the province to another while shifting the time between generation and end-use from hours, days or months.

Many technology pathways are being explored for storing energy in order to satisfy the challenges of integrating renewable energy sources into the existing power grid. Storing access energy in batteries are excellent from rapid charge/discharge perspectives but only for short time periods. Other energy technologies such as pumped-water for hydro and Compress Air Energy Storage (CAES) can offer longer time periods but are limited by the requirements of suitable geographic areas. Chemical conversion of electrical energy into hydrogen allows the existing NG-pipelines grid to be leveraged for massive-capacity, long-term, well distributed storage that can be in cost competitive with other energy storage technologies.

Limited academic publications have considered the power-to-gas concept, plus a limited working demonstrations of the concept have been conducted. In natural gas engines and natural gas turbines it is found that adding hydrogen to natural gas results in a cleaner and more efficient burn. The energy yield of the process increases, and emissions are generally reduced. Hydrogen assists the complete combustion of methane, decreasing unburned hydrocarbon and carbon monoxide emissions. Although in gas turbines, nitrogen oxide emissions may increase with the addition of hydrogen, they can be offset by adjusting reactor temperature and excess air ratio. It is found that excess air ratio also proves to be important in determining process efficiency and emissions (Ma, et al., 2007), (TerMaath, et al., 2006).

Power-to-Gas offers an incredible promise future of storing electricity in North America that should motivate the American/Canadian environmentalists to focus further on incorporating this technology into the existing grids and to follow the Europeans in their interest in this field. The Hydrogenics project that is assigned to store 2.5 MW of electricity within the grid in Ontario, Canada; followed by California power authorities (Cal ISO) who shared a project with NREL (National Renewable Energy Lab) to model the Western States Grid to identify Power-to-Gas opportunities. California authorities have come to realize how the Power-to-Gas represents a critical key towards integrate renewable energy sources into California's grid in order to meet some of the most aggressive renewable energy targets after Germany (Dodge, 2014). Canada has

long been the center of global hydrogen and fuel cell development, with an estimated 2,000 Canadians employed in the sector, according to the Vancouver-based Canadian Hydrogen and Fuel Cell Association (CHFCA). The CHFCA points out that hydrogen's greatest merit is its flexibility, since it can be produced from renewable sources at centralized manufacturing plants (from which it is then distributed by pipeline or tanker) or through on-site production (CHFCA, 2014).

The recognized advantages of the power-to-gas technology are examined when utilize the excess power from wind through generating hydrogen to be stored in the NG-pipelines distribution grid. The system's feasibility and its size are the key parameters, therefore a practical analysis is performed when generating hydrogen that would be injected into the natural gas grid.

The study considered the wind farms located in southwestern Ontario, Canada (Garmsiri, et al., 2014). Their model designed to consider the targeted rate of producing hydrogen as well as its rate when injected into the local NG-grid. The system is examined where located in a wind farm that have size of 100 MW integrating with a 16-MW capacity electrolysis process that can produce up to 4700 kg of hydrogen in a day. In this study, linking the capacity of wind energy to the reliability of producing hydrogen through electrolysis was examined. Mainly, the study compared the electrolysis capacity versus wind farm size to explore the daily maximum hydrogen production during one full year. A sensitivity analysis is performed for calculating the associated costs for this size of wind farm and for the electrolysis capacity. The simple payback periods were estimated for the 25-MW, 100-MW and 200-MW sizes of wind farms; their results were: 14.4 years, 13.1 years and 12.8 years, respectively. When the large cost associated with the 200-MW wind farm is considered and compared to the simple payback periods, the 100-MW wind farm was deemed to be the most likely choice for utilizing hydrogen in a power-to-gas system.

2.3 Technical Challenges of 'Power-to-Gas' Technology

In this section, the technical challenges that might face storing surplus electricity as electrolysis produced hydrogen in natural gas network are addressed in some details. Addressing these challenges is accomplished by cited the literature from different industrial backgrounds.

2.3.1 Hydrogen Leakage

Hydrogen is more vigorous in polymers than methane as the main element in natural gas, including the modern plastic pipes used in natural gas distribution system. Hydrogen's permeation coefficient is higher through elastomer polymers than through plastic materials (Zhou & Ersoy, 2010). It is found that in common polymer pipes in the U.S. NG-Grid, Hydrogen's permeation rates are about 4 - 5 times higher than that for methane. As well known, leakage from pipelines occurs in steel and ductile iron pipes mainly through threads or through joints. Leakage measurements that done by GTI (Gas Technology Institute) for steel and ductile iron NG-pipelines mentioned that the hydrogen's leakage rate is 3 times higher than that for NG (Zhou & Ersoy, 2010).

Based on technical relationships from literature compared the permeation coefficients of hydrogen and of natural gas in polyethylene pipes found that most gas leakage would occur through the pipes walls, rather than through pipes joints (EIA, 2012). It is mentioned that a hydrogen concentration of 20% in H_2-NG blend within the approximately 415,000 miles of polyethylene pipes in United States would result a loss of about 43 million ft^3 of gas blend per year, 60% of the losses being hydrogen and 40% being natural gas. This theoretical distribution main leakage rate (43 million ft^3 per year) would be 0.0002% of the 24.13 trillion cubic feet of natural gas consumed in 2010 (EIA, 2012). In general, due to the higher mobility of hydrogen molecules, injecting hydrogen into NG-pipelines would reduce the natural gas leakage, resulting in a net reduction in the greenhouse gas impact due to leakage. Based on experimental relations of permeation coefficients performed by Dutch to estimate the leakage percentage from their NG-pipelines system, it is found a 17% hydrogen blend would result a leakage rate of 0.00005% (Haines, et al., 2003).

2.3.2 Safety

All large-scale power generation systems including fossil-fueled and renewable energy systems are all accompanied with different types of human health and the environment risks. In general, NG-fueled power generation plants constitute with lower risk of severe accidents than do other large-scale power generation systems such as coal, petroleum, nuclear, and hydropower (Burgherr & Hirschberg, 2008), (Burgherr, et al., 2012).

It is found that higher concentrations of hydrogen in distribution NG-pipelines may lead to minor increase in overall risk (including probability and severity). The expected risks associated with increasing hydrogen concentrations inside NG- service-pipelines are considered differently due to their confined spaces that caused an accumulation when gas is leaked. If hydrogen concentrations exceed 20% in NG-service-pipelines, the risk will increase significantly and much more than that for other NG-distribution-pipelines (Melaina, et al., 2013).

The proper practices of risk management are critical to maintain the monitoring process for both distribution and service NG-pipelines in order to reduce the overall risk.

NaturalHy project appraised (theoretically through modeling and experimentally through pilot plant) three levels of risk when incorporate hydrogen into NG-pipelines, which are summarized in the following points (Lowesmith, 2011):

Gas buildup- For hydrogen concentration up to 50%, the gas buildup will be slightly higher than that for natural gas, but in general the behavior of the gas buildup of the blend was similar to that of pure natural gas (Melaina, et al., 2013);

Explosions in enclosures- Comparing the explosion of H_2-NG blend with hydrogen concentration of up to 20% to that of natural gas alone, it is noticed that there is relative increase in the severity when confined vented explosions are performed; and

Utilizing transmission pipelines risks- Basically the tendency for the severity will increase when hydrogen concentration increased in the H_2-NG blend inside NG-transmission-pipelines resulting in increasing closer to the point of explosion and decreasing further from the point of explosion. The key factor that has been noticed is the more accelerated dispersion of hydrogen blends inside NG-pipelines, the lower concentrations at shorter distances and therefore lesser sever related risks at the far point of the hazard area (Lowesmith, 2011).

2.3.3 Compression of H$_2$-NG Blend

Utilizing the large axial compressors originally designed for compressing/transferring pure natural gas in compressing H$_2$-NG blend (i.e. HENG fuel) will reduce the compressors head pressure and then will result in lower their capacity. Such additional gas compressing stations may be required to incorporate additional capacity and more support for the existing ones. It can be considered as a complex concern, but is not regarded as a critical short-term barrier to hydrogen blending process. Such a problem could be avoided by compressing hydrogen into the required extent pressure when generated using its specified compressors and then can be injected into NG-pipelines/grid; the H$_2$-NG blend would therefore only pass through modest booster compressors (Polman & Wolters, 2004).

The high pressure distribution pipelines is the cheapest way in transporting the gas for long distances, therefore blending hydrogen with natural gas will be the most cost effective step when performed at the high pressure entry points within the gas-grid. Producing hydrogen via electrolysis process and injecting it into NG-pipelines will be relatively cost effective due to the economies of scale, while the transportation step can be executed effectively via existing lines. When hydrogen transferred by the dedicated high pressure pipelines from its centralized production factory to the local blending facilities, more costs will be added; whereas will be cheaper to use the existing high pressure NG-pipelines within the grid (Polman & Wolters, 2004).

It has shown that hydrogen affected the physical properties of NG-steel pipes, but the deterioration of pipes properties is strongly related to the incidence of hard spots within the pipe which makes these spots rely on the specifics of the pipe's fabrication technique. The risks of cracking when adding hydrogen increase due to the increase in the stress within the pipe's wall resulting an increase in pressure swings. The potential for harmful interaction between hydrogen and steel has been known for many years and severe restrictions have long been in place. According to Europe regulation for compressed natural gas (CNG) vehicles, the H$_2$ content in CNG is limited to 2% by volume, if the tank cylinders are manufactured from steel with an ultimate tensile strength exceeding 950 MPa. This limit stems from the risk of hydrogen embrittlement which is known to cause accelerated crack propagation in steel and is, therefore, a critical safety issue (Altfeld & Pinchbeck, 2014).

2.3.4 Natural Gas Pipelines Capacity

Pressure loss per transported amount of energy (i.e. bar per MWh) is the parameter used when describing the capacity of a line in transporting specified quantity of a gas. This parameter is a function of gas physical properties such as its density, viscosity and calorific value as shown in Eqn. (2.1). All these physical properties will be influenced by the addition of hydrogen into natural gas. Polman, et al. (Polman & Wolters, 2004) calculated the effect of blending hydrogen with natural gas on the pipelines transport capacity at several pressures and their results are presented in Table (2.1).

$$\text{Pipeline Capacity} = \mathbf{f}(\text{Density, Viscosity, Califoric Value})_{\text{Gas Blend}} \qquad \text{Eqn. (2.1)}$$

Table (2.1): Hydrogen addition related to NG-pipelines capacity

Hydrogen Content [volume%]	Relative capacity at 0.05 bar	Relative capacity at 5 bar	Relative capacity at 50 bar
0	100	100	100
5	97.4	97.3	94.0
10	94.8	94.5	87.7
15	92.2	91.8	81.1
20	89.7	89.1	74.7
25	87.2	86.4	68.6
30	84.7	83.7	63.0

The NG-pipeline's capacity is reduced with increasing hydrogen concentration in HENG blend, and with increasing the pressure inside the pipes, the capacity is reduced even more.

The existing grid of NG-pipelines consists of distribution pipelines, compression stations and de-compression stations that are serving to transport the required amount of NG-energy to the end-users; but it can be used to store the gas whenever the gas supply exceeds the demand. This (short-term) storage of natural gas in pipelines is called "line-pack". Despite the fluctuating in gas demand, the line-pack permits a continuous supply of natural gas into the grid. More storage capacity requires higher pressures (Haeseldonckx & D'haeseleer, 2008). To meet the energy

demand (i.e. natural gas demand as an energy carrier), the flow rate of natural gas should be sufficiently high. This high flow rate is controlled alternatively by the pressure drop in the pipeline when transporting the gas. The gas flow through a pipeline is described by Eqn. (2.2) (Jacobs, et al., 1996).

$$\text{Flow}_{\text{gas}} = C * D_{\text{pipe}}^{2.5} * \text{Eff.} * \sqrt{\frac{(P_1^2 - P_2^2)}{\rho_{\text{gas}} * Z * T_{\text{gas}} * L_{\text{pipe}} * f}} \qquad \text{Eqn. (2.2)}$$

Where: Flow_{gas} is the normal flow rate, (Nm^3 per hour); C is the proportionality constant (0.000129); D_{pipe} is the pipe inner diameter (mm); Eff. is the pipeline efficiency; P_1 is the inlet pressure (kPa); P_2 is the outlet pressure (kPa); ρ_{gas} is the relative density compared to air; Z is the compressibility factor; T_{gas} is the gas temperature (K); L_{pipe} is the pipe's length (km); and f is the friction factor.

The High Heating Value (HHV) of hydrogen is about 13 MJ per Nm^3; the natural gas' one is 40 MJ per Nm^3 approximately. Therefore, in order to meet the same energy demand, the volume of hydrogen to be transported has to be three times that of natural gas; whereas the hydrogen's density is nine times smaller than that of natural gas. It can be seen that a greater flow rate of hydrogen results in the same pressure drop of natural gas which is being critical parameter in a pipeline network (Haeseldonckx & D'haeseleer, 2008).

2.3.5   Hydrogen-Natural Gas Blend Impacts End-Users

Adaptation of end-user systems is required at higher hydrogen concentrations in HENG blend. End-users impacts due to adding hydrogen to natural gas pipelines has been investigated by NaturalHy (De Vries, et al., 2007). Their study includes an estimation of the maximum hydrogen concentrations that don't require major adjustments for the end-users appliance. The conclusion was at hydrogen concentration of up to 28% in NG-pipelines can be used safely with well serviced existing appliances.

Haines et al. (Haines, et al., 2003) estimated the cost of upgrades/adjustments including (i.e. sensors modifications) required when using 3% hydrogen in NG-pipelines in the countries of United Kingdom, Netherlands, and France is found to be varied between $430,000 and $470,000. The cost estimation of modifying engine controls was $5.6 million in United Kingdom, $30 million

in Netherlands, and very limited cost in France; whereas cost estimation for modifying medium-pressure transmission lines was an average of \$500 - \$850 million per country. The cost estimation for updating end-users appliances when introducing a 12% hydrogen blend was around \$170 - \$470 million for each country. It is recommended by NaturalHy project that the outcomes of adding hydrogen into NG-pipelines for commercial/industrial combustion facilities be considered separately based on each individual case. For modernized power generation gas turbines, the natural gas as the desired fuel has a controlled specifications, adding hydrogen into NG-pipelines will require some adjustments to the turbine's control system in order to modify the parameters of the combustion process. Also, unexpected hydrogen concentration variations are unacceptable for gas turbines (Pinchbeck & Huizing, 2006).

The increase of the flame speed represents the most critical impact of using H_2-NG blend in burners, boilers or gas engines due to the flashback risk that accompanied. This problem could be reduced by modifying the combustion process. In general, within the flame detection system, the burner head and the sealing will need adjustment when HENG is used. The possible solutions to avoid multiple adjustments each time is: changing the composition of the input fuel; using multifunctional devices which can run both on natural gas and pure hydrogen; or a mixture of these two. The suggested applications are being developed in terms of efficiency, emissions, and safety and the results seem satisfactory (Ilbas, et al., 2005), (Akansu, et al., 2004).

The effect of increasing flame speed is most readily measured in laminar premixed flames. The increased flame speed consequences are as follows and as shown in Table (2.2), (Polman & Wolters, 2004):

- The temperature of the burner's surface will increase results in lowering the burner's lifetime;
- For both premixed and non-premixed laminar flame burners, the critical velocity gradient for light back will increase; and
- For both premixed and non-premixed laminar flame burners, the critical velocity gradient for blow off will increase.

Table (2.2): Hydrogen addition related to Gas Flame Speed

Hydrogen Content, by Vol.%	Flame Speed, cm/s
0	0.39
5	0.42
10	0.46
15	0.50
20	0.54
25	0.59

In Netherlands, a research was carried out by Gastec on gas cooking devices and domestic boilers to investigate the impacts of fueling them with a gas of up to 17 % hydrogen (Polman, et al., 2003). Three modern cooking devices and six different boilers were selected. The domestic appliances were selected to represent a different variety of the used ones through population in the country, while their variety in burner types and burner principles were specified. The gas composition for testing was a blend of 0 - 17% of hydrogen. Assessments included stability of burner's flame, burner's temperature, burner's pressure, emissions rates of CO and NOx, the loads and efficiency, the flame's detection and condensation rate. It is found that there is no technical obstacles observed when using H_2-NG blend of up to 17% hydrogen in cooking appliances and boilers.

Increasing the hydrogen concentration up to 25% in the fuel results in increase in burner's temperature which leads to increase the flame light back; whereas through the laboratory experiments, there was no increased burner's temperature and no light back seen when the percentage of hydrogen exceeds 17%. The wise choice of burner's materials seems good fit to avoid any expected flame light back. The H_2-NG blend used for light back tests across most of Europe has limit of up to 23% hydrogen (Polman, et al., 2003).

In general, for large scale power-generation and gas transport, gas turbines are currently the most critical facility in supporting energy demand. Almost all commercial fuel gases such as natural gas, syngas and any combination of these gases can be used to fuel the gas turbines. Gas turbines are designed to satisfy specifications/agreement between the manufacturer and end-user. The gas quality specifications are significant condition for achieving best performance of gas turbines.

All different-originated natural gas have similar combustion properties, however blending hydrogen (at different concentrations) will change the combustion properties of the new blend significantly. There is always a risk of moving the H_2-NG fuel quality outside the agreed turbine's design limits. Practically, gas turbines can be designed to be fueled with any fixed H_2-NG blend (i.e. HENG fuel). The manufacturer's assistance is necessary when adapting of a gas turbine to be fueled with a fixed ratio natural gas – hydrogen mixture which may be modified at moderate cost. Gas turbines that use mixed fuel are commercially available, they may suite for a fixed ratios of H_2-NG fuel; whereas modifying of a gas turbine to use natural gas with variable hydrogen concentrations is a challenge. Significant modifications will be required particularly when the turbine is designed to satisfy the contractual specifications of power supply, rather than simple operational specifications. The re-design technology for this application is still to be developed (Polman & Wolters, 2004).

2.4 Storing Electrical Energy

Storing electrical energy has shown great improvements in maintaining power supply for meeting demand through three main roles: (1) It reduces the cost by storing inexpensive electricity from renewable sources at off-peak periods, for sale at on-peak periods at higher prices; (2) It boosts the power supply reliability by supporting consumers when power network failures occur due to natural disasters; and (3) It maintains and enhances the quality of the power. The current capacity of existing electrical energy storage is less than 5% of the world's total generation capacity of 5550 GW (IEC, 2011). It has been suggested by technical performance studies that energy storage should represents not less than 10% of the total power capacity for better peak shaving and daily charge/discharge cycles (Chen, et al., 2009). There is a significant potential to cut the cost of power generation through minimizing the costlier modes by storing electrical energy generated by low-cost sources (or the surplus power from renewables) during off-peaks being reused into the grid during on-peaks periods.

Due to the flexibility and reliability needed, introducing mixed energy sources into electrical power grid became an urgent target for many researches. In general, power grid faces major challenges in transmission and distribution activities during the remarkable variations in hourly,

daily, and seasonal demand. As a pack up, storing the surplus of electrical energy and recover it when needed, is the most promising solution for these challenges. Storing electrical energy refers to the technology of transforming the surplus power into a storable state (energy carrier) in order to be retained back at maximum efficiency (Chen, et al., 2009).

Storing electricity as a technical approach can be defined as the delivery of energy from the upstream power suppliers to the downstream end-users, therefore it is providing buffering capacity in order to motivate the suppliers and the end-users maintain their transactions needed in a none simultaneous way. The bulk of the gathered energy by a specific society for variety of applications comes from a few primary power generation sources, of which the fossil fuels have the major part at about 80.9% (IEA, 2012). Since the location of the primary fossil-fuels energy resources are located at far distances from the different demands locations, therefore there is a need to store/transport energy to the final destination in which consumed (Birol, 2013). Scale-up the electrical energy storage has gathered significant research interest due to the commitment of the power grid reliability especially when the share of the intermittent renewable power generation is rising significantly. The classical approach for overcome the fluctuation in power demand is done by adjusting the power supply; whereas the outputs of the renewable energy sources such as wind and photovoltaics cannot be dispatched due to their intermittent nature. Utility-scale energy storage has been proposed as a tool to maintain grid reliability at the required level, while enabling the integration of renewable energy sources (Denholm, et al., 2010).

The main target for electrical energy storage is to increase the use of the renewable energy sources and to be more effective in matching power demand, this will enable the power operators to run at a higher capacity while meeting demand and at the same time reducing the need for peaking power plants. In general, electrical energy storage technologies are desired to improve the power's system responsiveness, power grid's reliability, and the overall flexibility while minimizing the whole related costs for both suppliers and customers (Schaber, et al., 2004).

Storing electrical energy from the intermittent renewable sources during off-peaks demand adds value to the supplied demand during on-peak by making this type of energy predictable and guaranteed (e.g. when deliver electrical power upon needed). This kind of buffer storage should be regulated and maintained by cost, efficiency and retrieval time. As a function of time, the power demand varies considerably during the day or from season to season; therefore the electrical energy

can be stored only to satisfy just a limited portion of the nominal demand, while it should be made available as a result of a contractual compromise (Ibrahim, et al., 2008).

The electrical energy systems can be classified as shown in Figure (2.3) into mechanical, electrochemical, chemical, electrical and thermal systems; whereas for large energy quantities, secondary systems such as hydrogen and hydrogen enriched natural gas (HENG) can be used as energy carriers via electrolysis process and/or via methanation process to produce methane (IEC, 2011). The main idea is use surplus generated electricity from renewable sources during off-peak periods to produce hydrogen via water-electrolysis process and to be used as energy carrier either as pure hydrogen or as HENG fuel. In addition, although the efficiency of this system is not high at the current time, but the significant advantages of the large amount of energy that can be stored and for long time encouraging researches for improving the system efficiency.
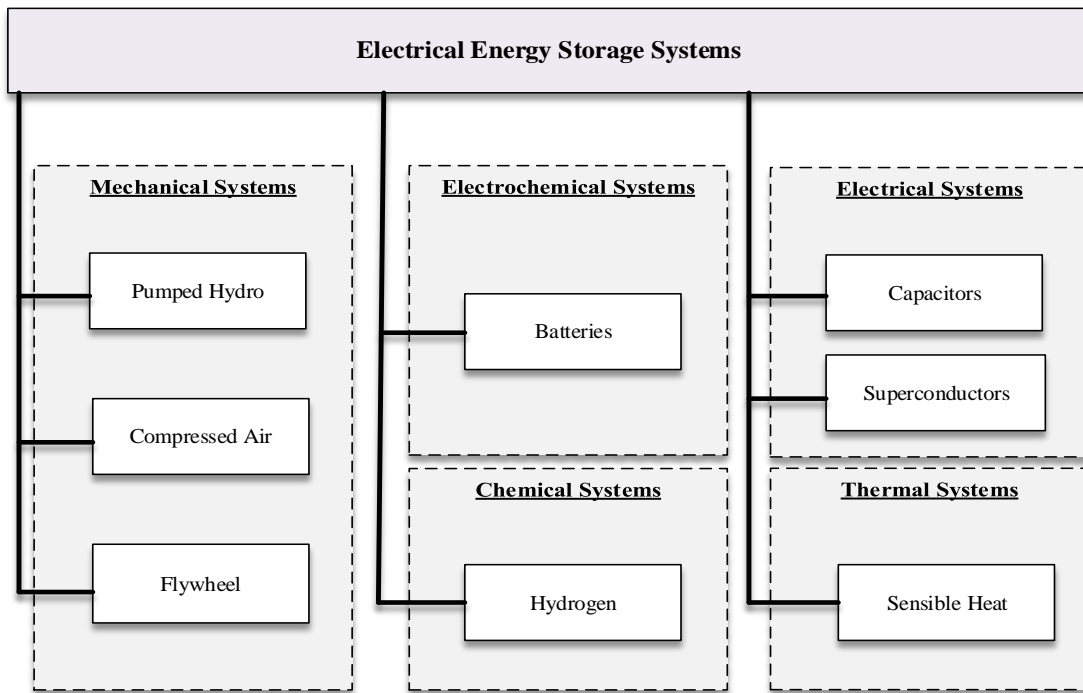
Figure (2.3): Electrical Energy Storage Systems of different categories

Power-to-Gas represents a feasible and relatively low-cost technology to large-scale electricity storage; whereas electrolyzers can be used in other grid functions such as rapid demand or supply response, spinning reserve, and frequency and voltage regulations. This technology is close to the scale of compressed air but it is much more modular and flexible in siting while it can be utilized its vast storage capacity within the NG-grid (see Figure 2.4). There is about 130 billion cubic feet

of natural gas storage capacity exists in Southern California (California Hydrogen Business Council, 2015), this is enough to supply all of the gas-fired generation in the whole region for more than two months.
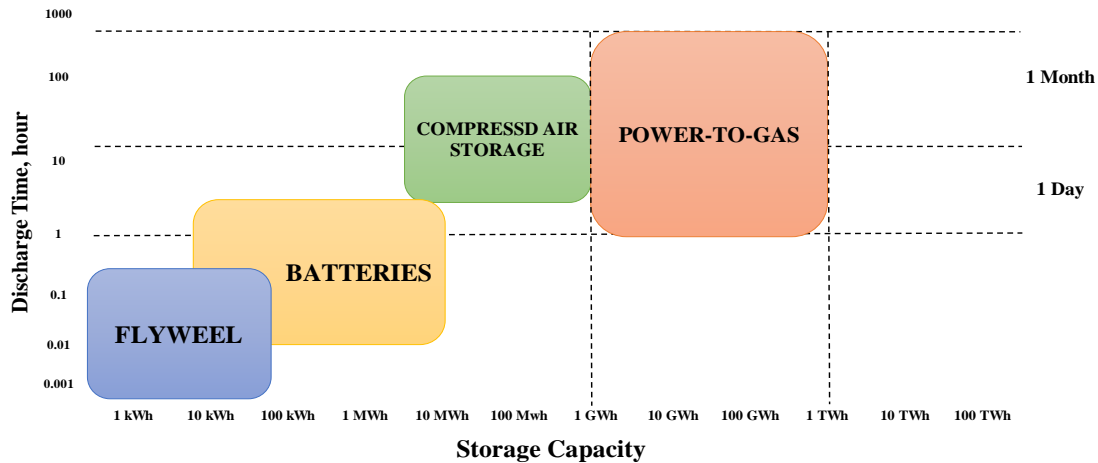
Figure (2.4): Electricity storage technologies

Hydrogen is one of the most favorable choices to store electrical energy due to its cleanness and reproducible capability as an energy carrier for both transportation and stationary applications. Interest in the research of hydrogen energy has developed dramatically to investigate the best for utilizing hydrogen as an alternative fuel due to its high energy density; therefore, the hydrogen energy development proceeds through three major areas: production, storage, and utilization (Liu, et al., 2010). In general, such an electrical energy storage system that utilize hydrogen as energy carrier can contain an electrolyzer, hydrogen storage tank and a fuel cell; all of these facilities are subject to specific characteristics based on system capacity, operation, and supply-demand. Different approaches studied for storing generated hydrogen, either as a gas under high pressure, a liquid at very low temperature, or adsorbed on metal hydrides; whereas gaseous hydrogen under pressure represents the most common method.

Storing energy is a unique method for adjusting the time discrepancy between power supply and demand. To improve the power quality and make the renewable energy generation resources more reliable, energy storage systems can play a crucial role. In the near future electrical energy storage will become crucial in emerging IEC-relevant markets in the use of more renewable energy, to achieve CO_2 reduction and for Smart Grids.

2.4.1 Storing Electrical Energy in Ontario

Ontario is working to manage periods of surplus base-load generation (SBG) from emissions free renewable sources and from nuclear power plants. Storing energy for long periods of time (i.e., months) would have opportunity to time-shift surplus baseload energy, to supply Ontario demand. For storage technologies with longer storage cycles, there would be an opportunity to mitigate, approximately 25% of the expected annual SBG (IESO, 2016). Gas energy storage offers the equivalent of a system-wide, distributed storage system during periods of surplus power, off-peak power periods, or when system operators need to immediately absorb spikes in generation during high wind periods. Also, in Ontario, fluctuations from renewables will increase, to 10,000+MW of new renewables (non-hydro) to be connected through 2018. Stemming from increased penetration of intermittent renewables, grid operators will have increased need to control power fluctuations, grid frequency, etc. and energy storage is an alternative to curtail renewables or operating thermal plants in the off-peak periods to control system stability.

By converting "excess" renewable energy and surplus base-load power into 'stored electrical energy', the constraints on increased renewable energy deployment are lifted and costly infrastructure additions (i.e. electric transmission towers and lines) are not required. Through the convergence of the electric distribution grid with the gas distribution and storage infrastructure, Ontario can achieve more flexible and adaptive operations across multiple vectors in the provincial energy system. Ontario's electricity sector is blessed with a relatively low-carbon electricity grid; however, with over 50% of the energy supplied by nuclear energy the grid has less operational flexibility to balance supply and demand during off-peak periods.

Balancing the grid will be even more challenging when the existing 2,000+ MW of variable generation, like wind, is expanded to 10,000 MW of variable generation by 2018. There are short periods when the intermittent nature of new renewable power sources will result in surplus electricity supply being available to the grid and this surplus is a necessary and expected result of Ontario's diverse portfolio of power sources and the need to ensure peak system capacity at all times. With additional quantities of must-run hydroelectric power, the province can anticipate significant periods of surplus power going forward.

Ontario's natural gas infrastructure can accommodate the equivalent of 80 TWh of energy that can be stored for many months. To offer a sense of scale for this energy storage, this is the equivalent of approximately 55% of the provinces annual electricity consumption. The peak, daily capacity for existing gas storage systems is so large it could accommodate the entire daily energy output from Ontario's nuclear fleet. This can be repeated for months without the need to discharge the stored energy. The conundrum - this surplus power must be converted to a gas to access this existing and cost-effective infrastructure.

As a gas, surplus energy can be stored, transported and converted into a dis-patchable and renewable power using existing NG-pipelines through utilizing Combined Cycle Power Plants (CCPP). Using CCPPs with renewable HENG-fuel could optimize these assets for lower overall costs of operation.

Storing electricity as electrolytic-produced hydrogen inside NG-pipelines has the potential to reduce the impact of extreme or sudden changes in power demand and renewable sources (i.e. wind and solar) availability, which would lessen the need and utilization of peaking plants (i.e. CCPP) and lower overall system costs.

Seasonal electrical energy storage and energy distribution are required in Ontario, and electrolysis-produced hydrogen can provide this storage vector as it can be generated from off-peak electricity, and then stored with natural gas in existing pipelines network storage facilities. To make the energy network "smart", energy storage will need to be deployed, including the existing gaseous energy storage.

2.5 Modelling and Optimization Tools

In this research, two modeling tools are used: General Algebraic Modelling System (GAMS) which is used for modelling and optimizing the objective functions; the second tool is Air Quality Benefits Assessment Tool (AQBAT) which is used for monetizing health impacts associated with emissions from NG-fueled CCPP.

2.5.1 General Algebraic Modelling System 'GAMS'

GAMS is a high level Computer programming language for modeling and solving optimization problems such as linear, non-linear, and mixed integer programs. It is especially useful for handling large and complex problems. GAMS enables the user to model problems in a natural way, so it can be easily change the formulation – even convert a model from linear to nonlinear with few steps. The goal from developing was to create a powerful but easy-to-use computer programming language that would greatly simplify the modeller's task of formulating and solving complex optimization problems. GAMS offers many advantages over other conventional computer optimization, it enables the modeller to:

(1) Describe the model to a computer in an easy and simple way. The model can be formulated using concise algebraic statements that is easy to read by computers and by humans.

(2) The specified statements can be created in one statement; whereas other optimization software requires entering individual constraint. GAMS can generate the constraint equation based on the input and specified data values.

(3) GAMS allows the modeller to enter data only once, the basic data can be entered as table which saves time and reduces the possibility of making mistakes.

(4) GAMS allows to include explanatory text as a definition of any symbol or equation. Furthermore, GAMS automatically incorporates the comments into the output report which making the results easy to understand.

(5) GAMS compiles the desired model while searching for any errors before run the model. It checks for errors in numerical operations and mathematical consistency. GAMS tells the modeller where the errors occur in the model and what sort they are.

GAMS is designed for modeling linear, nonlinear and mixed integer optimization problems; it is especially useful for handling large, complex, one-of-a-kind problems (McCarl, 2012). The MCP is a natural format for expressing a variety of economic models for markets. Algorithms for solving MCPs are relatively reliable and efficient (Rutherford, 2002). GAMS is used in the current research to model and to optimize the costs-emissions as the main objective functions. Mixed Complimentary Problem (MCP) and Mixed Integer Linear Programming (MILP) are the simulation-models that used in the four different studies; the related results are presented in the following chapters.

2.5.2   Air Quality Benefits Assessment Tool 'AQBAT'

The Air Quality Benefits Assessment Tool (AQBAT) is developed by Health Canada as a computerized simulation tool to calculate the burden of illness and economic impact caused by air pollution. The economic impact of air pollution, including health damage, can be calculated by the AQBAT. Within this approach, health outcomes are monetized using health endpoint valuations. The AQBAT is based on the people WTP approach, which has been used to assess the value of doing riskier jobs and assessing the level of wages required in order to encourage participation in those jobs. Minimization of mortality risk is used in AQBAT when performing mortality valuation; whereas the cost of a treatment approach is used in evaluating the morbidity outcomes, including direct medical expenses, lost productivity, and all other averting expenditures. Utilizing the AQBAT for evaluating the external cost of air pollution is not new. It has been used for similar studies in Hamilton, Ontario, and in British Columbia while evaluating the transportation sectors across Canada. In addition, this tool has been applied to estimate the burden of illness due to traffic-related air pollution by the TPHD (Toronto Public Health Department, 2007).

As a computer-based simulation tool, it allows to define different scenarios and models by incorporating flexibility to connect air pollutants such as CO, NO_x, PM, and SO_2 into health impacts while considering other variables such as geographic areas and time under the study. It requires to utilize a dispersion model to calculate the pollutants concentrations in μg per m^3 and then related them to the distance (in meter) from the pollution source at which the highest pollutant's concentration can be reached. More flexibility can be found in AQBAT by

considering a wide range of health impacts within the impacted area; i.e. mortality, morbidity, respiratory & cardio-vascular, asthma, reduction in lung capacity, hospitalization, restricted activity, and cancers. The fundamental calculation when using AQBAT is presented by Eqn. (2.3):

$$\text{No. of Accidents} = \text{Risk}_{\text{Coff.}} * \Delta C_{\text{Pollutant}} * \text{HIR} * P \tag{2.3}$$

Where: **Risk**$_{\text{Coff.}}$ represents the percentage of health impacted due to an increase of pollutant's concentration; $\Delta C_{\text{Pollutant}}$ is the increase in pollutant concentration; **HIR** represents the health incidence rate, i.e. number of health impact incidents per million of population; and **P** is the population under study in millions.

AQBAT is used in this research to monetize health impacts associated with emissions from utilizing combined cycle power plants (CCPP) in meeting power demand. Monetizing health impacts is critical to investigate the hidden cost of electricity generated by fossil fuels such as natural gas (NG). Expected pollutants from NG-fueled CCPP is specified, whereas health impacts matrix is addressed as shown in Table (2.3):

Table (2.3): Air Pollutants – Health Impacts Matrix

Primary Air Pollutants	*Health Impacts*							
	Mortality	Morbidity	Respiratory and Cardio-Vascular	Asthma	Reduction of lung capacity	Hospitalization	Restricted Activity	Cancers
Carbon Monoxide, CO	High	N/A	High	N/A	N/A	Low	N/A	N/A
Nitrogen Oxides, NO$_x$	Very high	N/A	High	N/A	N/A	N/A	N/A	N/A
Particles Matters PM$_{2.5}$	Very high	N/A	Medium	Medium	N/A	Medium	N/A	Very high
Sulfur Dioxide, SO$_2$	Medium	N/A	Medium	N/A	N/A	N/A	N/A	N/A

Chapter Three

3. Design of an energy hub based on natural gas and renewable energy sources

3.1 Introduction

This research focuses on generation, exchange, and conversion of energy between many types of energy generators such as combined cycle power plant (CCPP) as a critical energy source within the proposed hub. In a CCPP, a natural gas-turbine generates electricity, while the exhaust heat is used to generate steam in order to drive a steam turbine to generate additional electricity. The CCPP is utilized for a dis-patchable and reliable power supply, while the renewable energy sources of wind turbines (WTs) and photovoltaic (PV) solar cells are utilized for sustainable and emission-free power supply. The surplus electricity from the WTs and the PV solar cells during off-peak times can be used by alkaline electrolyzers to generate hydrogen which is proposed to be used for direct sale to the hybrid electric vehicles. The main objectives is to assess the combination of a conventional NG-fuelled CCPP with the renewable energy sources of WTs and PVs in terms of costs and emissions that could be save. In general, Ontario's policies recommended increasing the integration of renewable energy sources into existing power grid to reduce the environmental impacts of the power generation sector (IESO, 2009). Furthermore, based on 2005 projection, Canada's government plan to reduce the GHGs by 17% by 2020 would offer a more stable and secure energy supply through the use of local energy resources of NG, wind, and solar (Goverment of Canada, 2010). Figure (3.1) shows the major constituents of the proposed energy hub. The CCPP dispatches the power demand, while WTs and PV solar cells provide a clean power intermittently. The surplus power of WTs and PVs during the off-peak periods is to be utilized by alkaline electrolyzers to generate hydrogen. Storing hydrogen is a vital step through what is named "hydrogen-economy". The inverters and/or transformers that located within the power conditioning system (PCS) are used to enhance electricity interchange among the hub units. Storing NG and H_2 did not included in the proposed energy hub's model.

This energy system technology could be used to support existing power grid or to meet limit demand of such a remote area. The capacity of this system is generated by utilizing CCPPs, WTs, and PVs. Excess energy from wind and solar during permitted weather conditions can be

transformed into another form of energy such as hydrogen using energy conversion technologies such as alkaline electrolyzers.
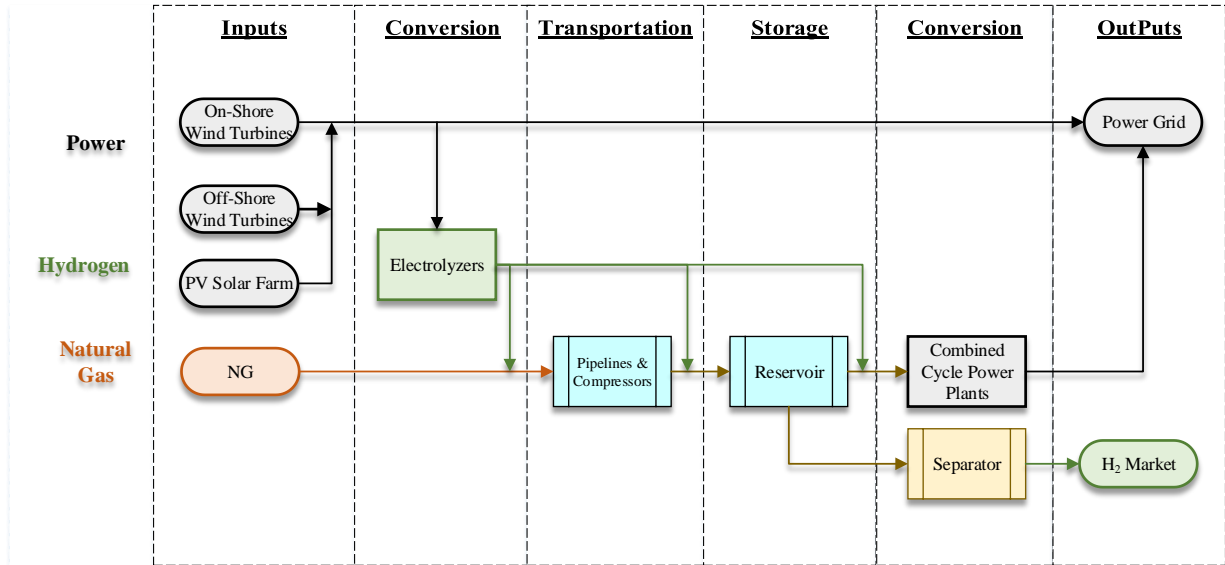
Figure (3.1): The configurations of the proposed energy hub

3.2 Developing the Simulation Model

GAMS is used to develop the simulation process using the mixed complementary problem (MCP) solver. Different hourly inputs such as air temperature, solar insolation, and power demand were used for better reality, accuracy and significance to the research's results. The input and output of the hourly parameters over a one full year are coupled with Micro-Soft Excel for better visual and organized manner. The simulation-model was designed based on the fundamental laws of thermodynamics, economics, and process design. The process flow diagram of the proposed CCPP has been showed by Figure (3.2).

3.2.1 Developing Cost Model for CCPP

The main parts of the combined cycle power plant as the only fossil-fueled power source used for meeting dis-patchable demand are presented in Figure (3.2).
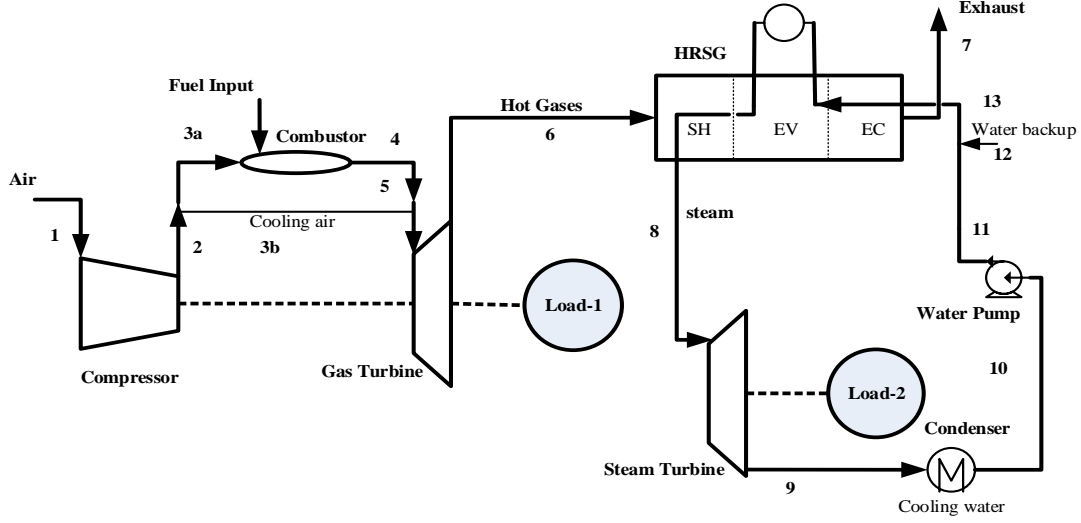
Figure (3.2): The CCPP's main parts

The net of power generated by CCPP in MWh per hour is calculated as shown in Eqn. (3.1):

$$Power_{CCPP,i} = Power_{Gas-Turbine,i} + Power_{Steam-Turbine,i} - Power_{Compressor,i} - Power_{Pump,i} \qquad (3.1)$$

The main power generator in CCPP is the gas-turbine which is burning natural gas to generate electricity, the hourly power output of this generator in MWh is calculated using Eqn. (3.2):

$$Power_{Gas-Turbine,i} = M_{5,i} * R * T_{5,i} * \left(\frac{n}{n-1}\right) * \left[\left(\frac{P_{5,i}}{P_{6,i}}\right)^{\frac{n-1}{n}} - 1\right] * t \qquad (3.2)$$

Where: $M_{5,i}$ is the molar flow rate of the air–fuel mixture in mole per hour, n is the expansion-compression index, R is the gas constant, $T_{5,i}$ is the stream temperature at point 5 of Figure (3.2), t is the time interval in hours, and $P_{5,i}$, $P_{6,i}$ are the streams pressures at points 5 and 6 of Figure (3.2) respectively.

The relationship between inlet and outlet conditions is governed by the adiabatic compression-expansion relations. The pressure drop due to the flow of air-fuel mixture through the combustion chamber should be considered in the calculations. The stream's pressure at the combustion chamber exit (i.e. at point 4 in Figure (3.2)) is calculated as a difference between the combustor's inlet pressure P_{3a} and the pressure drop at the combustion chamber which is assumed to be 3% of P_{3a}. Energy balance around the combustion chamber is used to calculate the stream's temperature at point 4 $T_{4,i}$ of Figure (3.2), this temperature is called of the "adiabatic flame temperature" or the combustion temperature of the gases that exit the chamber. The adiabatic temperature as been determined by (Smith, 2005) is calculated by trial and error method to find an approximate value as shown by Eqn. (3.3):

$$\Delta H^o_{Combustion} = \Delta H_{Products} - \Delta H_{Reactants} \tag{3.3}$$

Where: $\Delta H_{Products}$ represents the change in enthalpy of the products of the combustion reaction in the combustion chamber, and $\Delta H_{Reactants}$ represents the enthalpy change of the reactants. The $\Delta H^\circ_{Combustion}$ is the standard heat of combustion at 298 K. The enthalpy change ΔH_j of a component is a function of its heat capacity as shown in the Eqn. (3.4):

$$\Delta H_j = \int_{T_i}^{T_o} C_{p,j} \cdot dT \tag{3.4}$$

Where: The heat capacity $C_{p,j}$ is given by Eqn. (3.5):

$$C_{p,j} = \alpha_j + \beta_j . T + \gamma_j . T^2 + \delta_j . T^3 \tag{3.5}$$

Where: The parameters α_j, β_j, γ_j and δ_j are constants for a given component j. The $\Delta H^\circ_{Combustion}$ of combusted natural gas (NG) is calculated using the combustion reaction of methane CH_4 as shown in Eqn. (3.6):

$$CH_4 + 2*(O_2 + 3.7*N_2) \rightarrow CO_2 + 2*H_2O + 7.52*N_2 \tag{3.6}$$
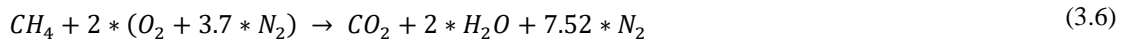
The heat recovery steam generator (HRSG) is the unit that utilizes the excess energy from exhaust gases that exit from gas-turbines to be used for generating steam in the steam-turbine. This unit consists of super-heater, evaporator and economizer; whereas the total energy transferred to the steam in point 8 of Figure (3.2) is calculated using Eqn. (3.7):

$$\text{Energy}_{\text{HRSG,i}} = \int_{T_{7,i}}^{T_{6,i}} \sum_j (M_{j,i} * C_{p,j}) \, dT_i \tag{3.7}$$

Where; $\text{Energy}_{\text{HRSG,i}}$ represents the energy transferred from the hot gases exhaust at point 6 of Figure (3.2) to the generated steam, $M_{j,i}$ represents the molar flow of component j at hour i, and $C_{P,j}$ is the heat capacity of component j at hour i. The power generated by steam turbine in MWh per hour is calculated as shown in Eqn. (3.8):

$$\text{Power}_{\text{Steam-Turbine,i}} = M_{8,i} * R * T_{8,i} * \left(\frac{n}{n-1}\right) * \left[\left(\frac{P_{8,i}}{P_{9,i}}\right)^{\frac{n-1}{n}} - 1\right] * t \tag{3.8}$$

Where: $M_{8,i}$ represents the molar flow rate of the steam at point 8 of Figure (3.2). The power consumed by air compressor in MWh per hour is calculated using Eqn. (3.9):

$$\text{Power}_{\text{Compressor,i}} = M_{1,i} * R * T_{1,i} * \left(\frac{n}{n-1}\right) * \left[\left(\frac{P_{2,i}}{P_{1,i}}\right)^{\frac{n-1}{n}} - 1\right] * t \tag{3.9}$$

Where: $T_{1,i}$ represents the stream's temperature at point 1 of Figure (3.2), it is assumed to be equal to the ambient temperature T_0. $P_{1,i}$ represents the stream's pressure at point 1 of Figure (3.2), this pressure is equal to the difference between ambient pressure and the pressure drop at the compressor inlet. The pressure drop is assumed to be 2% of the ambient pressure; n is the expansion-compression index.

The heat energy removed by the condenser is calculated based on (Sinnott, 2005). The shell-and-tube type condenser with an overall heat transfer coefficient range of 1250 W/(m^2.$^{\circ}$C) is considered in this research. Eqn. (3.10) is used to calculate the heat energy removed by the condenser:

$$Energy_{Condenser,i} = U_{Condenser} * A_{Condenser} * LMTD_{Condenser,i} \tag{3.10}$$

Where; $\text{Energy}_{\text{Condenser, i}}$ represents the heat energy transferred at any hour i, $U_{\text{Condenser}}$ is the heat transfer coefficient in W per m^2.K, $A_{\text{Condenser}}$ is the heat transfer area in m^2, and $\text{LMTD}_{\text{Condenser, i}}$ represents the Log Mean Temperature Difference at any hour i which is calculated as shown in Eqn. (3.11):

$$LMTD = \frac{\Delta T_h - \Delta T_c}{\ln(\Delta T_h/\Delta T_c)} \tag{3.11}$$

Where: ΔT_h represents the difference in hot terminal temperature; whereas ΔT_c represents the difference in the cold terminal. These equations are used to rate, size and to estimate the cost of the condenser.

The work energy consumed by the boiler-feed pump (water pump) is calculated using incompressible fluids-Bernoulli's equation as shown in Eqn. (3.12):

$$\text{Power}_{\text{Pump,i}} = \left(9.81 * m_{11,i} * \Delta h_{10-11}\right) + \left(\frac{m_{11,i}}{\rho_{H_2O}} * \Delta P_{10-11,i}\right) + \left(\frac{m_{11,i}}{\rho_{H_2O}} * \Delta P_{10-11,i}^{\text{friction}}\right) \quad (3.12)$$

Where: $\textbf{Power}_{\textbf{Pump}}$ represents the pump's power in Watt required at any hour $\textbf{i}$ given, $\textbf{m}_{\textbf{11,i}}$ represents the steam's mass flow rate in kg per second, $\Delta \textbf{h}_{\textbf{10-11}}$ represents the difference in altitude measured in meter, $\Delta \textbf{P}_{\textbf{10-11,i}}$ represents the pressure drop in Pa between the points 10 and 11 as shown in Figure (3.2), and $\Delta \textbf{P}_{\textbf{10-11,i}}^{\textbf{friction}}$ represents the pressure drop in Pa due to the friction between the points 10 and 11.

Air pollutants emissions represent critical parameters that are considered in modeling the combustion of the combined cycle power plant (CCPP). In general, the rate of emission of the different pollutants is a function of the temperature of the exhaust gases and pressure drop through the combustor chamber. The semi-empirical relations are adopted from (Rizk & Mongia, 1993) to calculate the rates of gas emissions as shown by the following Eqns. (3.13), (3.14), and (3.15).

$$\text{Rate}_i^{\text{NO}_x} = \frac{0.15\text{E}16 * \tau^{0.5}\exp(-71100/T_{4,i})}{p_{3,i}^{0.05}(\Delta p_{3a-4}/p_{3,i})^{0.5}} \quad (3.13)$$

$$\text{Rate}_i^{\text{CO}} = \frac{0.18\text{E}9 * \exp(7800/T_{4,i})}{p_{3,i}^2 * \tau * (\Delta p_{3a-4}/p_{3,i})^{0.5}} \quad (3.14)$$

$$\text{Rate}_i^{\text{UHC}} = \frac{0.755\text{E}11 * \exp(9756/T_{4,i})}{p_{3,i}^{2.3} * \tau^{0.1} * (\Delta p_{3a-4}/p_{3,i})^{0.6}} \quad (3.15)$$

Where: $\textbf{Rate}_{\textbf{i}}^{\textbf{NO}_{\textbf{x}}}$, $\textbf{Rate}_{\textbf{i}}^{\textbf{CO}}$ and $\textbf{Rate}_{\textbf{i}}^{\textbf{UHC}}$ represent the rates of emissions (Nitrogen Oxides, Carbon mono-Oxide, and Un-burned Hydro-Carbons) measured in gram of pollutant per kg of the fuel which is NG at any hour $\textbf{i}$, and $\boldsymbol{\tau}$ is the residence time in the primary zone and it is assumed to be 2 milliseconds (Lazzaretto & Toffolo, 2004).

Calculating costs is a key step in modeling CCPP as it represents the crucial part of the total cost of electricity (COE). The CCPP's cost estimation is divided into capital costs and operating & maintenance (O&M) costs. The following relationships are used to calculate the capital costs of the main equipment of CCPP in $US (Attala, et al., 2001).

$$\text{Capital Cost}_{\text{Gas-Turbine}} = 3,832 * \text{Nominal} - \text{Power}_{\text{Gas-Turbine}}^{0.71} \tag{3.16}$$

$$\text{Capital Cost}_{\text{HRSG}} = 17,000 * \sum (\frac{\text{Heat Removed}_{\text{Condenser}}}{\Delta T_{\text{Condenser}}})^{0.6} \tag{3.17}$$

$$\begin{aligned}\text{Capital Cost}_{\text{Steam-Turbine}} \\ = 3,197,280 * \text{Area}_{\text{Steam-Turbine}}^{0.261} + 823.7 \\ * \text{Nominal} - \text{Power}_{\text{Steam-Turbine}}^{1.543}\end{aligned} \tag{3.18}$$

$$\text{Capital Cost}_{\text{Condenser}} = 162 * \text{Area}_{\text{Condenser}}^{1.01} \tag{3.19}$$

$$\text{Capital Cost}_{\text{Pump}} = 1,293.44 * \text{Nominal} - \text{Power}_{\text{Pump}}^{0.8} * \left(1 + [\frac{0.3}{1 - \eta_{\text{Pump}}}]^{-0.46}\right) \tag{3.20}$$

Where: η_{Pump} is the efficiency of the pump.

In order to estimate the annual payment for the calculated capital costs over the entire life of the project, the following Eqn. (3.21) is used:

$$\text{Payment} = \text{Current Value} * (\frac{\text{Interest} * (1 + \text{Interest})^{N}}{(1 + \text{Interest})^{N} - 1}) \tag{3.21}$$

Where: the **payment** will be in $ per year and **N** represents the number of payments; whereas the interest is assumed to be 5%.

The CCPP's O&M costs are divided into fixed and variable costs. The fixed O&M costs are function of the nominal power plant; whereas the variable O&M costs are function of the CCPP's generated electricity as shown in the following Eqn. (3.22).

$$\text{Cost}_{\text{O\&M}} = c_{\text{Fixed}} * \text{Nominal} - \text{Power}_{\text{CCPP}} + c_{\text{Variable}} * \text{Power}_{\text{CCPP}} \tag{3.22}$$

Where: **CFixed** is assumed to be $20 per (kW.year), and **CVariable** is $0.002 per kWh (Mansouri, et al., 2012).

The natural gas cost is calculated based on the following Eqn. (3.23):

$$\text{Cost}_{\text{NG}} = \sum_{i=1}^{8760} \text{Cost}_{\text{NG,i}} * \text{Mass Flow}_{\text{NG,i}} \tag{3.23}$$

Therefore, the average COE of generated electricity by CCPP in $ per kWh can be calculated as shown in Eqn. (3.24):

$$\text{COE}_{\text{CCPP}} = \frac{\text{Capital Cost}_{\text{CCPP}} + \text{Cost}_{\text{O\&M}} + \text{Cost}_{\text{NG}}}{\text{Power}_{\text{CCPP}}} \tag{3.24}$$

3.2.2   Developing Cost Model for Wind Turbines

The proposed wind farm is based on Port Dover & Nanticoke wind (PDN); the plan is to generate 105 MW of electricity utilizing 58 wind turbines of V-90, which each turbine produces 1.8 MW of power as stated by Capital Power (Capital Power, 2015). The PDN Wind project is located on privately-owned leased lands within Haldimand and Norfolk Counties, Ontario, near the north shore of Lake Erie.

For the on-shore wind farm, the data of wind speed, air temperature, etc. for this farm is adopted from Environment Canada at 42.791 N, -80.168 W, and at altitude of 80 m. Table (3.1) provides the seasonal wind profile of the proposed wind farm.

Table (3.1): The expected wind speed data for on-shore farm

Season	Mean wind speed, m/s
Annual	6.96
Winter	8.26
Spring	6.91
Summer	5.53
Fall	7.26

The cost model for proposed wind turbines starts by calculating the power generated by each turbine in watts as shown in Eqn. (3.25) (Wizelius, 2007):

$$\text{Power}_{\text{WT,i}} = 0.5 * \rho_{\text{air}} * A_{\text{rotor}} * \text{Coff}_{\text{Performance}} * \eta_{\text{WT}} * \eta_{\text{Mech.}} * V^3_{\text{air,i}} \tag{3.25}$$

Where: the η_{WT} and $\eta_{\text{Mech.}}$ represent the efficiency of generator and the mechanical efficiency of gear box respectively. Based on Kurtulan et al. (Kurtulan & Sevgi, 2009), the performance coefficient can assumed to be 0.35; whereas the mechanical efficiency is assumed to be 0.95 (Kurtulan & Sevgi, 2009) and the $V_{\text{air, i}}$ is the wind speed at any hour in meter per second.

Calculating the costs of wind turbine represents the next step in modeling development, the cost of electricity (COE) for WTs is governed by capital costs, O&M costs and other auxiliary costs. The on-shore WTs capital cost for the proposed capacity is varied from 1100 to 1400 € per kW (Blanco, 2009). As an average value of $1700 per kW is assumed for this model, therefore the capital cost in $ per year is presented as shown in Eqn. (3.26):

$$\text{Capital Cost}_{\text{WT}} = 1700 * \text{Nominal} - \text{Power}_{\text{WT}} \tag{3.26}$$

The O&M costs for on-shore WTs vary with the size of wind farm, it include maintenance, spare parts, and administration fees. In the current model, it is assumed the O&M costs is an average of 0.7 ¢ per kWh (Fingersh, et al., 2006) as shown in the following Eqn. (3.27):

$$\text{Cost}_{\text{O\&M}} = \sum_{\text{i}=1}^{8760} 0.007 * \text{Power}_{\text{WT,i}} \tag{3.27}$$

In the last step for WTs cost of electricity calculation, the COE is calculated similar to the one of CCPP before, as shown in the following Eqn. (3.28):

$$COE_{WT}^{On-Shore} = \frac{\text{Capital Cost}_{\text{WT}} + \text{Cost}_{\text{O\&M}}}{\text{Power }_{\text{WT}}} \tag{3.28}$$

For the off-shore wind turbines, the location is in Lake Erie, Nanticoke region. The related wind speed data is adopted from Environment Canada at 42.772 north, 80.116 west at altitude of 80 m as shown from Table (3.2):

Table (3.2): Expected wind speed data for off-shore farm

Season	Mean wind speed, (m/s)
Annual	7.47
Winter	8.83
Spring	7.38
Summer	5.97
Fall	7.78

The off-shore's WTs characteristics are selected based on the model SWT 2.3-93 from Siemens (Siemens AG, 2009). The turbine has a nominal power of 2.3 MW makes it superior for moderate wind speeds. By the same way that has been followed in calculating on-shore WTs, cost calculations for off-shore WTs are modelled; the capital cost as per specified capacity is assumed to be $2,924 per kW (Blanco, 2009).

The O&M costs of off-shore WTs are higher than that of on-shore WTs due to the extra costs of the special equipment needed as the maintenance process is more complex for the off-shore WTs, therefore, an assumed cost of 2 ¢ per kWh is considered in this model based on an estimation from the National Renewable Energy Lab (Fingersh, et al., 2006). The average COE of off-shore WTs is presented in Eqn. (3.29):

$$\text{COE}_{\text{WT}}^{\text{Off–shore}} = \frac{\text{Capital Cost}_{\text{WT}} + \text{Cost}_{\text{O\&M}}}{\text{Power}_{\text{WT}}} \tag{3.29}$$

3.2.3 Developing Cost Model for PV-Solar

The PV's SPR-400 is an existing design brand in the market from Sunpower Corporation (Sunpower Corporation, 2008). This solar panel has 128 monocrystalline cell incorporates with an efficiency of 18.5% and an ability to generate 400 W maximum. Based on market information from Solarbuzz (Solarbuzz, 2011), the inverter's cost was 71.4 ¢ per Watt.

The power generated by PV-solar is calculated as a function of the hourly solar insolation, G_i (in Watt per m^2) and the modular efficiency $\eta_{Solar,i}$ for generating power as shown from Eqn. (3.30) (Russell & Bergman, 1986):

$$Power_{PV,i} = G_i * Area_{Solar} * \eta_{Solar,i} \tag{3.30}$$

Calculating the cost of the power generated by PV-solar is the next step, the capital costs of grid-connected solar farm is assumed to be $7000 per kW for this model based on Ayoub et al. report (Ayoub, et al., 2010). The O&M costs of solar is assumed to be $0.01 per kWh as per PV cost factors report (Muneer, et al., 2011), therefore the COE of power generated by solar farm is calculated as shown in Eqn. (3.31):

$$COE_{PV} = \frac{Capital\ Cost_{PV} + Cost_{O\&M}}{Power_{PV}} \tag{3.31}$$

3.2.4 Developing Cost Model for Electrolyzers

The electrolyzers as the main equipment used for generating hydrogen from water through the electrolysis process, the alkaline electrolyzer HySTAT-60 model from Hydrogenics is chosen in this study as well-known brand in Ontario's market. The following Table (3.3) is presenting the main characteristics of the proposed electrolyzers:

Table (3.3) Specifications of the proposed alkaline electrolyzer

Specification	Value	Reference
Electrolyte	H_2O + 30% wt. KOH	(Hydrogenics Corporation, 2009)
Power Constant, kWh/Nm^3	5.2	(Hydrogenics Corporation, 2009)
Max H$_2$ generated, Nm^3/h	60	(Hydrogenics Corporation, 2009)
H$_2$ purity, %	99.998	(Hydrogenics Corporation, 2009)
H$_2$ output pressure, bar (g)	10	(Hydrogenics Corporation, 2009)
Temperature range, ºC	(-20) - (+40)	(Hydrogenics Corporation, 2009)
Electrolyser running capacity range, (Nm^3/h of H$_2$)	24 - 60	(Hydrogenics Corporation, 2009)

As per Hydrogenics Corp., the HySTAT-60 alkaline electrolyzer can generate 60 m^3 of hydrogen per hour at Normal-operating conditions of pressure and temperature, thus the hydrogen that can be produced hourly is calculated as shown from Eqn. (3.32):

$$\text{Flow} - \text{Rate}_{H_2,i} = \text{Flow} - \text{Rate}_{Normal-Conditions} * N_{Elz,i} \tag{3.32}$$

Where: $N_{Elz,i}$ represents the number of electrolyzers in operation in each hour.

In order to calculate the total costs of producing hydrogen via electrolysis process, it is to note that these costs are impacted significantly by capital costs of electrolyzers and the cost of electricity that will be used in electrolyzers. The capital costs of electrolyzers is a function of electrolyzer's capacity for producing hydrogen as shown in Eqn. (3.33):

$$\text{Capital Cost}_{Elz} = 224.49E3 * \text{Flow} - \text{Rate}_{Normal-Conditions}^{0.6156} \tag{3.33}$$

The O&M costs of the proposed electrolyzers are assumed as a percentage of 5% of the capital costs of the electrolyzers (Saur, 2008) as shown by the following Eqn. (3.34):

$$\text{Cost}_{O\&M}^{Elz} = 0.05 * \text{Capital Cost}_{Elz} \tag{3.34}$$

The electricity consumed by the proposed eletcrolyzers is calculated as shown in Eqn. (3.35) and Eqn. (3.36); whereas the cost of this electricity is calculated by Eqn. (3.37):

$$\text{Power}_{Elz} = \sum_{i=1}^{8760} \text{Power}_{Elz,i} * N_{Elz,i} \tag{3.35}$$

$$\text{Power}_{Elz,i} = 5.2 \left(\frac{\text{kWh}}{\text{Nm}^3}\right) * 60 \left(\frac{\text{Nm}^3}{\text{hour}}\right) \tag{3.36}$$

$$\text{Cost}_{Power-Elz} = \sum_{i=1}^{8760} \text{COE}_{Renewable-Power} * \text{Power}_{Elz,i} * N_{Elz,i} \tag{3.37}$$

The cost of water Cost_{Water} used in eletcrolyzers for generating hydrogen can be included in the total costs of electrolyzers, therefore the total costs of utilizing alkaline electrolyzers in generating hydrogen is expressed as shown in Eqn. (3.38):

$$\text{Cost}_{Total}^{Elz} = \text{Capital Cost}_{Elz} + \text{Cost}_{O\&M}^{Elz} + \text{Cost}_{Power-Elz} + \text{Cost}_{Water} \tag{3.38}$$

The cost of producing hydrogen in $ per kg is calculated using the following Eqn. (3.39):

$$Cost_{Hydrogen} = \frac{Cost_{Total}^{Elz}}{Flow - Rate_{H_2,i}} \qquad (3.39)$$

3.3 Running Different Scenarios

Three different scenarios are designed in this research to examine techno-economic performance of the proposed energy hub; each scenario is presented with a unique simulation model to study, assess and to investigate the feasibility of the energy hub in terms of: electricity cost, CCPP-emissions, renewable generated energy by WTs & PV-solar, and utilizing hydrogen as an energy carrier as seen from the following scenarios:

i.   Scenario A: Meeting demand by utilizing CCPP only,

ii.   Scenario B: Meeting demand utilizing energy hub, and

iii.   Scenario C: Hydrogen as an energy carrier.

Accordingly, an hourly input data are fed into each scenario; whereas an outputs such as electricity generated, CCPP's emissions, hydrogen generated, and all related costs, are collected and presented in results and discussions section.

3.3.1   Scenario A: Meeting Demand by Utilizing CCPP only

This scenario is proposed for utilizing NG-fueled CCPP to meet the desired power demand (i.e. through all times periods including off-peaks and on-peaks), therefore this scenario is used as a base step in performing all the needed calculations including generating electricity, related CCPP's emissions and all related costs. The objective of this scenario is to be the reference point for the subsequent scenarios in terms of electricity cost, emissions, and CCPP's efficiency. The power demand reflects the 2009's profile that provided by Independent Electricity System Operator (IESO). The NG cost is assumed to be an average of monthly price. The hourly outputs such as electricity produced, air pollutants emitted, and all related costs are considered and presented to be used for comparison later on among other scenarios.

It is assumed that NG is a pure CH_4 in the calculation of mass and energy balance and it is sulfur free, i.e. emissions of SO_x at the exhaust is neglected as well as PM_x emissions. Table (3.4) summarizes the inputs/outputs parameters as well as related variables that are modelled in this scenario.

Table (3.4): Scenario A: Meeting Demand by Utilizing CCPP, inputs/outputs

Inputs	Hourly power demand in MWh
	NG monthly average cost in $ per kg
	CCPP's design parameters such as $T_{5,i}$ and $P_{5,i}$
	Exhaust gases properties such as heat capacity C_p
Outputs	Hourly electricity generated in MWh
	Cost of electricity (COE) in $ per kWh
	Average CCPP's efficiency η_{CCPP}
	Hourly emissions of CO_2, CO, NO_x, and UHCs in kg

3.3.2 Scenario B: Meeting Demand Utilizing Energy Hub

This scenario is proposed for utilizing energy hub including NG-fueled CCPP, on-shore WTs, off-shore WTs and solar to meet the desired power demand, therefore incorporating the renewable energy sources of wind and solar is what this scenario differs from Scenario A. In addition to the inputs that included in Scenario A, the inputs for scenario (B) are including wind speed, insolation, air temperature, etc. plus the specifications of WTs and solar as the design parameters. In this scenario, the wind speed inputs for on-shore and for off-shore WTs are of seasons average, while the air density is assumed to be un-impacted by air temperature variance. Table (3.5) summarizes the main inputs/outputs of this scenario.

Table (3.5) Scenario B: Meeting Demand Utilizing Energy Hub, inputs/outputs

Inputs	Scenario A inputs
	Hourly wind speed for on-shore WTs, nominal power, number of WTs, and WTs specifications
	Hourly wind speed for off-shore WTs, nominal power, number of WTs, and WTs specifications
	Hourly insolation for PV-solar, air temperature, nominal power, number of PV modules, and module specifications
Outputs	Hourly power generated from energy hub in MWh
	Cost of electricity (COE) in $ per kWh
	Hourly emissions of CO_2, CO, NO_x, and UHCs in kg

3.3.3 Scenario C: Hydrogen as an Energy Carrier

This scenario is proposed to utilize the surplus power from renewable energy sources of WTs and solar in eletcrolyzers for producing hydrogen while meeting the power demand. The surplus power during off-peak periods will be used in electrolyzers to produce hydrogen, which can then be sold to fuel power cell vehicles. The proposed energy hub in this scenario includes NG-fueled CCPP in addition to the renewable energy sources and alkaline electrolyzers. For inputs, this scenario showed the hourly excess electricity and its cost in addition to the inputs that mentioned in scenario B. For outputs, this scenario showed the hydrogen generated hourly and its cost. Table (3.6) summarizes the inputs/outputs of Scenario C.

Table (3.6): Scenario C: Hydrogen as an energy carrier, inputs/outputs.

Inputs	Scenario B inputs
	Electrolyzer's design parameters, such as power constant, operating pressure, etc.
	Hourly surplus power in MWh from WTs and Solar after meeting the demand.
	Hourly renewable energy cost (COE) to feed the electrolyzers in $ per kWh.
Outputs	Hourly H_2 generated in kg per hour.
	Hourly cost of H_2 in $ per kg.
	Hourly power produced in MWh.
	Hourly Cost of electricity (COE) in $ per kWh.
	Hourly emissions of CO_2, CO, NO_x, and UHCs in kg

3.4 Results and Discussions

The following sub-sections are specified for assessing the performance of the three scenarios abovementioned based on the generating electricity for meeting demand, cost of electricity (COE), NG-emissions levels, and using hydrogen as an energy carrier.

3.4.1   Scenario A: Results and Discussions

The NG-fueled CCPP is the only energy source used to generate the required power for meeting the demand, a maximum power of 3150 MW in year of 2009 is used to size the proposed CCPP. Based on the low heating value (LHV) of NG, the CCPP's efficiency is considered to be around 60%. The proposed power demand profile is presented in Figure (3.3) and based on this simulated profile, the CCPP units were at low-capacity for 1456 hour (i.e. about 17%); whereas the operating time at medium/high capacity was about 83% during the year.
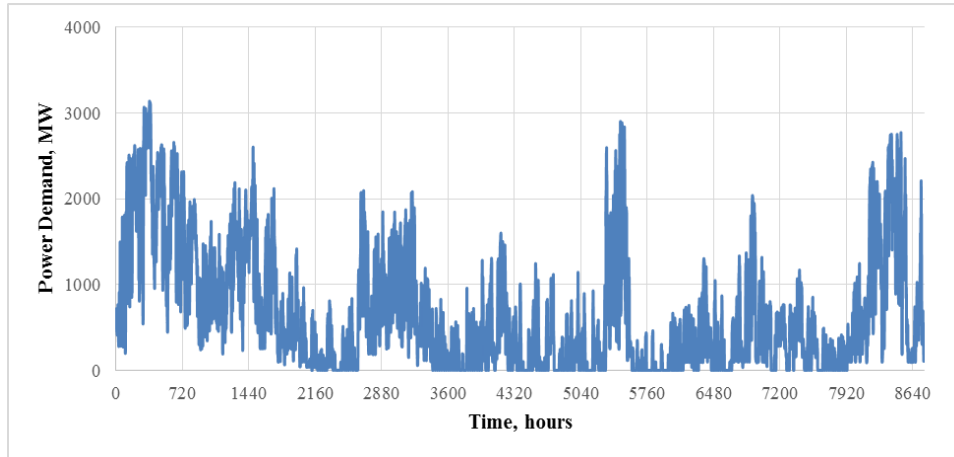
Figure (3.3): Hourly power supply by the CCPP unit through Scenario A

The average cost of electricity produced by the NG-fueled CCPP is basically a function of the capital costs, O&M costs, and NG price. Maximum of 8 CCPP units were utilized at a time, while the average COE produced while meeting the demand is about \$0.074 per kWh as shown in Figure (3.4) for different months of the year. It is noticed that as the rate of generating electricity growing up, the COE is going down.
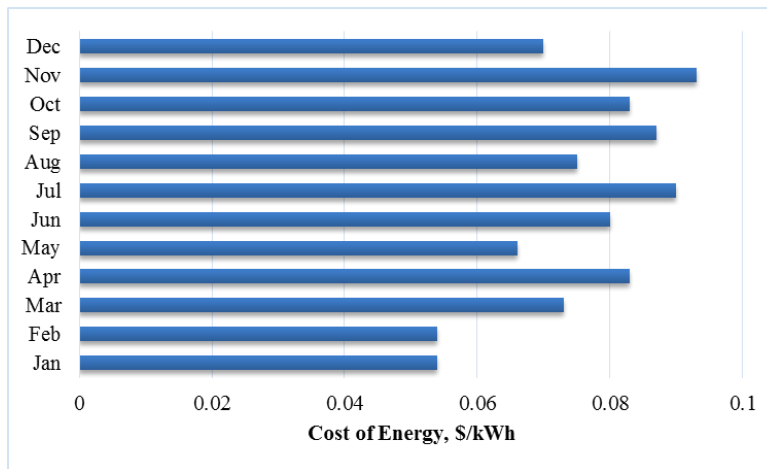
Figure (3.4): The average monthly COE for Scenario A.

As this scenario proposed to utilize the conventional CCPP as the only energy source for meeting the demand, it is expected to have the highest levels of emissions during the operating hours. The emission rates of CO_2, NO_x, CO, and UHCs reached the maximum levels during on-peak periods and felt down to the minimum levels during off-peaks ones. Table (3.7) presents the emission rate of every pollutant measured based on the operating conditions of CCPP.

Table (3.7): Scenario A emissions rates

Air pollutants gases	Emission rate, kg per kWh
CO_2	0.317
NOx	0.015
CO	0.004
UHCs	0.002

3.4.2   Scenario B: Results and Discussions

Energy hub system is used in this scenario to generate the required power for meeting the demand, the NG-fueled CCPP, on-shore and off-shore WTs and PV-solar cells were all utilized to fill the gap between the power demand and its dis-patchable supply.

As the power demand profile is kept same as well as the desired CCPP's capacity and efficiency in this scenario, about 97% of the proposed demand is met by CCPP units. The rest of the demand which is only 3% are met by:

- A 30 MW capacity of on-shore WTs by using 20 turbines,
- A 46 MW capacity of off-shore WRs by using a 20 turbines, and
- A 20 MW capacity of PV-solar by using 50,000 modules that occupied around 108,100 m^2 of land.

Figure (3.5) presents the contribution of each energy source into the required power demand as an average operating hours during the year. For the renewable energy sources, the contribution of on-shore WTs was 0.9%, the contribution of off-shore WTs was the highest of about 1.6%, while the contribution of solar (mainly during summer time) was the lowest at about 0.4%. In this scenario, the surplus power of renewable energy sources during off-peak periods was uncontrolled i.e. as it is assumed to be curtailed.
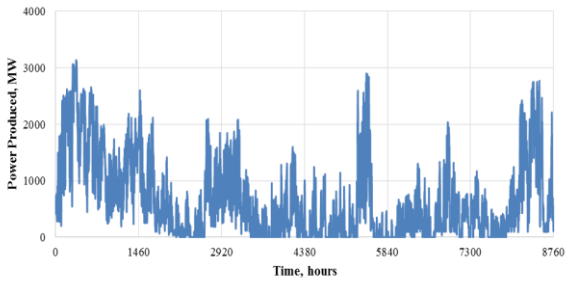
(a) CCPP units profile
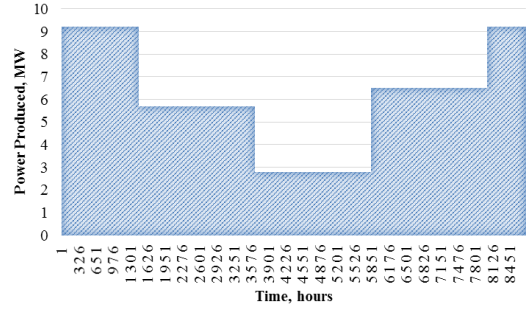
(b) On-shore WTs profile
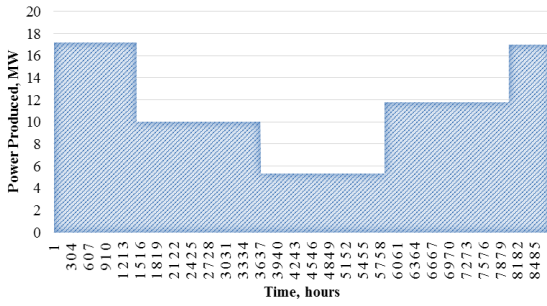
(c) Off-shore WTs profile
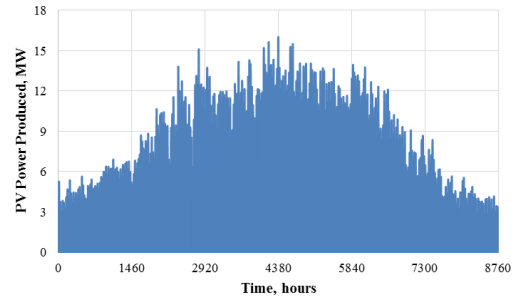
(d) PV solar farm profile
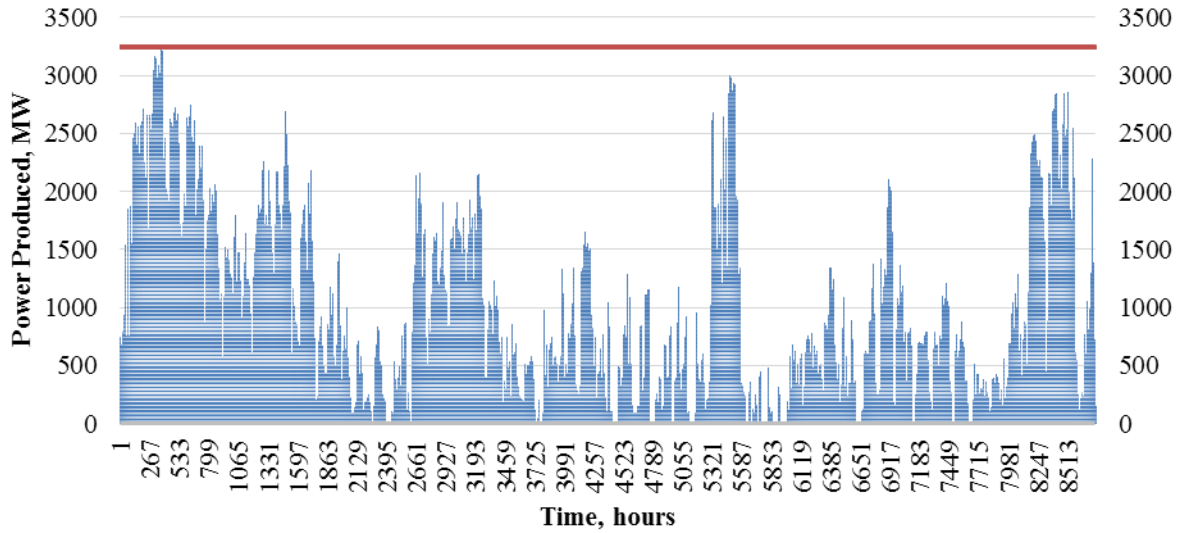
(e) Energy hub profile

Figure (3.5): Power generated utilizing Scenario B: (a) CCPP, (b) On-shore WTs (c) Off-shore WTs (d) PV solar farm, and (e) Energy hub.

The COE for each power generation technology is calculated in this scenario, the average of solar's COE is the highest at about 18 ¢ per kWh followed by the off-shore's COE at about 15.8 ¢ per kWh, followed by the COE of on-shore at 10.2 ¢ per kWh. The COE of CCPP has the least value at an average of 7.5 ¢ per kWh. Although CCPP's share in generating the required power within the energy hub is the main at around 97%, incorporating the renewable energy technologies has increased the COE from the energy hub into 9.2 ¢ per kWh, i.e. by about 23%. On the other hand, utilizing the renewable energy sources resulted in an emission abatement at about 3% when compared to the emissions in Scenario A.

3.4.3 Scenario C: Hydrogen as an Energy Carrier

The integration of the alkaline electrolyzers is what characterized this scenario when compared to scenario B, they were utilized in producing hydrogen when needed. The eletcrolyzers operation is restricted to employ the excess power from WTs and solar cells whenever they are available during the off-peak periods to generate hydrogen. It is counted that about 490 electrolyzers were available for use at a time to employ power at a range of 12 – 42 MW per hour from available renewable sources as seen from the profile of the renewable electricity generated in Figure (3.6).

| (a) Wind Turbines Profile during operation | (b) PV Solar profile during operation |
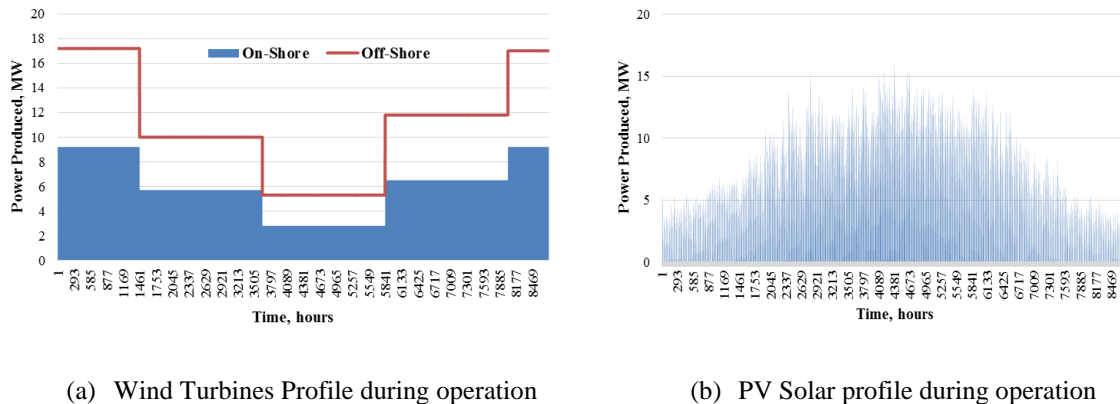
Figure (3.6): The renewable electricity consumed by electrolyzers in Scenario C.

The on-shore wind turbines operate for 1,795 hour per year with a capacity factor of 20.5%; whereas the off-shore ones operate for 2,099 hour per year with a capacity factor of 24%. The solar farm operated for 3,837 hour per year with a 13.7% of its maximum design capacity.

The average production capacity of the electrolyzers at operation is about 400 kg of hydrogen per hour with an efficiency of 68%. The monthly hydrogen generated from the electrolyzers units is shown in Figure (3.7).
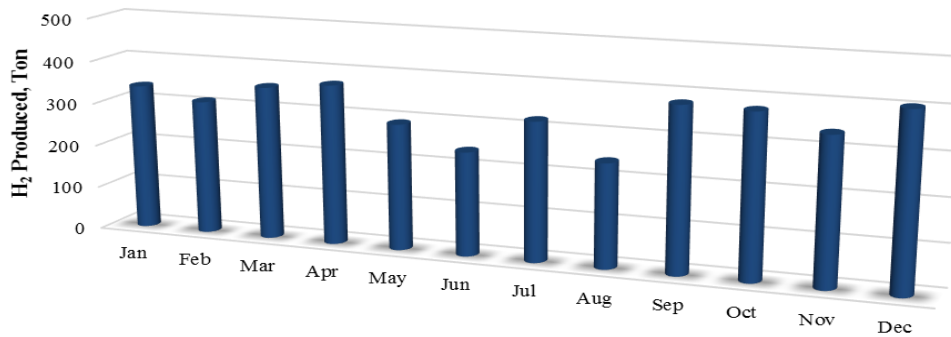
Figure (3.7): The monthly hydrogen production.

The average estimated cost of producing hydrogen was about 17 $ per kg, this relative high cost is due to the COE's high value of renewables that used in electrolyzers for producing hydrogen. Average seasonally produced hydrogen as well its production cost are presented in Table (3.8), more off-peaks periods during winter resulted in producing more hydrogen and therefore its cost is dropped, while the summer with less off-peaks periods resulted in less hydrogen produced and therefore its cost went high.

Table (3.8): Average hydrogen production and its cost during different seasons

Seasons	Average H_2 production, kg	Average H_2 production cost, $ per kg
Winter	1,054,000	11.1
Spring	1,018,400	15.8
Summer	803,360	26.9
Autumn	1,098,300	14.8
Annual	*3,974,000*	17.1

As expected, Cost of Electricity (COE) increased with incorporating renewable energy sources of wind and solar as seen from scenario A versus scenario B, and other hand the reduction in emissions is achieved when the shares of wind and solar increased in meeting power demand. Due to the amount of hydrogen that produced in scenario C, therefore this scenario looks the most feasible one from the economic perspective when selling hydrogen to the market is considered.

3.5 The Conclusions

Simulation-mathematical model is developed in GAMS based on materials/energy balance, thermodynamic and techno-economic relations to investigate the feasibility of integration the renewable energy resources into NG-fueled energy hub in terms of costs and emissions.

Utilizing NG-fueled CCPP alone in meeting power demand has the lowest cost but the highest emissions, while integrating wind and solar has increased the cost of electricity by about 23% and decreased the emissions by about 3%. Among the renewable energy sources, COE of solar power generated has the highest value of 18¢ per kWh followed by off-shore's COE value of 15.8 ¢ per kWh, and followed by on-shore's COE value of 10.2 ¢ per kWh due to the main cost components that included in the model such as capital costs, O&M costs, etc.

The feasibility of utilizing the surplus power of wind and solar during off-peak periods is investigated and approved, alkaline electrolyzers used this power for producing hydrogen that can be sold as a storable, clean and viable energy to the market.

Fast-paced developments of the wind and solar are critical for minimizing their cost and maximizing their performance to increase their integration into existing power grids. Based on the current results, improving the hydrogen-fueled technologies offers clean power and more of grid flexibility due to the use of curtailed electricity.

Chapter Four

4. Integration of renewable energy sources into combined cycle power plants through electrolysis generated hydrogen in a new designed energy hub

4.1 Introduction

The current energy infrastructures built 30-40 years ago, will have difficulty meeting the growing energy demand while considering emission issues for the future. In Ontario-Canada, many electricity generation facilities are approaching the end of their lifetime. In addition, electricity demand is rapidly growing, therefore, new and clean energy generation capacity has to be built or replaced. Replacing old power plants, continuing to meet the electrical demand while considering climate change issues are critical challenges. Green House Gases (GHGs) and criteria air emissions of Nitrogen Oxides (NO_x), Sulphur Oxides (SO_x) and Particulate Matters (PM_x) from fossil-fuelled power generation are the constraints in any future energy plans. Furthermore, the intermittent and the non-dis-patchable nature of renewable sources such as wind and photovoltaic solar will raise the question of how to integrate these sources into the current energy network. The intermittent nature of wind and solar needs to be balanced when connected to the grid for stability purposes, therefore electricity storage is required. In Germany, e.g., the estimated residual power is about 60 GW (Gotz, et al., 2016); whereas the shortage in suitable capacity to store the surplus-energy from renewable sources for long time represents one of the main challenges (Bucher, et al., 2015). All of these challenges motivate the researchers to adopt new ideas for the future of energy or the energy for the future. The power-to-gas technology is one of the favorable options since it enables both temporal and spatial solutions for aforementioned challenges at a time with respect to power supply and required storage (Jentsch, et al., 2014). Utilizing power-to-gas in a competitive way can be employed in five different pathways including: power-to-gas-to-electricity, power-to-gas-to-NG pipeline, power-to-gas-to-industrial hydrogen, power-to-gas-to-methanation process, and power-to-gas-to-mobile fuel (Walker, et al., 2016) which adds more flexibility to the operating power-system.

An energy hub is a simulated framework representing 'power-to-gas' concept where multiple energy sources can be converted, conditioned, and stored in a synergistic fashion. It provide an interface between different energy infrastructures and/or loads (Geidl, et al., 2007), (Bakken & Holen, 2004). Modelling energy hub from techno-economic perspective will help to understand the feasibility of adopting 'power-to-gas' technologies when connected to the grid. In addition to renewable sources of wind and solar, the conventional energy sources such as natural gas (NG) as well as energy carriers such as electricity and hydrogen are considered in the network of energy hub model; whereas their costs and emissions are to be optimized. The main advantage of modelling the energy hub in the current study is to improve the incorporation of the combined cycle power plants (CCPPs) as a dis-patchable energy source with renewable energy sources (REs) as zero-emissions sources. The rationale of adopting energy hub is to reliably meet electricity demand, to maintain affordable cost, and to achieve optimum efficiency while minimizing emissions. This study explores the possibility of utilization CCPP as base-load linking with wind turbines (WTs) and photovoltaic solar panels (PVs). The CCPP is a competitive power plant as a result of the rapid development and the wide availability of low-cost NG in North America. CCPPs respond to changes in outside conditions as well as their short start-up time and high-loading gradients which make them favoured in meeting power demand (Kehlhofer, et al., 2009). Hydrogen is utilized in the current energy hub as the energy carrier. Producing hydrogen using water electrolysis is currently one of the most promising methods. Electrolysis technologies have been successfully integrated into renewable- and hydrogen-energy-based systems (Harrison & Miller, 2012). In particular, highly effective alkaline electrolysis systems generally have larger hydrogen production capacities were integrated successfully with CCPPs using RE sources (Saur & Ramsden, 2011). Hydrogen as an energy vector within the hub was studied by Hajimiragha et al. (Hajimiragha, et al., 2007); it is shown that due to storage capability of this energy vector, more flexibility on energy conversion inside the hub is provided, which brings more freedom in system planning and operation. Electrical energy obtained from REs can be converted to hydrogen using electrolyzers which, in turn, can be converted back to electrical energy by mixing hydrogen with NG as feed stock for fuelling CCPP to reduce emissions. Hydrogen assists in the complete combustion of methane, decreasing unburned hydrocarbons and carbon monoxide emissions; whereas hydrogen-enriched natural gas (HENG) fuel represents the potential option to minimize GHG emissions (Melaina, et al., 2013), (TerMaath, et al., 2006) and (Atlantic Hydrogen, 2009).

Sharif et al. (Sharif, et al., 2014) present a deterministic simulation model for an energy hub consisting of NG turbines as the main source of energy in addition to the two RE sources of WTs and PVs. It has been found that CCPP and REs would offer energy production that not only meets the demand but also reduces emissions. Nevertheless, the high electricity costs continue to remain an obstacle in adopting the energy hub concept in today's economy.

The Ontario Power Authority (OPA) projects that 15,700 MW of future electricity demand will have to be met either by new REs or by adding CCPPs. This is due to an expected increase in peak demand in Ontario, and the fact that 80% of the current power generation will have to be replaced or refurbished over the next 20 years (Ministry of Energy, 2013). HENG-fuelled CCPP represents such a creative and successful solution to enhance the performance of the CCPPs and to reduce their GHG emissions to minimum levels. The HENG fuel has the potential for reducing NO_x emissions without the limitations found in other NO_x control methods (Melaina, et al., 2013). Integrating sustainable, zero-emissions and non-dis-patchable resources such as WTs and PVs into the grid through producing hydrogen represents the main advantage for health and the environment (Goldstein & MacDougall, 2012). This method offers cleaner, more flexible and secure energy supply while utilizing local energy resources of NG, wind, and solar. The importance of this research is to exhibit the possibilities for different energy sources to operate in a synergistic manner in order to meet the market electricity demand at reasonable prices while minimizing hub fossil impacts on the environment.

The proposed energy hub consists of CCPPs, WTs and PVs as the energy sources. CCPPs are set up to meet the power demand while REs are designed to meet electrolyzer's power demand as shown in Figure (4.1). Renewable-produced hydrogen by alkaline electrolyzers (AELs) is injected directly into NG pipelines. Utilizing REs for supplying power to the AELs will stabilize the cost while maintaining hydrogen availability. The current study is targeted to meet a proposed load profile (CHFCA, 2008).
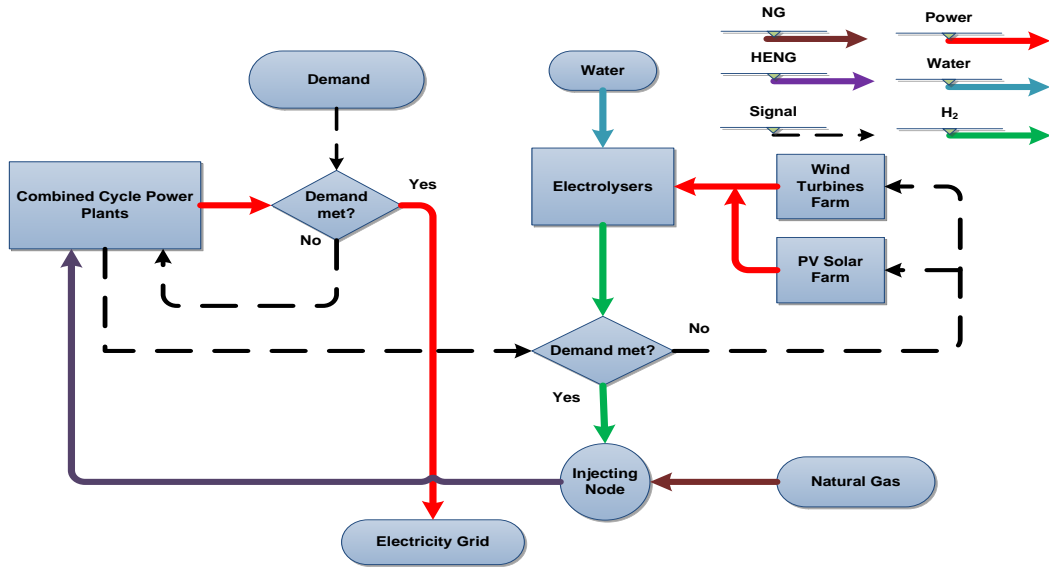
Figure (4.1): Block diagram of the modeled energy hub

4.2 Developing Simulation Model

The energy hub cost model is developed in the current study by using General Algebraic Modeling System (GAMS) as a Mixed Complementarity Problem (MCP) and solved by the CPLEX solver. The objective function is to maximize revenue from selling electricity and from emissions credits; whereas hydrogen concentration in CCPP fuel (range from 0.0 to 5.0% vol.) is to be tested for maximum revenues. Meeting power demand and the limits of the hydrogen concentration in CCPP fuel are the most effective constraints for the model. Hourly inputs such as load profile, wind speed, air temperature, solar insolation, and other inputs in a whole full year are fed into the energy hub model rather than average monthly or seasonal data in order to get more accurate and reliable results. The current energy hub model is built based on laws of thermodynamics, economics, and power plant process designs. The proposed energy hub consists of: a fixed number of CCPPs each has capacity of 555 MW; on-shore wind turbines each has capacity of 1.8 MW; off-shore wind turbines each has capacity of 3.0 MW; PV-solar modules each has capacity of 0.191 kW; and alkaline electrolyzers with a production normal capacity of 60 m^3 per hour (power constant of 5.2 kWh per m^3). The main costs including capital costs, operating & maintenance (O&M) costs, the fuel cost, and other technical and services costs for the CCPP and the RE sources are considered

and discussed in the following sections. The CCPP configuration is evaluated and presented in this section. The design of the CCPP is based on a market-ready technology that is commercially available. The plant consists of two advanced F-class Combustion Turbine Generators (CTGs), two Heat Recovery Steam Generators (HRSGs) and one Steam Turbine Generator (STG). In Figure (4.2), the block flow diagram of CCPP with process data for the streams is given (Black, 2013).

Point	Flowrate, kg h^{-3}	Temp. ^{0}C	Press. MPa	Enthalpy kJ (kg K)$^{-1}$	Density kg m^{-3}
1	3,154,735	15	0.1	3023	1.2
2	75,901	38	3.1	463	22.2
3	3,230,636	629	0.11	835.81	0.4
4	3,230,636	106	0.1	248.81	0.9
5	388,927	566	16.65	3,472.36	47.7
6	514,240	38	0.01	160.61	992.9
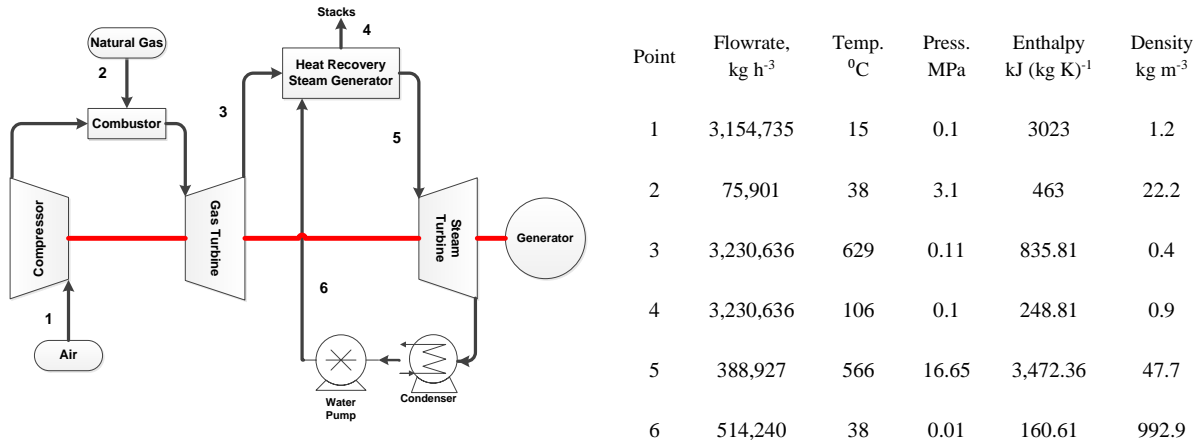
Figure (4.2): CCPP power plant configuration

The considered power plant has two NO_x reduction technologies; the first is the Dry Low NO_x (DLN) burner, and the second is the Selective Catalytic Reduction (SCR) system. An existing CCPP design with the characteristics shown in Table (4.1) (Black, 2013) is used in the model.

Table (4.1): CCPP's specifications and performance summary

NG Turbine	Nominal Power, P_{GT}	184,400 kW	Water Pump	Nominal power, P_{PUMP}	5,400 kW
	NG mass flow rate	75,969 kg h^{-1}		Isentropic Pump Efficiency, η_{Isen}	90%
HRSG	Heat Recovered, Q_{HRSG}	174,578 kW	Condenser	Cooling Duty	1,139*10^6 kJ h^{-1}
				Surface Area, S	1,388 m^2
Steam Turbine	Nominal Power, P_{ST}	213,000 kW	Air Compressor	Pressure in P_{In}	1.013 bar
	Section Area, A	4,577 m^2		Pressure out P_{Out}	8.634 bar
				Air flow rate, $Flow_{Air}$	877 kg s^{-1}
Emissions					
CO$_2$	365 kg per MWh	NO$_x$	0.027 kg per MWh	SO$_2$ & PM$_x$	Negligible

The cost of electricity (COE) produced by CCPP in $ per kWh is calculated using Eqn. (4.1).

$$COE_{CCPP} = \left[C_{Fuel} + \frac{C_{Capital} + C_{O\&M}}{n} \right] / AEP_{CCPP} \qquad \text{Eqn. (4.1)}$$

Where: C_{Fuel} is the fuel's cost, $C_{Capital}$ is the capital cost, $C_{O\&M}$ is the operating and maintenance costs, AEP_{CCPP} is the annual electricity produced in kWh, and n is the number of units. The capital costs of the main equipment and auxiliaries are calculated based on the cost relationship used by Attala et al. (Attala, et al., 2001) as shown in Eqns. (4.2) and (4.3).

$$C_{Capital} = C_{Equipment} * A_f \qquad \text{Eqn. (4.2)}$$

$$C_{Equipment} = C_{GT} + C_{ST} + C_{HRSG} + C_{COND} + C_{PUMPS} + C_{GEN} + C_{COMP} \qquad \text{Eqn. (4.3)}$$

Where: C_{GT} is the gas turbine's cost, C_{ST} is the steam turbine's cost, C_{HRSG} is the cost of the heat recovery of steam generator, C_{COND} is the condenser's cost, C_{PUMPS} is the pumps cost, C_{GEN} is the generator's cost, and C_{COMP} is the compressor's cost. The amortization factor A_f is calculated in Eqn. (4.4).

$$A_f = D_r * \frac{(1 + D_r)^n}{(1 + D_r)^{n-1}}$$

<div align="right">Eqn. (4.4)</div>

Where: D_r is the discount rate, and n is the number of years; the other cost factors of equipment that appeared in Eqn. (4.3) are calculated in the following equations (4.5 – 4.11) (Attala, et al., 2001):

$$C_{GT} = 3832 * P_{GT}^{0.71}$$

<div align="right">Eqn. (4.5)</div>

Where: P_{GT} is the nominal power of gas turbine; the cost of steam turbine is calculated by using Eqn. (4.6).

$$C_{ST} = 3,197,280 * A^{0.261} + 823.7 * P_{ST}^{1.543}$$

<div align="right">Eqn. (4.6)</div>

Where: A is the heated surface area of the steam turbine, P_{ST} is the nominal power of steam turbine. The cost of HRSG is calculated based on Eqn. (4.7).

$$C_{HRSG} = 17,000 * Q_{HRSG}^{0.6}$$

<div align="right">Eqn. (4.7)</div>

Where: Q_{HRSG} is the heat recovered by HRSG; the cost of condenser is calculated based on Eqn. (4.8) as follow:

$$C_{COND} = 162 * A_{Surface}^{1.01}$$

<div align="right">Eqn. (4.8)</div>

Where: $A_{Surface}$ is the condenser's surface area; the pump's cost is calculated based on Eqn. (4.9).

$$C_{PUMPS} = 37.6 * P_{PUMP}^{0.8} * \left[1 + \left(\frac{1 - 0.7}{1 - \eta_{Isen}}\right)^{-0.46}\right] * 34.4$$

<div align="right">Eqn. (4.9)</div>

Where: P_{PUMP} is the nominal power of the pump, and η_{Isen} is the isentropic efficiency of the pump. The cost of gas and steam generators is calculated in Eqn. (4.10) based on Kotowicz et al (Kotowicz & Bartela, 2010):

$$C_{GEN} = 3082 * (P_{GT} + P_{ST})^{0.58}$$

<div align="right">Eqn. (4.10)</div>

Where: P_{GT} and P_{ST} are the nominal powers of gas turbine and steam turbine respectively. The cost of air compressor is calculated in Eqn. (4.11) as previously determined by Siemiatycze et al (Sieniutycz & Jezowski, 2013) :

$$C_{COMP} = \left[\frac{F_{Air} * M_{Air}}{0.9 - \eta_{AC}}\right] * \frac{P_{Out}}{P_{In}} * Ln(\frac{P_{Out}}{P_{In}})$$ Eqn. (4.11)

Where: F_{Air} is air fraction, M_{Air} is the air's molecular weight, η_{AC} is the air compressor efficiency, P_{In}, and P_{Out} are the inlet and outlet pressures respectively. The NG fuel cost in $ is calculated in Eqn. (4.12) based on Cetin et al (Cetin, et al., 2008).

$$C_{Fuel} = 3,600 * 8,760 * Price_{NG} * P_{CCPP} * Load_{factor}/(HHV_{NG} * \eta_{CCPP})$$ Eqn. (4.12)

Where: HHV_{NG} is the high heating value of the natural gas, η_{CCPP} is the CCPP's efficiency. The thermal efficiency η_{CCPP} that appears in Eqn. (4.12), is calculated in Eqn. (4.13) as follow:

$$\eta_{CCPP} = \frac{P_{CCPP}}{Q_{NG}}$$ Eqn. (4.13)

The fuel thermal energy Q_{NG} that appears in Eqn. (4.13) for natural gas is calculated in Eqn. (4.14) as follows:

$$Q_{NG} = M_{NG} * HHV_{NG}$$ Eqn. (4.14)

Where: M_{NG} is the natural gas molecular weight; the O&M cost $C_{O\&M}$ that appeared in Eqn. (4.1) is calculated in Eqn. (4.15) based on Black, J. (Black, 2013):

$$C_{O\&M} = 0.00132 * AEP_{CCPP}$$ Eqn. (4.15)

The Annual Energy Produced (AEP) by CCPP in kWh AEP_{CCPP} that appeared in Eqn. (4.1) is calculated in Eqn. (4.16):

$$AEP_{CCPP} = \sum_{i=1}^{8,760} (P_{CCPP} * Load_{factor})$$ Eqn. (4.16)

The On-shore WTs that designed by Vestas (Vestas, 2008) as well as the off-shore WTs (Vestas, 2004) are considered in the model; all specifications are summarized in Table (4.2).

Table (4.2): Wind turbines specifications

Specifications	On-shore WTs	Off-shore WTs
WT Nominal Power, N_P	1,800 kW	3,000 kW
Hub height, H_h	80 m	90 m
Rotor Diameter, R_D	80 m	90 m
Area swept, A_{Rotor}	5,027 m²	6,362 m²

The cost of electricity (COE) generated by wind turbines in $ per kWh is calculated in Eqn. (4.17) as follows:

$$COE_{WT} = (Cost_{Capital} + Cost_{O\&M} + LRC + LLC)/AEP_{WT} \qquad \text{Eqn. (4.17)}$$

Where: **LRC** represents the levelized replacement cost, and **LLC** is land lease cost; the capital cost of WTs as a sum of the individual costs of parts and services accompanied with the installation stages are calculated in Eqn. (4.18).

$$Cost_{Capital} = \sum_l C_l + \sum_m C_m \qquad \text{Eqn. (4.18)}$$

Index 'l' represents the main parts of WTs such as blades, hub, gear box, tower, yaw, etc.; whereas index 'm' represents the services accompanied such as connections, transportation, civil work, and engineering. The capital cost relationships are adopted based on Fingersh et al (Fingersh, et al., 2006). Further capital costs are considered for off-shore WTs such as support and structure cost, turbine installation cost, and other costs (Fingersh, et al., 2006). The O&M costs as a function of WTs power produced **AEP$_{WT}$** are considered in Eqn. (4.17); it is 0.008 $ per kWh for on-shore WT and it is 0.02 $ per kWh for off-shore WTs (Fingersh, et al., 2006).

$$Cost_{O\&M} = f_{O\&M} * AEP_{WT} \qquad \text{Eqn. (4.19)}$$

Where: **f$_{O\&M}$** is the operating & maintenance factor. The annual energy produced **AEP$_{WT}$** in kWh that appeared in Eqn. (4.17) is calculated in Eqn. (4.20):

$$AEP_{WT} = \sum_{i=1}^{8,760} Power_i \qquad \text{Eqn. (4.20)}$$

The hourly power produced by WTs in Watts is calculated using Eqn. (4.21) as follows:

$$Power_i = \frac{1}{2} * \rho_{Air} * V_i^3 * A_{Rotor}$$

Eqn. (4.21)

Where: A_{Rotor} is the rotor area; whereas the air density ρ_{Air} is modified at different elevated WT's rotor heights and is calculated in Eqn. (4.22):

$$\rho_i = (\frac{\rho_{Air}}{R * T_i})^{\frac{-g*h}{R*T_i}}$$

Eqn. (4.22)

Where: ρ_i and T_i are the air density and air temperature at any hour respectively; h is the height and R is the gas constant. According to Vestas WTs specifications, the wind speed range of $3 - 25$ meter per second is required for best achievement. The on-shore Levelized Replacement Cost LRC is calculated in Eqn. (4.23) based on Fingersh et al (Fingersh, et al., 2006):

$$LRC = 10.7 * N_P * N_T$$

Eqn. (4.23)

Where: N_P is wind turbine nominal power, N_T is the number of wind turbines. For the off-shore wind turbines, the LRC is calculated in Eqn. (4.24) based on Musial et al (Musial & Ram, 2010).

$$LRC = 17 * N_P * N_T$$

Eqn. (4.24)

The Land Lease Cost LLC is principally based upon the land used by the WTs. The factors applied in different wind farms developments vary widely depending on the wind class of the particular site, the nature and value of the land, and the potential market price (Fingersh, et al., 2006). The LLC for on-shore wind turbines is calculated using Eqn. (4.25); and for off-shore ones, the LLC is calculated as in Eqn. (4.26):

$$LLC = 0.0012 * AEP_{WT}$$

Eqn. (4.25)

$$LLC = 0.0008 * AEP_{WT}$$

Eqn. (4.26)

The CS6P-256mm PV-Solar module is selected to represent the base unit of solar energy model from Canadian Solar (CanadianSolar, 2013). Table (4.3) presents the module's specifications and its operating conditions.

Table (4.3): PV-solar specifications and operating conditions

Specifications		Operating Conditions	
Nominal power, N_p	0.191 kW	Nominal operating temperature, T_{nom}	45 ^{0}C
Life span of PV cells, LS_m	25 years	Ambient air temperature, T_o	20 ^{0}C
Module efficiency, E_i^{ff}	17%	Operating temperature, $T_i^{operating}$	(- 40) - 85 ^{0}C
Module's area, A_{module}	0.02434 m^2		

The cost of electricity (COE) in $ per kWh is calculated using Eqn. (4.27):

$$\text{COE}_{\text{PV}} = \text{Cost}_{\text{total}}/\text{AEP}_{\text{PV}}$$ Eqn. (4.27)

The total PV costs as a sum of capital, O&M and labor are calculated in Eqn. (4.28) as follows:

$$\text{Cost}_{\text{total}} = \text{Cost}_{\text{Capital}} + \text{Cost}_{\text{O\&M}} + \text{C}_{\text{Labor}}$$ Eqn. (4.28)

The capital cost as a function of equipment cost and land cost is calculated using Eqn. (4.29):

$$\text{Cost}_{\text{Capital}} = \text{C}_{\text{Equipment}} + \text{C}_{\text{Land}}$$ Eqn. (4.29)

Based on Buzz Solar (Buzz Solar, 2012), the cost of equipment **C**Equipment is $0.215 per kWh; for labor cost, each MW of newly installed PV-solar requires 44 jobs (Mitchell, 2010). Median of Canadian employed income by 2006 was $41,400 per year (CanadaStatistics, 2011). As a result, the cost of labor as part of installation cost will be $1822 per kWh per year. The cost of land **C**Land is calculated based on proportional land market prices as $ per kWh per year (Gwartney, 2015). The O&M cost is calculated as a factor of $0.01 per kWh as per Bing, J. M. (Bing, 2007). The annual PV-solar power produced **AEP**PV in kWh is calculated in Eqn. (4.30).

$$\text{AEP}_{\text{PV}} = \sum_{i=1}^{8,760} \text{Power}_i$$ Eqn. (4.30)

The hourly power produced from PV-solar is calculated in Eqn. (4.31) based on (Earth Observation System, 2012):

$$\text{Power}_i = \text{G}_i * \text{E}_i^{ff} * \text{A}_{\text{module}}$$ Eqn. (4.31)

Where: G_i is the hourly insolation, E^{ff} is the hourly efficiency, and A_{module} is the module's area. For the eletcrolyzers, the model HySTAT-60 from Hydrogenics (Hydrogenics, 2011) is considered in calculating the costs of the electrolysis process. Hydrogen production cost in $ per kg is calculated in Eqn. (4.32):

$$Cost_{Hydrogen} = (Cost_{Capital}^{AEL} + Cost_{O\&M}^{AEL} + Cost_{Consumed}^{Power} + Cost_{Consumed}^{Water})/Hydrogen_{Produced} \qquad \text{Eqn. (4.32)}$$

The capital cost of the AEL is calculated in Eqn. (4.33) based on (Zoulias & Lymberopoulos, 2007) and (Li, et al., 2009).

$$Cost_{Capital}^{AEL} = 250,000 * (AEL_{Capacity} * \rho_{Hydrogen})^{0.6} \qquad \text{Eqn. (4.33)}$$

Where: $\rho_{Hydrogen}$ is the hydrogen's density; the AEL's production capacity is 60 Nm^3 per hour (Hydrogenics, 2011). The power consumed by each AEL is calculated by multiplying power consumption (5.2 kWh per m^3) by the capacity at operating conditions; whereas the hydrogen produced in kg per hour is calculated in Eqn. (4.34).

$$Hydrogen_{Produced} = AEL_{Capacity} * \left[\frac{P_{oper} * MW_{Hydrogen}}{R * T_{oper}}\right] \qquad \text{Eqn. (4.34)}$$

Where: $MW_{Hydrogen}$ is the hydrogen's molecular weight, P_{oper} and T_{oper} are the operating pressure and temperature respectively. The cost of renewable power consumed by the electrolyzers has a significant impact on the cost of hydrogen production and is calculated in Eqn. (4.35) as follows:

$$Cost_{Consumed}^{Power} = \frac{(COE_{WT} * AEP_{WT}) + (COE_{PV} * AEP_{PV})}{(AEP_{WT} + AEP_{PV})} \qquad \text{Eqn. (4.35)}$$

The O&M cost of the electrolyzers is considered to represent 2% of the direct installed capital cost as per Saur et al (Saur & Ramsden, 2011); and the cost of water is calculated based on the cost of demineralized water cost ($1.04 per 1,000 kg) as in Eqn. (4.36):

$$Cost_{Consumed}^{Water} = 1.04 * \left(\frac{MW_{Water}}{MW_{Hydrogen}}\right) * Hydrogen_{Produced} \qquad \text{Eqn. (4.36)}$$

Where: MW_{Water} is the water's molecular weight.

4.3 Storing Electrical Energy as Hydrogen in NG Pipeline

Storing electrolytic-renewable produced hydrogen in the NG pipelines network as an innovative idea is adopted in this research which is based on assumptions of the 'Power-to-Gas' projects (Hydrogenics, 2012), (Eichman, 2015), and (California Hydrogen Business Council, 2015). This clean energy solution establishes a bridge between the electricity and NG networks to bring seasonal storage capabilities to electricity networks. It also underscores the importance of pipelines in meeting the objective of increased REs penetration. The technology could be particularly advantageous in markets with large amounts of intermittent RE sources. By converting the electricity to gas and storing it in the vast NG pipelines, more RE's energy can be stored for long periods while increasing the amount of clean energy that is available for consumers. A mathematical model developed by Tabkhi et al (Tabkhi, et al., 2008) based on NG-H_2 blend transport through pipelines and compressors to be compensated for the pressure drops by implying mainly the mass and energy balances on the basic elements of the network. This work deals with the quantitative amount of hydrogen that can be added to the NG network. Their quantitative results show that the addition of hydrogen to NG pipelines significantly decreases the transmitted power; whereas, the maximum fraction of hydrogen that can be added to natural gas is around 6 mass percent.

4.4 The Methodology

A flow diagram of the calculations is presented in Figure (4.3). The hydrogen concentration in CCPP fuel (as a starting point) is to be used to determine the number of REs in operation including WTs and PVs and to determine the required number of electrolyzers for operating to produce hydrogen. The next step is to calculate all the related costs of the energy hub parts including CCPPs, on-shore WTs, off-shore WTs, PVs and AELs considering capital costs, O&M costs, NG fuel cost, and related auxiliaries. Based on the calculation of the energy hub cost model, the unit power cost in $ per kWh will be calculated. This unit will be compared to two scenarios: (1) the retail cost equivalent value for the electricity which is based on smart meter in $ per kWh; (2) the set of wholesale price equivalent value for the electricity. Injecting electrolytic-renewable produced hydrogen into CCPP's fuel will improve emissions. The objective function is to maximize the annual revenues that will be gained from selling power to meet the demand and to maximize the emissions credits that will be achieved. In order to measure the emissions

improvements in terms of monetary value, the Monetary Value of Carbon (MVC) and the Marginal Abatement Cost (MAC) were considered. The MVC measures the full global cost of an incremental unit of carbon emitted, summing the full global cost of the damage it imposes over the whole time in the atmosphere (Thornton, et al., 2007). MAC refers to the sum of the marginal costs, or the area under the MAC curve which is plotting CO_2 prices against a corresponding reduction amount for a specific time and region (Mrris, et al., 2008). Based on the aforementioned studies including Ball et al (Ball & Kennett, 2012), \$13 per ton is considered for CO_2 emission reduction credit and \$55 per ton for NO_x. The CO_2 and NO_x emissions credits will be added to the revenues in the objective function to balance the high cost of using REs in producing hydrogen. Sensitivity analysis is carried out to compare power unit cost before and after adding hydrogen to the CCPP's fuel, and to compare CO_2 and NO_x emissions credits achieved. Sensitivity analysis results will determine the best hydrogen concentration in HENG fuel in terms of optimum annual revenue.
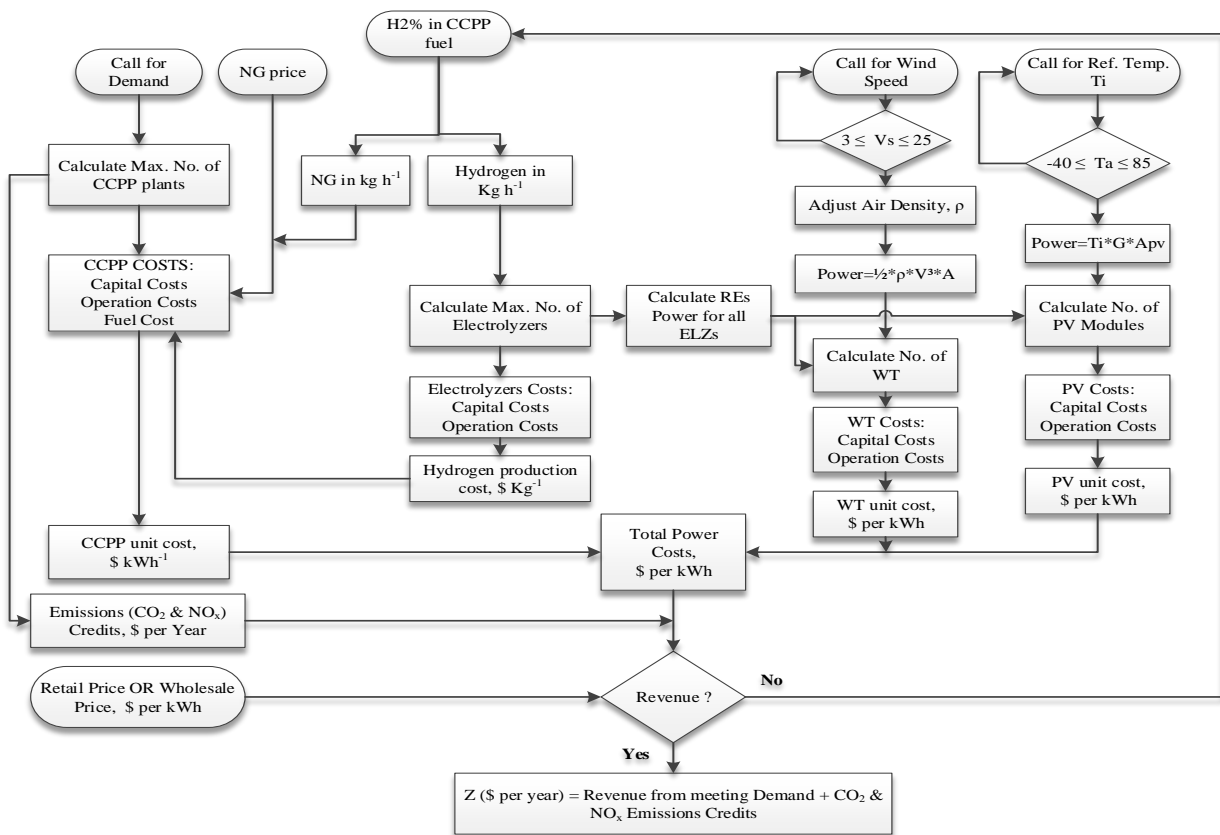
Figure (4.3): Block diagram of the applied methodology for cost's model

4.5 Results and Discussions

In the following sections, two scenarios are discussed: (1) cost model results when meeting proposed load profile (power demand) utilizing NG-fueled CCPPs; and (2) cost model results when meeting same power demand utilizing HENG-fueled CCPPs. In scenario (2) and in order to examine the achieved revenues, two sub-scenarios will be discussed: (A) comparing the power cost calculated to retail price equivalent value; and (B) comparing the power cost calculated to a set of wholesale price equivalent values. The proposed load profile is used to determine the number of CCPPs required to meet the dis-patchable demand as shown in Figure (4.4).
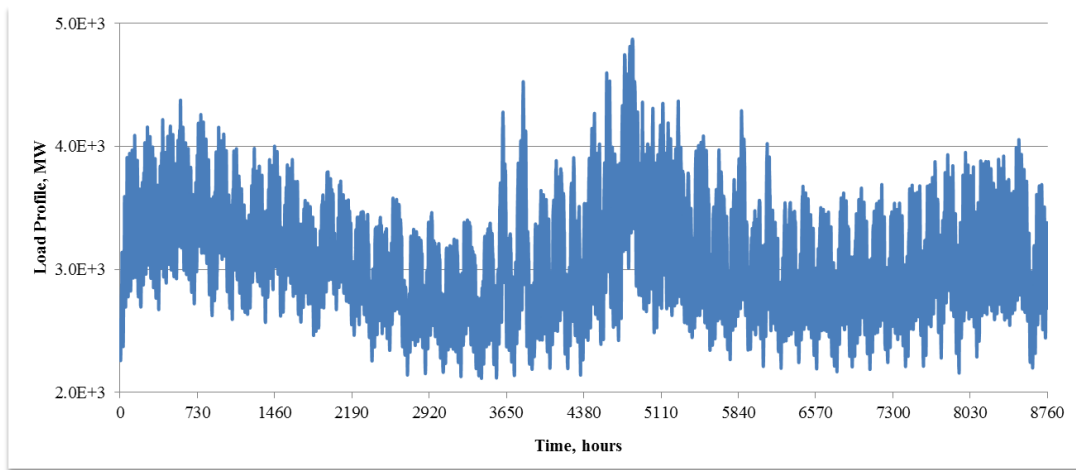
Figure (4.4): Hourly proposed load profile

The expected hourly demand is varied between 2,116 – 4,873 MW, and based on this range the number of CCPP required is 9 power plants to be available for hourly response operation. Emissions in ton per year from the desired CCPPs are calculated based on load factor and operating time. CO_2 has the highest emission level followed by NO_x as seen in Figure (4.5).
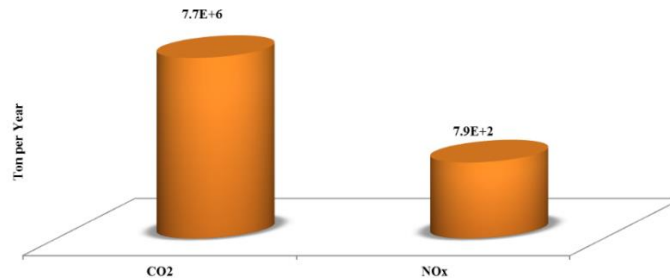
Figure (4.5): Calculated CCPP's annual emissions

71

4.5.1 Scenario (1): Cost Model for NG-fueled CCPP

CCPP's cost model is used to calculate all the required capital cost, O&M cost, NG fuel cost; Eqn. (4.1) is used to calculate the CCPP's unit power cost in $ per kWh. The results are summarized in Table (4.4).

Table (4.4): CCPP power cost model results

CCPP required to meet variable power demand	9 plants
Average hourly power produced, MW	3,162
Average NG fuel used, kg per hour	469,581
Average efficiency, low heating value basis	42.7%
Average fuel cost, $ per hour	9,190.5
Average cost of electricity COE, $ per kWh	0.087
Average load factor	90%

As seen from Table (4.4), the average energy power cost is high when compared to the average unit power cost of base-load sources like nuclear and hydro. In North America, combined cycle power plants are designed for meeting high peak demand. Thus their power cost of about $0.09 per kWh is acceptable when compared to the high peak market price.

4.5.2 Scenario (2): Cost Model for HENG-fueled CCPP

Based on the hydrogen concentration in CCPPs fuel and REs availability (required wind speed and insolation), the number of on-shore, off-shore wind turbines, PVs and AELs in operation are calculated and illustrated in Table (4.5). Hydrogen rate is varied between 2,000 kg per hour at H_2 equal to 1% (low rate) and up to 22,000 kg per hour at H_2 equal to 4% in CCPP's fuel.

Table (4.5): No. of REs and AELs at different %H_2 in CCPP fuel

H_2 Concentration in HENG fuel	No. of RE Sources			No. Of AELs
	On-shore WTs	Off-shore WTs	PV-Modules	
1%	444	274	115,111; (42 acre)	78
2%	887	543	228,577; (83 acre)	156
3%	1330	812	342,043; (124 acre)	234
4%	1773	1085	457,154; (167 acre)	312

The target in this scenario is to calculate the unit power cost in $ per kWh after blending hydrogen with NG to fuel CCPPs. This calculation is performed by adding the hydrogen production costs to the CCPP's unit power cost that calculated previously. The hydrogen production cost is based on the mathematical equations introduced in previous section. In Table (4.6), the aforementioned calculated costs are summarized based on 2% hydrogen as an example of the results. It is found that electrolytic-renewable produced hydrogen costs about $4.1 per kg, which is about $0.13 per kWh of the renewable power supplied to AELs.

Table (4.6): HENG Blend costs for 2% H_2 (sample of results)

Calculated Costs	$ per kWh
On-shore unit power	0.098
Off-shore unit power	0.141
PV-Solar unit	0.370
Average Renewable Power	0.1023
Average Hydrogen Production	0.13

The renewable electricity used in AELs to produce hydrogen costs more than 80% of the total hydrogen production costs in $ per kWh as shown in Table (4.6). There is a significant potential to reduce the costs of renewable power in short term future, and then the cost of electrolytic-renewable produced hydrogen will have more chance to compete other methods for producing hydrogen.

4.5.3   Scenario (2A): Power Cost vs. Retail Price

As discussed above, the power cost from CCPP is high when it is used to meet the base-load of the proposed load profile. In this scenario, the target is to compare power cost to Ontario retail price equivalent value which is based on smart meter readings and at different hydrogen concentrations in CCPP fuel as shown from Figure (4.6). The cost of power produced varies between an average of $0.09 per kWh at H_2 equal to 1% and an average of $0.13 per kWh at H_2 equal to 4%. Power cost is compared to the retail price of 2011 as shown from Figure (4.6). When the hydrogen concentration equal to 1% and 2%, revenue is achieved when the CCPPs are operated for almost the whole year. While when the hydrogen concentration equal to 3%, revenue is achieved after the month of May to the end of the year; whereas at 4% hydrogen barely any revenue is made.
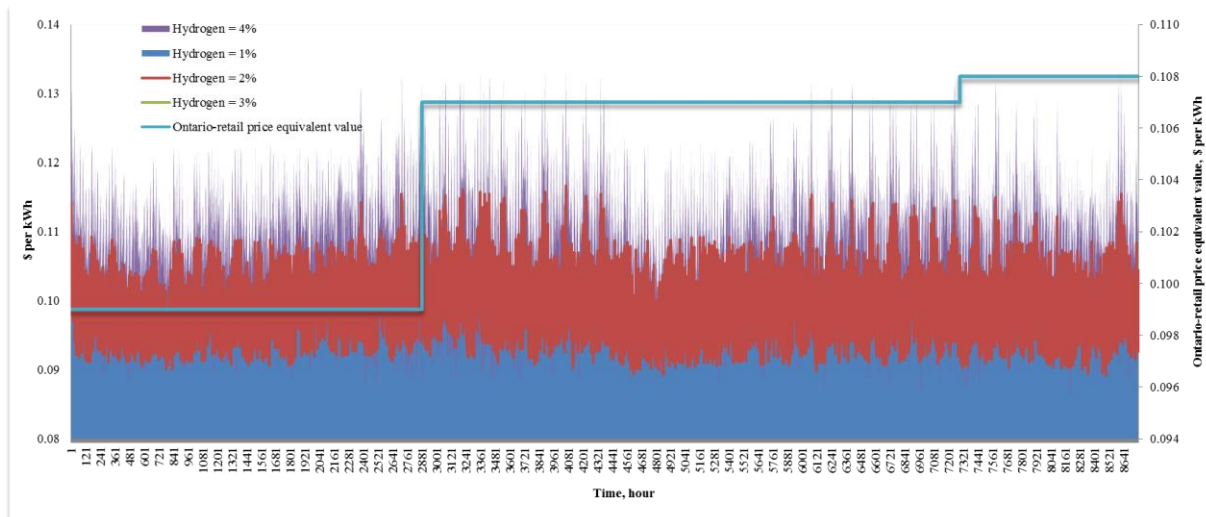
Figure (4.6): Power cost vs. hydrogen concentrations compared to Ontario-retail price

4.5.4   Scenario (2B): Power Cost vs. Set of Wholesale Price

While increasing the amount of hydrogen in CCPP's fuel, the drop in revenue is greater than emissions credits gained as shown from Figure (4.7). It is found that revenue made from selling electricity to meet the demand is the most effective part of the objective function. In general, losing

profitability when adding hydrogen into CCPP's fuel is expected and can be adjusted by examining different weights for the emissions credits in the objective function. The curve of the annual revenue is intersecting with the CO_2 & NO_x emissions credit curve at hydrogen concentration of 3.7%, it means that the objective function is derived by two paths: exponential drop in revenue up to H_2 equal to 3.7% followed by slow linear incremental emissions credits.
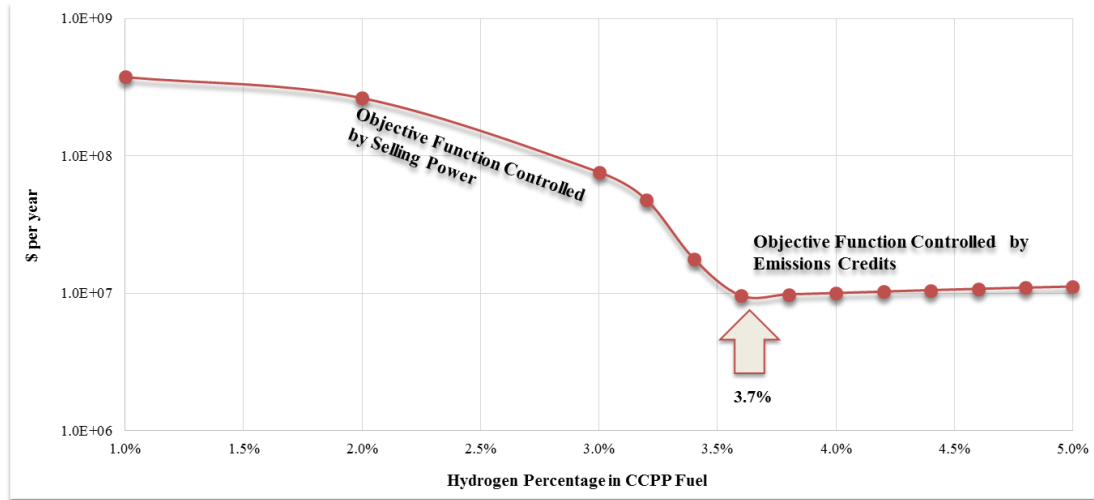
Figure (4.7): Selling power revenue & emissions credits vs. Hydrogen concentrations in CCPP fuel

This scenario is performed in order to find out the best price to sell electricity at different hydrogen concentrations in CCPP fuel. The wholesale price values is ranged from $0.03 per kWh up to $0.37 per kWh while examining the annual revenue as shown from Figure (4.8). At lowest hydrogen concentration and at highest wholesale price, the highest revenue can be achieved. At wholesale price of $0.12 per kWh the model starts to make revenue when the hydrogen concentration ranged from 1 to 3%. At hydrogen concentration 3.7% the wholesale price should be above $0.12 per kWh. The wholesale price of $0.12 per kWh is critical point towards making revenue, and this agrees with what Ontario set for on-peak price.
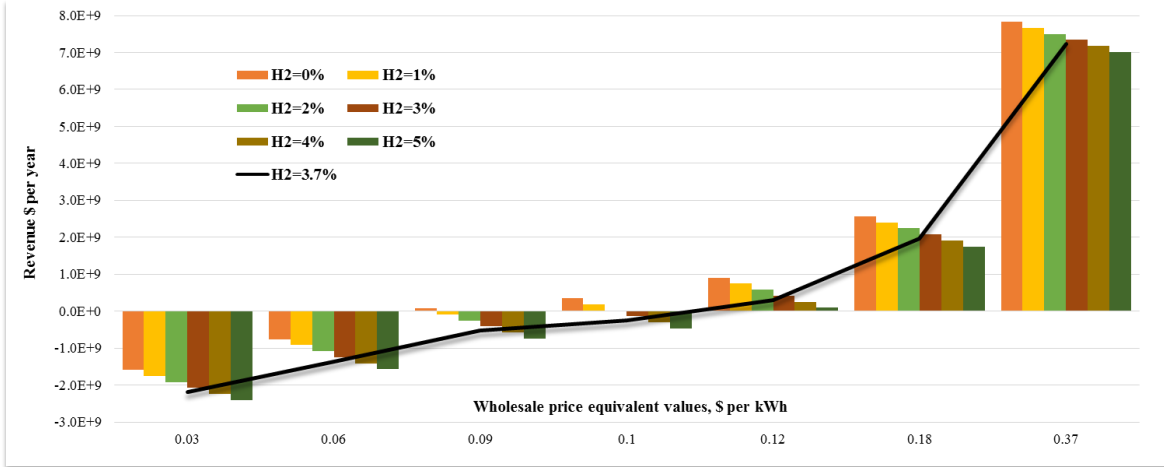
Figure (4.8): Annual revenue compared at a set of wholesale price at different H_2-concentration in HENG fuel

4.5.5 Results Sensitivity Analysis

A sensitivity analysis is performed in this section to examine the uncertainty of hydrogen concentration in CCPP fuel and how changing this parameter will impact the emissions credits. Credit of CO_2 emission is found to be more sensitive to the increase in hydrogen concentration than the credit of NO_X emission as seen from Figure (4.9). This approach is due to two facts: (1) the amount of CO_2 emissions released in ton per MWh is much larger than the amount of NO_x emissions; and (2) the CCPPs that are considered in the current study incorporated with SCR and DLN units, but they don't have the CO_2 capture unit.
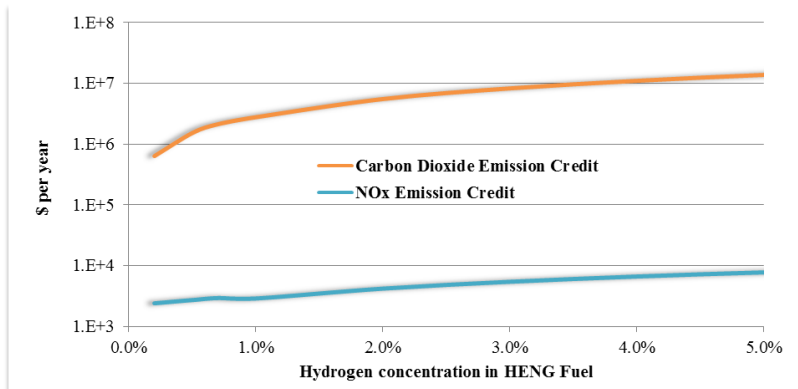
Figure (4.9): Emissions credits of CO_2 and NO_x at different hydrogen levels

4.6 The Conclusions

The energy hub is modelled as a framework of 'Power-to-Gas' concept to incorporate the zero-emissions renewable sources into dis-patchable combined cycle power plants via introducing hydrogen as an energy vector to be a replacement of the conventional fossil-fuelled power plants. Adding hydrogen into natural gas as a fuel for combined cycle power plants will create extra costs and reduce annual revenue, but at the same time will increase the CO_2 and NO_x emissions credits. Selling electricity at a price of $0.12 per kWh when hydrogen is 3.7% in CCPP's fuel represents a starting point towards increasing annual revenue. Revenue from selling electricity is more sensitive to increasing hydrogen concentration in CCPP's fuel than revenue from CO_2 and NO_x emissions credits. The credit of CO_2 emission is more sensitive to adding hydrogen into HENG CCPP's fuel than the credit of NO_x emission.

Chapter Five

5. Cost-analysis of health impacts associated with emissions from combined cycle power plant

5.1 Introduction

Power generation plants fueled by fossil fuels including natural gas (NG) have remarkable environmental impacts. The impacts associated with human health are the most important ones that can result in increased mortality in terms of reducing life expectancy. Additionally, the airborne pollutants can result in increased morbidity in terms of cardiovascular and pulmonary illnesses. Exposure to carbon monoxide (CO), particulate matters (PM_x), nitrogen oxides (NO_x), or sulfur oxides (SO_x), has a noticeable impact on human's health in both the long and short term during normal plant operations. Airborne pollutants impact human health directly, thus having a significant effect in the form of hidden costs in many different ways, including increasing the cost of health care and the number of missed working days, as well as reducing the productivity of impacted workers. Airborne pollution costs society and related economies billions of dollars every year (OMA, 2005). The real direct and indirect social costs of air pollution are even higher. The costs of health and social impacts due to air pollution also include indirect impacts such as losses in social welfare, suffering from pain, and early death. Airborne pollution from power plants has been related to a wide range of health concerns, starting with asthma and extending to cardiovascular diseases. Previous studies performed by the Toronto Public Health Department (TPHD), the Government of Canada and the OMA, show that air pollution can have serious impacts that may increase the rate of workers' absence and the numbers of emergency room visits and hospital admissions, and may lead to premature death (OMA, 2005).

When electricity generation costs do not adequately reflect all associated health and societal costs, the monetary value assigned to all causal impacts, considered damages, are "hidden" in the sense that governments and decision makers are not aware of the full economic impact of their actions on the public. These "hidden" impacts should motivate governments to adopt and establish protective actions such as regulations, taxes, and fees, or other restrictions for better recognition (National Academy of Sciences, 2009). The hidden costs of generating electricity can be defined as the costs of all health, social, and environmental damages imposed by the power generation

facilities that are not included in the market price of electricity (Molnar, et al., 2008); therefore, all of these related costs should be considered when evaluating the entire impact of the energy sector and should be expressed in terms of external costs per energy unit. The hidden costs are considered external due to their undeclared impacts within the normal pricing system, they can also be considered by-products generated by techno-economic activities that are unrelated to the parties involved in the activity (El-Guindy, 2013). The impact pathway approach (IPA) developed as part of the External Costs of Energy (ExternE) Project (Bickel & Friedrich, 2005) is one of the most common practical methods for assessing the environmental effects of different energy sectors; it is a unique tool for estimating the damage costs of airborne pollution to health and society. This step-by-step approach conceptualizes pollution as a burden and links it to its related impacts (Bickel & Friedrich, 2005). Calculating the actual cost of electricity will impact existing regulations in planning and undertaking the investments in new energy systems and operating existing power generation facilities. The main approach used in calculating the actual costs of generating electricity is conceptualizing the damage function as a relationship between pollutant emissions and the direct environmental impacts followed by monetizing the accrued damages. In general, this approach is considered superior when compared to the other approaches due to the intensive technical data required before utilizing this approach (Burtraw, et al., 2012).

With increased penetration of renewable energy sources such as wind and solar facilities, there is a need for additional peak power generation facilities to account for the intermittent nature of these sources. In addition, the power generated by intermittent renewable sources may not provide supplied power at the right time in order to be consistent with demand, nor is it likely to be in an appropriate location. Thus integrating these resources into the existing grids requires a unique energy system that can connect the inputs and the outputs of different energy flows in order to convert, conditioned and stored the energy; such a system called the energy hub (Buhler, 2010).

Thus, energy hub is designed for providing benefits for the transportation of energy as well as load-matching capabilities from different sources of energy. Hydrogen generated via electrolysis process from renewable sources as an energy carrier in energy hub system can be fed with NG and consequently used by combined cycle power plants (CCPPs), thus capturing the full value of the intermittent renewable capacity. Both provide the added benefit of reducing air pollution from power generation facilities.

This work is to explore the health impacts as one of the most significant environmental damages, and to monetize these damages in order to reveal the hidden costs of generating electricity from NG-fueled CCPP. In this manner, it continues to detect the potential of utilizing the energy hub system that designed in the previous study (AlRafea, et al., 2016) with respect to reduced emissions and society health impacts through a case study of NG-fueled CCPP.

The CCPP under study operates during times of higher electricity demand, which typically occur during daytime hours on summer and winter business days, but this may vary depending on changes in the spot market prices for electricity and NG (Greenfield South Power Corporation, 2012). Southwest Ontario is the assumed air-shed under consideration using the annual scenario of 2014. This location provides appropriate electrical transmission assets as well as the potential for the location of large-scale wind and solar facilities.

5.2 Air Quality-Health Assessment

Investigating the relationship between the quality of air and its impact on human health has been an objective for researchers for more than two decades. Burnett et al (Burnett, et al., 2004) examined the impact of short-term exposure to different concentrations of NO_2 on daily mortality cases registered in different Canadian cities under study.

Burnett and his colleagues linked the air pollution activities to the mortality cases recorded within the same areas of study using statistical methods. Their study can be used to provide unbiased estimation of the uncertainty in such air pollution-mortality association. This study showed that within certain groups of people, and in specific areas and time periods, there are direct relationships between a person's age at death and warmer months of the year. The conclusions from this work and other related studies suggest that, by reducing the number of fossil-fueled combustion power plants and utilizing cleaner facilities, public health benefits will result.

Understanding the sources of the air pollution, the characteristics of the emission, and the geographic and meteorological conditions as the main contributors to local air quality are required in order to achieve successful assessments (Barn, et al., 2011).

The Air Quality Health Index (AQHI) was established by Environment and Climate Change Canada in June 2015 as an effective tool in forecasting air pollution levels within 17 different locations in Ontario. It is designed for protecting people's health by guiding them to make the right decisions in minimizing short-term exposure to air pollution and by engaging in daily activity during periods with low levels of air pollution. This tool can provide valuable guidance on the best means to enhance the quality of the air breathed (Environment and Climate Change Canada, 2015). Evidence from observational studies indicates that higher daily pollutant concentrations are associated with increased incidences of asthma attacks, hospital admissions, daily mortality, and other markers of morbidity (Fig 5.1) (US EPA, 2014). Quantifying the health impacts associated with emissions from power generation facilities was applied through the impact pathway approach (IPA) Gunatilake et al (Gunatilake, et al., 2014). They applied a proposed methodology to an 800 MW coal-fired power plant facility located in India to demonstrate practically how a reduction in air pollution is feasible and economically applicable. They were successful in reducing the health impact costs associated with air pollution from CAD $12.58 per kWh to only CAD $1.05 per kWh.
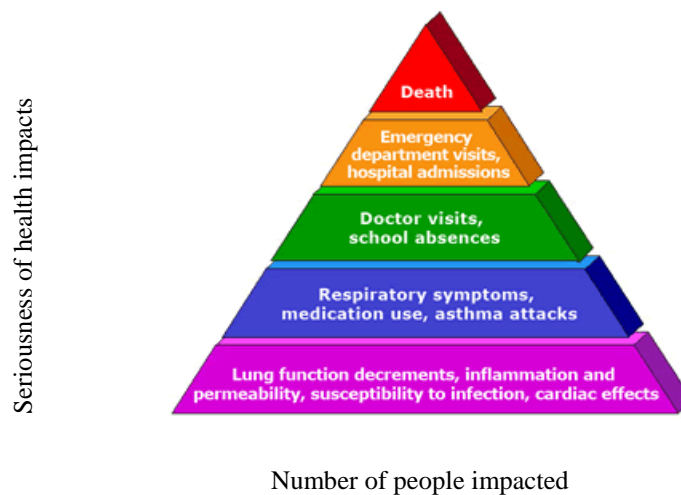
Figure (5.1): Health impacts vs. population impacted

5.3 Measuring Health Impacts Paths

A limited number of approaches are used to measure health impacts associated with emission from power plants. In an epidemiological path, people in the same exposure area with different pollutant concentrations can be compared. The health impacts then can be measured based on real human populations by observing models and relationships between pollutant concentrations and the resulting health impacts. Unfortunately, the uncertainties in an epidemiological path are large (Rabl, 2005). Another option is to measure health impacts through a toxicological path. In this approach, the mechanisms of pollutants' actions can be identified through animals, which are the only way to identify carcinogenic effects. Toxicology can also suggest new questions to be investigated by epidemiology (Rabl, 2005); however, the toxicological approach is omitted in this work due to the difficulty of extrapolating the results to humans. In order to carry out an epidemiological approach, two types of studies can be employed: cohort and time studies. Cohort studies are observational studies in which a group of selected people is specified and related information can be collected to determine which subjects have specific characteristics that are suspected of being related to exposure to a possible epidemiological agent. Setting a period of time is the followed step, and then incidents of impacted individuals are compared to the incidents of non-impacted individuals within the same group and living in the same area. In general, these studies are designed for exploring long-term exposure health impacts associated with air pollution. Although they are expensive, they can be used to observe serious impacts such as chronic symptoms that require observations over many years. Unlike other studies, they started by classifying exposed people according to their exposure-level followed by observing their reactions to certain health events such as early death, hospital admission, or an emergency department visit (Region of Waterloo Public Health, 2008). In contrast, time studies are designed for discovering health impacts associated with short-term exposure to different levels of pollutant concentrations. Within large cities, relations can be made between pollutants' concentrations and the occurrence of health impacts during the subsequent days. These studies are inexpensive, but only acute impacts can be observed. As another approach, the health impacts associated with air pollution for a specific exposure and at certain levels can be measured and linked to the risks of expected health illness. These determined links were used to form rational relations for counting the likelihood of each impact to occur (Robinson, 2008). The direct relationship between costs and illness can be found through cost of illness (COI) or burden of disease (BOD) approaches that consist of various

aspects of measuring a disease's impact on an individual's health while living in a country, region, or small community (Changik, 2014). Measuring the direct costs of medical treatment, nursing care, and drugs; and indirect costs such as related expenses associated with expected diseases. Estimating the savings from eliminating these diseases is also another approach.

A related measurement can be performed via a human capital survey. Such assessments estimate how the illness as a health outcome might lower productivity. This approach also monetizes the loss of an exposed person's life based on the association between economic losses and premature mortality; therefore, the conclusion is that the value of people's WTP should be greater or at least equal to their earnings that they would lose when dying prematurely (Remoundou & Koundouri, 2009). The quality-adjusted life year (QALY) as an approach to employ the cost-effectiveness concept in measuring health impacts; it aims to guide the decision makers to allocate rare resources across competing health care programs (Weinstein, et al., 2009). It directs to merge the health interventions of both mortality impacts as well as morbidity impacts into a unique index through a common currency to enable comparisons across various diseases. Within a certain timeframe, different health impacts appear on those who have been exposed to certain pollutants, therefore, the next step is to weigh these impacts according to specified scores associated with the impacts (Whitehead & Ali, 2010). Cost of damages is a simple way to place a value upon changes in air pollution levels and allow researchers to estimate the cost to society of a change in the emission of different pollutants. It can be determined for a specific pollutant, source, and location (DEFRA, 2015a). Per ton, the damage's cost of NO_x from the energy supply industry is £1,263, of PM_x is £2,906, and of SO_x is £1,956. These damage costs are used to assess national policies, programs, and projects by location and source (DEFRA, 2015b).

5.4 Atmospheric Dispersion Models

The atmospheric dispersion model can be defined as a function in the form of a mathematical relationship describing the dispersion of air pollutants in the ambient atmosphere. It can be executed by computer programs that solve sets of equations and algorithms to mimic the dispersion mechanism of air pollutants.

Dispersion models are significant due to their role in estimating the air pollutant concentrations at different distances from the source as well as their ability in incorporating atmospheric chemistry into the model when secondary pollutants are formed. Additionally, these models are useful in examining a new air pollution source when it will impact a specific area or in forecasting the best ways to control a specific source. Dispersion models are utilized when a forecast of ambient concentrations is required, specifically to review a new air pollution source or evaluate suggested plans for emission reduction (EPA, 2015a) and (Stockie, 2011). Selecting a relevant model from a wide range of models is significant in meeting the requirements of the proposed task followed by applying quick estimations of the highest air pollutant concentrations that are likely to occur. These models will be used when the study area is large (e.g. province-wide) or when ordinary models are unable to address such an exceptional situation (Alberta Environment, 2010). The approved dispersion models as per the Ontario Ministry of the Environment (OME) for discharge of a contaminant are AERMOD and SCREEN3 (Ministry of the Environment, 2008). The SCREEN3 dispersion model provides a simple method of estimating contaminant concentrations. The SCREEN3 methods were structured based on the EPA's publication Screening Procedures for Estimating the Air Quality Impact of Stationary Sources (Jesse, et al., 2007).

As it is capable of measuring the worst-case dispersion (maximum concentration) of various pollutants, SCREEN3 is a useful tool to simulate the dispersion of different emission sources (i.e., points, areas, volumes, and flares). The emission from an area sources represents a homogenous distribution of the air pollutants from a two-dimensional surface area; whereas the emission from volume sources represents emission of air pollutants from buildings or roof monitors (Abdelwaheb, et al., 2014) and (Taha, et al., 2005).

SCREEN3 is chosen for measuring pollutant concentrations in the current study due to: (1) its ability to provide ground-level concentrations of pollutants for different areas, flare, and variable sources; (2) its ability to conservatively estimate the impact from several sources, and modeling several sources that emit the same pollutant with similar parameters; and (3) its ability to provide 1-hour, 3-hours, 8-hours and 24-hours measurements of air pollutants concentrations (US EPA, 2005). Its schematic diagram is represented in Fig. (5.2). Pollutant concentrations modeled by SCREEN3 are compared with cited literature in the results section.

Inputs

Outputs

| Pollutants Emissions Rates, g s^{-1} |
| Pollutants Flow Rates from Specific Units, m^3 s^{-1} |
| Stacks Specific Design, Chimney height, Diameter, Stack exit Temp., etc. |

SCREEN3 Dispersion Model

Max. and Min. Distance from Stack

Correlation of Pollutant Concentration in g m^{-3} with the Distance from Emission Source
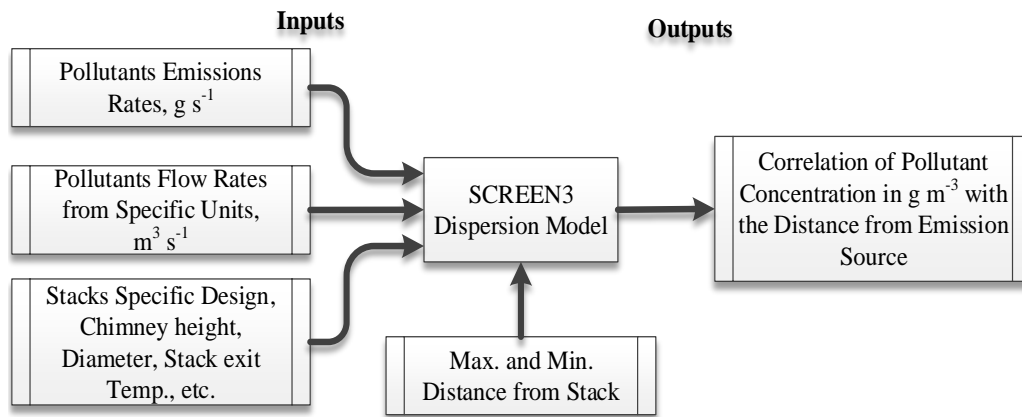
Figure (5.2): Schematic diagram of SCREEN3 dispersion model.

5.5 Integration Renewable Energy Sources – Energy Hub Model

In the present work, the demonstration of the integration of these technologies is not specifically modelled; however, the analysis considers a scenario where hydrogen enriched natural gas (HENG) is used to fuel the CCPP. Future works will demonstrate the overall optimization of all the technologies together. A simulation of blending hydrogen with NG to fuel CCPPs in order to examine its potential for reducing air emissions is adopted in the current study. The reason for this approach is to drive interest in analyzing the use of HENG in matters of cost and emission effectiveness; HENG enhances significantly flame stability lean combustion and so permits a stable combustion at low temperatures, which are required for minimizing the emissions of NO$_x$ (Schefer & Oefelein, 2003).

The objectives of the current study are: (1) measuring the concentrations of the most considerable air pollutants that emit from CCPP while using NG fuel and then to be compared to the ones from using HENG fuel; (2) studying the impacted areas by air pollution that surrounded the proposed CCPP facility in terms of population's health impacts; (3) monetizing the population's health impacts that associated with exposure to the specified air pollutants within the impacted areas; and (4) performing a cost analysis in order to investigate the hidden costs of health impacts that will be added to the main costs of generating electricity.

5.6 The Approach

Attempting to estimate the cost of health damage due to air pollutant emissions from a specific source is inconsistent with a considerable number of uncertainties accompanied by the effect and range of the damage. Because of uncertainties surrounding global climate change and due to the length of time required to determine its effects, the current study does not consider global climate change damage but simply regional impacts within an air shed. The principal steps in evaluating the health impact of a pollutant by carrying out an IPA assessment and tracing its passage from the emission's source to the impacted receptors can be grouped as follows:

(a) Specifying the technologies and environmental burdens they impose (e.g., kg of NO_x emitted per MWh generated by the CCPP);

(b) Calculating pollutant concentrations that have increased in all affected regions (e.g., using models of atmospheric dispersion, such as SCREEN3);

(c) Calculating the extent of the increased exposure and its impact, which can be stated as damage in physical units using a concentration-response function (e.g., number of asthma incidents associated with increases in a pollutant's concentration;

(d) Evaluating the health impact (e.g., how much does an asthma incident cost?); and

(e) Evaluating the health impact of using HENG-fired fuel in CCPP and then comparing that impact to health impacts caused by utilizing NG-fired fuel.

In the present proposed study, the emission factors for various pollutants based on NG characteristics will be used to evaluate the emissions from electricity generation. Estimations of health damage will then be used to provide a monetary valuation of the damage costs. The current study will be constituted of the following major steps (Fig 5.3). First, an up-to-date, efficient, emission-controlling NG-fired CCPP will be recruited to the study. Preferably the plant will be able to control emissions as part of the Ontario government's plan for replacing coal-fired power plants. Although different equipment within the power plant emits different pollutants, the study will propose the desired CCPP as the only source of emissions. The second step is to consider the CCPP's emission rate of CO, NO_2, $PM_{2.5}$, and SO_2 and the severity of the associated health impacts. Based on the power plant's location, the population distribution in the specified area of study is assessed in terms of age, distance from the emission source, and the time period during which the statistical data are available. In addition, the design specifications of the plant's emissions stacks is used to implement the dispersion model for calculating the emissions'

concentrations. Anticipated health impacts are considered and tabulated using a matrix according to daily exposure. Health damage, including mortality, morbidity, cardiovascular disease, and asthma are considered and measured based on epidemiological studies. In this stage of the study, the conditions of people in the same exposure area will be correlated with different concentrations of pollutants. In order to connect the change in the concentrations of pollutants on the relevant receptors, the exposure response function (ERF) is used within the AQBAT. The ERF for health impacts is calculated from semi-empirical relations which are mainly based on a survey of epidemiological studies (Hainoun, et al., 2010). The dose from the increased exposure to the surplus contaminants, as well as the impacts from this dose, is identified using a concentration-response function. For optimal implementation, one needs to know the level of the damage caused by specific pollutants emitted from specific sources. The last stage of the process is the monetary valuation of the counted health impacts. Converting the counts of various human health impacts to monetary values allows for a summation of valuations across health endpoints to estimate the overall monetary value of health incidents (Judek, et al., 2012).
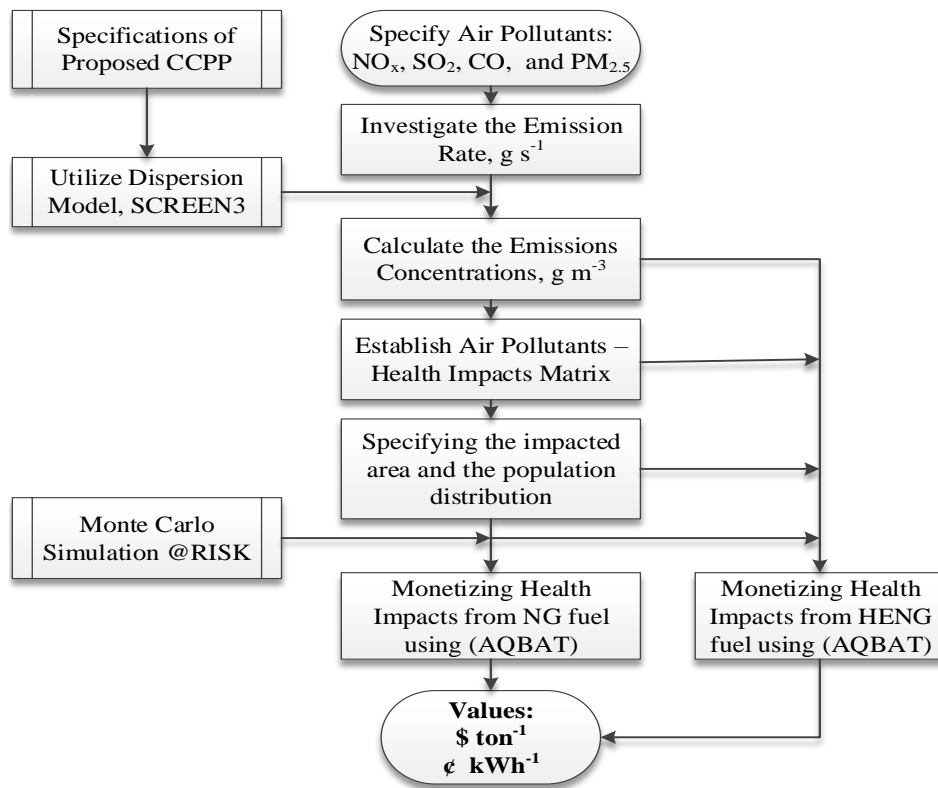
Figure (5.3): Flow diagram of steps for calculation the monetized value of emissions impacts

5.7 Methodology

Five steps are considered in the methodology, which focus on calculating health impacts' costs resulting from specified emissions of air pollutants from the proposed CCPP. The first step in this process is to propose a CCPP facility that would meet the incremental power demand. The second step is to specify the air pollutants that are being emitted from the proposed CCPP. The third step is to calculate the concentration of each pollutant using the SCREEN3 model. The fourth step is to correlate the health incidents with the air quality change in the region under consideration. Finally, the fifth step is to utilize AQBAT software for monetizing health impacts. The location in southwest Ontario was selected to be consistent with earlier work (AlRafea, et al., 2016). It is worth noting that this location is suitable for an energy hub as it has suitable wind and solar resource potential, the potential for hydrogen storage, and available electrical transmission grid capacity. As the epidemiological path is chosen in this study in calculating exposure response function (ERF) as well as the concentration response function (CRF) within AQBAT tool; the related uncertainties are large. The methodology is designed to justify and to reduce the accompanied uncertainties by employing real inputs and data while correlating air pollutants to health damages costs.

5.7.1   Step 1: Propose CCPP - Green Electron Power Project

The Green Electron Power Project is a NG-fueled CCPP facility with an annual average capacity of 289 MW located in St. Clair, Ontario; it is an existing power plant and is chosen to be the source of actual data in meeting the proposed demand. It consists of one gas turbine generator fueled by NG, one heat recovery steam generator (HRSG), and one triple pressure, reheat, full-condensing steam turbine generator. The plant utilizes an existing transmission infrastructure which feeds the regulator controlled grid (IESO, 2014). The thermal efficiency of the plant is 48%. The gas turbine is equipped with dry low NO_x burner technology which was selected to reduce NO_x emissions. The power plant is projected to operate at near 100% capacity for up to 10.9 hours per non-holiday weekdays or 2,676 hours per year (Eastern Power Limited, 2012); and (Greenfield South Power Corporation, 2012).

5.7.2   Step 2: Specify the air pollutants from the CCPP

The atmospheric emissions from the specified NG-fueled CCPP during operations hours include: NO_x's emissions which is consisting of NO and NO_2; CO's emission which is resulting from incomplete combustion; SO_2's emissions which is resulting from a mercaptan odorant additive; and PM_{10}, and $PM_{2.5}$ emissions (Vogt & Holbein, 2012). The proposed HENG-generation facility would emit only about 9.1% of the NO_x, 0.035% of the SO_2, and none of the mercury that is emitted under current models. The annual expected emissions are presented in Table (5.1) (Vogt & Holbein, 2012). For the purpose of consistency, the emission rates from other NG-fired CCPPs are compared to what is considered in the current study (Table 5.2) and demonstrates that the simulated emission profile is consistent with values reported in other studies.

Table (5.1): Expected annual emissions from the proposed CCPP

Species	Emissions (tons)	Species	Emissions (tons)
NO_x	94.9	PM_x	92.5
CO	148.4	SO_2	12.8
UHC (CH_4)	0.90	Hg	None

Table (5.2): Comparing emissions rates from current study with other CCPPs from cited literatures

Pollutants	Emissions rate (kg per MWh)				
	Current Study	Cited literatures			
		(NETL, 2010)	(Black, 2013)	(Spath & Mann, 2000)	(NPI, 2012)
CO	0.24	0.100	-	0.287	0.10
NO_2	0.16	0.370	0.027	0.570	0.54
$PM_{2.5}$	0.15	0.006	-	0.133	-
SO_2	0.021	0.014	-	0.324	-

5.7.3 Step 3: Calculating Pollutants' Concentrations using SCREEN3

The SCREEN3 dispersion model is used in the current study to predict the emission concentrations from the proposed CCPP. According to Canada's Ministry of the Environment (MOE), only CO, NO_2, $PM_{2.5}$, and SO_2 are evaluated because of their significant impact on the surrounding air quality. The receptors of interest have been specifically chosen to be close to the proposed CCPP. The input required to run SCREEN3 are the emission rates for each pollutant, the stack's height and it's inside diameter, the gas velocity from the stack's exit, the stack's gas exit temperature, and the ambient air temperature (Table 5.3).

Table (5.3): The expected emissions from all CCPP auxiliaries and the stack characteristics of the CCPP

Emission Sources	Emission rate (g/s)				Stack height (m)	43
	CO	NO_x	$PM_{2.5}$	SO_2	Stack inside diameter (m)	5.5
HRSG	9.76	10.40	1.63	0.12	HRSG stack exit temperature (K)	360
Cooling Towers (4 Stacks)	-	-	4*0.005	-	Ambient air temperature (K)	293
NG-Fired Heaters (12 heaters)	0.014	0.07	0.004	0.0004	HRSG's stack exit flow rate (m^3/ s)	500

In order to calculate the emission's flow rate from each stack, a relationship by Madrzykowski and Kerber (Madrzykowski & Kerber, 2009) is used as shown in Eqn. (5.1).

$$Q = C * A * \sqrt{2 * g * H * (Ti - To)/Ti}$$

(5.1)

Where: Q is the pollutants' flow rate that exit from the stack in m^3 s^{-1}; C is the discharge coefficient of gas flow through a channel, its value can be determined based on the characteristics of fluid flow as well as channel's dimensions, and it is a dimensionless factor; A is the cross sectional area of the stack, measured by m^2; g is the gravitational acceleration in $m.s^{-2}$; H is the stack height in m; Ti is the stack's inside temperature in K; whereas To is the stack's outside temperature in K.

The gases' flow is proportional directly to the discharge coefficient and to the cross-sectional area of stack; direct proportional to the square root of both the height of the stack and the

inside/outside temperatures. This equation is a well-known tool for measuring volumetric gas flow through channels (Bahrami, et al., 2013).

5.7.4 Step 4: Correlate the health incidents during exposure periods

This step represents the AQBAT calculations for quantifying health incidents due to the changes in pollutant concentrations. In the AQBAT, the concentration response function (CRF) is employed to measure the frequency of the occurrence of health damages which occurred when an increase in pollutant concentrations happened. The AQBAT's calculations are based on risk coefficients from epidemiological studies in previous scientific literature (Table 5.4).

Table (5.4): Risk Coefficients that are used by AQBAT

Pollutants	Risk Coefficient Estimates		
	Exposure Mortality, (% change per 10 units pollutant)	Respiratory Admissions (% change per 10 units pollutant)	Cardiovascular Admissions (% change per 10 units pollutant)
CO (ppm)	0.19	-	2.77
NO_2 (ppb)	0.75	-	-
$PM_{2.5}$ ($\mu g/m^3$)	6.8	0.75	0.71
SO_2 (ppb)	0.46	-	-

The number of health events is the product of the four factors: the CRF which is expressed as excess adverse endpoints per unit of increase in pollutant concentrations; the change in pollutant concentrations; the baseline rate of the incidence of the health endpoint in the specified population to which the CRF is applied; and the specified population. Estimates of the health impact related to air quality in the region under consideration are performed by the AQBAT, which is modeled according to a literature review of air pollutants and health impacts (Rabel, et al., 2011); (Rabl, 2005); and (Region of Waterloo Public Health, 2008). The methodology used to estimate the number of health incidents due to air pollution exposure in the Air Pollution Burden of Illness in Toronto report (Toronto Public Health Department, 2007) was adopted for use in the current study, whereas Equation (5.2) is used to calculate the health incidents.

$$N = HE * RC * \Delta PC * Pop \tag{5.2}$$

Where: $\mathbf{N}$ is the number of health incidents due to exposure to the specified air pollutants; $\mathbf{HE}$ is the expected health end points (health impacts); $\mathbf{RC}$ is the risk coefficient as a relationship between relative risk increased due to increase in the concentration of an air pollutant; $\mathbf{\Delta PC}$ is the concentration change of the air pollutant that expected to cause such a health impact (measured in micro gram per m^3); $\mathbf{P_{op}}$ is the population number that under investigation.

5.7.5 Step 5: Using AQBAT in Calculating Health Impacts' Costs

Based on the AQBAT approach discussed earlier and according to current studies, three components of: air pollutants, health endpoints, and scenario year are linked to four key model input factors in estimating health impacts. Each of these components are indices of the factors involved in estimating the health impact outputs. The air pollutants and health impacts are linked by assigning CRF, the first key input factor, and a quantification of the influence of a pollutant on a health. The change in a pollutant's concentration is the second key input factor to estimate health impact, which can be expressed as a baseline health endpoint occurrence. For long-term exposure mortality, corresponding CRFs applied to the concentration changes are also transformed to estimate changes in life expectancy. The monetary valuation estimate assigned to one occurrence of a health outcome is termed a health impact valuation, which is the third key input factor. As is the case with CRFs, the health impact valuation estimates are generally statistically derived and revealed in the choice of a distribution form and its corresponding parameter values. Other factors involved in the determination of health impacts are the baseline health endpoint occurrence rates, population counts, and various global constants. All of these factors are deterministic values and are collectively considered the fourth key input factor. Monetary valuations are expressed in Canadian dollars. The cited values of CRF for each pollutant that are considered in the AQBAT are summarized in Table (5.5).

Table (5.5): The CRFs for each pollutant considered in AQBAT and their respective cited literature

Pollutant	CRFs used by AQBAT	Reference(s)
CO	24 hour CO-Concentration (ppm) - Acute Exposure Mortality	(Burnett, et al., 2004)
	1 hour CO (ppm) - Elderly Cardiac Hospital Admissions	(Burnett, et al., 1997); (Sctwartz & Morris, 1995)
NO_2	24 hour NO_2 (ppb) - Acute Exposure Mortality	(Burnett, et al., 2004)
$PM_{2.5}$	24 hour $PM_{2.5}$ (µg per m^3) - Acute Respiratory Symptom Days	(Krupnick & Harrington, 1990)
	24 hour $PM_{2.5}$ (µg per m^3) - Adult Chronic Bronchitis Cases	(Abbey, et al., 1995)
	24 hour $PM_{2.5}$ (µg per m^3) - Asthma Symptom Days	(Ostro, et al., 1991)
	24 hour $PM_{2.5}$ (µg per m^3) - Cardiac Emergency Room Visits	(Burnett, et al., 1995)
	24 hour $PM_{2.5}$ (µg per m^3) - Child Acute Bronchitis Episodes	(Dockery, et al., 1996)
	24 hour $PM_{2.5}$ (µg per m^3) - Respiratory Emergency Room Visits	(Burnett, et al., 1995); (Stieb, et al., 2000)
	24 hour $PM_{2.5}$ (µg per m^3) - Chronic Exposure Respiratory Mortality	(Pope III, et al., 2001)
SO_2	24 hour SO_2 (ppb) - Acute Exposure Mortality	(Burnett, et al., 2004)

The four components of the AQBAT model are pollutants, health endpoints, geographic areas, and scenario year (Fig. 5.4). Each of these components is an index to the factors involved in estimating the health impact outputs. The pollutant, health endpoint, and geographic area components are linked by CRF, whereas the pollutant, geographic area, and scenario year components are linked by the pollutant concentration change factors. The geographic area and scenario year components are linked by the factor of end-point evaluation. In AQBAT, mortality and/or morbidity impacts as outcomes are the last step in cost valuations. The value of statistical life (VSL) path is used for mortality valuation as a measurement of how much people are willing to accept different levels of risk, whereas losing wages, treating health issues, averting expenditures, and suffering from pain

are all related to morbidity outcomes. The database block represents other factors that are deterministic, including baseline health endpoint occurrence rates, population counts, and various global constants. Health benefit (or damage) counts and monetary valuations are the AQBAT outputs.
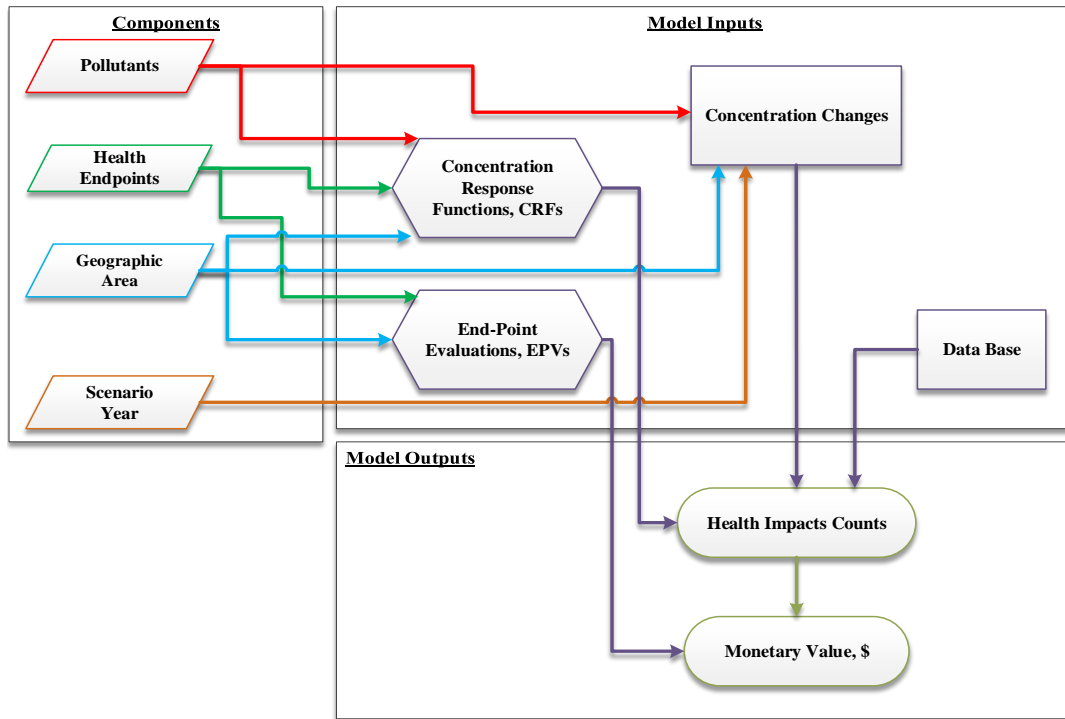
Figure (5.4): AQBAT Schematic Diagram

5.8 Results and Discussions

In this section, the outcomes are collected and presented according to their performance in the following scenarios:

5.8.1 Scenario 1: Meeting the demand utilizing the NG-fueled CCPP

In this simulation, the proposed CCPP was used to encounter the on-peak power demand. The hourly power demand is simulated based on the aforementioned projected design in section 5.6.1 and the desired operation of the proposed CCPP under consideration. The proposed hourly operation scenario of this power plant is presented in Fig. (5.5); whereas the load factor of the CCPP is varied between 73 - 99% during the 2,676 operating hours per year.
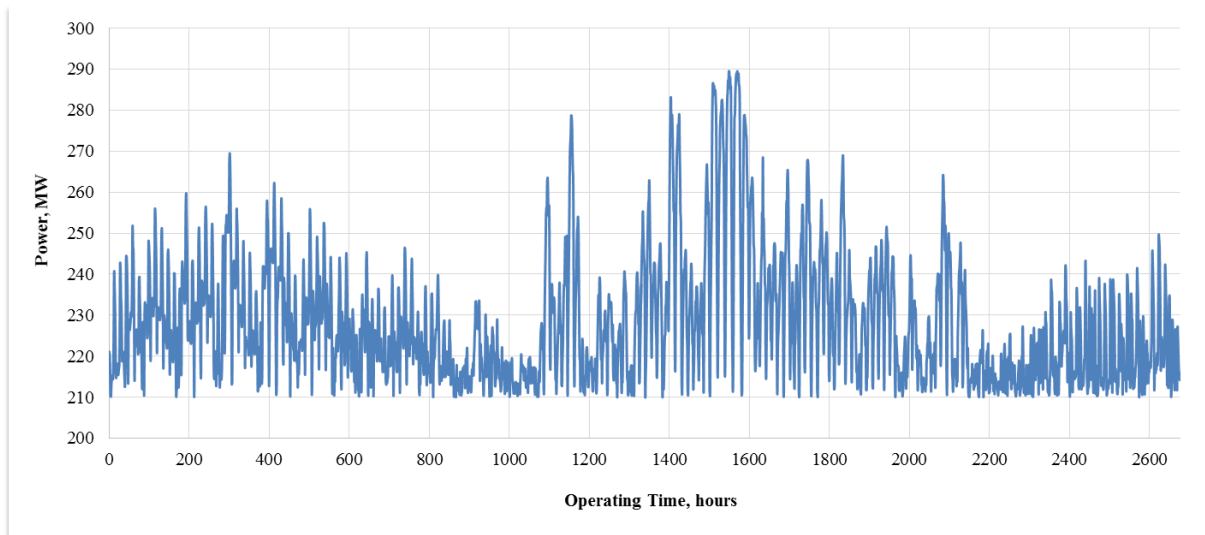
Figure (5.5): Proposed operating scenario for NG-fired CCPP, hourly basis

Based on the hours of the CCPP's operation and its load factor, and based on the expected emissions from the CCPP's auxiliaries as shown in Table 3, the hourly emissions that are expected are presented in Fig. (5.6). The emission rates of NO_2 and CO have similar profiles and vary between 25 - 37 kg per hour. The $PM_{2.5}$ emission rate is less impacted by a CCPP's operation and is almost stable at five kg per hour; whereas the emission rate of SO_2 has a minimum value of about 0.35 kg per hour.
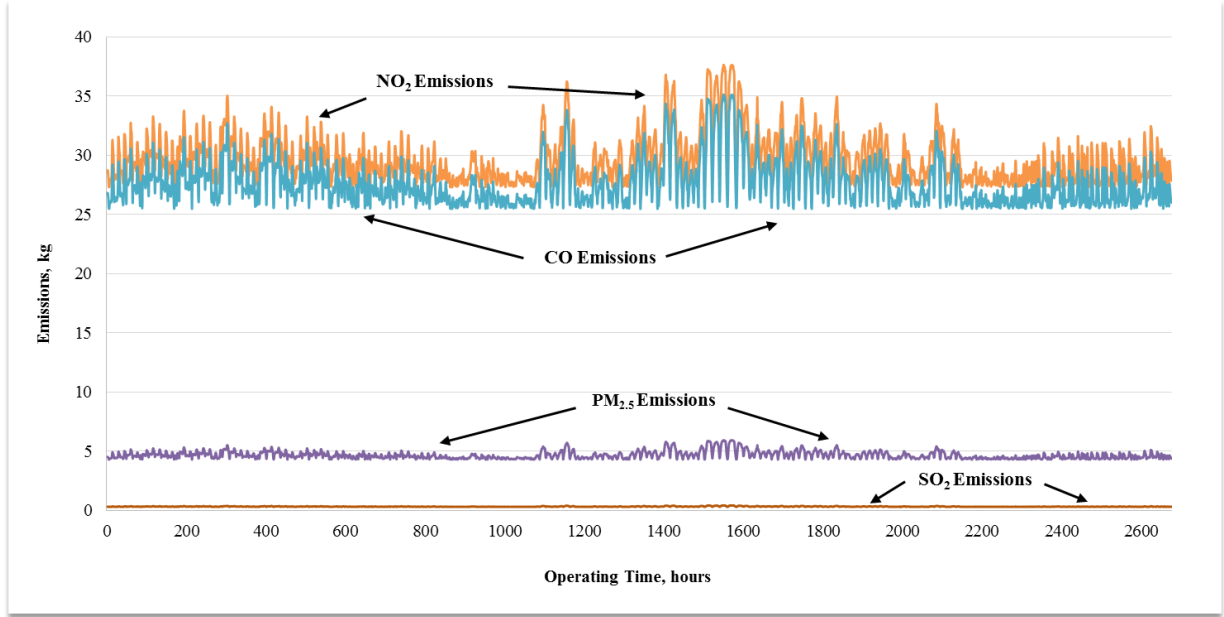
Figure (5.6): The expected emissions rates in kg from proposed NG-fueled CCPP

In order to measure the concentrations of the specified pollutants, SCREEN3 dispersion model is run (Fig. 5.7). The pollutant's concentration in μg per m^3 as the results are related to the distance from the pollutant's source which is measured in meters. The pollutants reached their maximum concentration value at almost the same distance from the source, which is varied from 1,000 to 1,200 meters (Fig. 5.7).
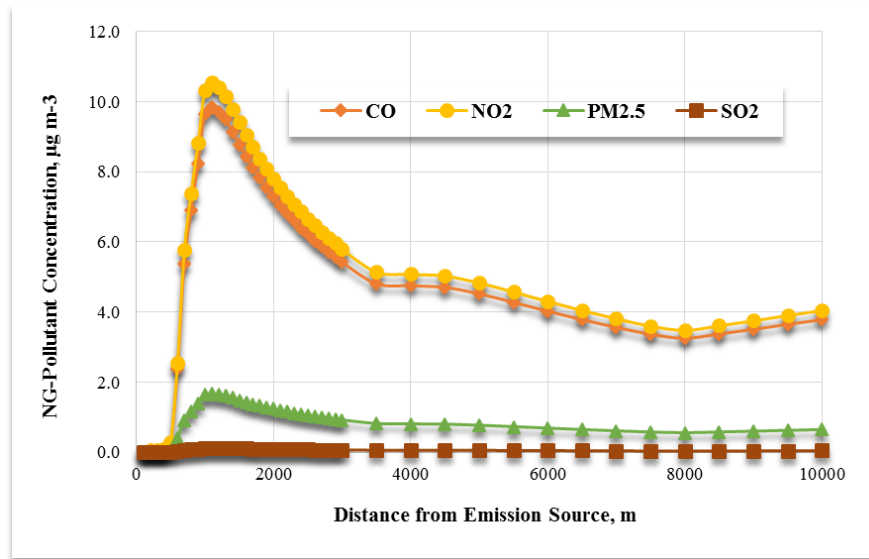
Figure (5.7): SCREEN3 results, NG-pollutants concentrations vs. distance

This finding means that all of the receptors living within this area will be impacted by different levels of pollution. The pollutant concentrations are then used in the AQBAT as one of the required inputs. In order to measure the additional pollutant concentrations in the affected area due to the CCPP's operation and to be compared to the existing pollutant concentrations measured by Eastern Power Limited (Itliong, et al., 2012), a comparison is presented in Table (5.6).

Table (5.6): Impact of the expected emissions on existing emissions in air shed

Species	Existed 5 years average pollutants concentration (μg per m^3)	Additional pollutants concentration caused by operating CCPP, calculated by SCREEN3 (μg per m^3)	Expected increased percentage in the existed air shed
CO	385.6	9.9	2.6%
NO$_x$	48.9	10.8	22.1%
PM$_{2.5}$	21.8	1.7	7.8%
SO$_2$	17.9	0.122	0.7%

The specific pollutant that most impacted the outlined area was NO$_2$. An analysis by Eastern Power Limited (Itliong, et al., 2012) showed that the proposed power plant's emissions will meet MOE Guideline A-5 for limits of oxides for N$_2$, CO, and SO$_2$. At this stage, all the required inputs for the AQBAT software are specified: the four pollutants under study, the impacted health endpoints, the geography of Sarnia, Ontario, and the scenario year of 2014. Health impacts are monetized by running the AQBAT software (Fig. 5.8).
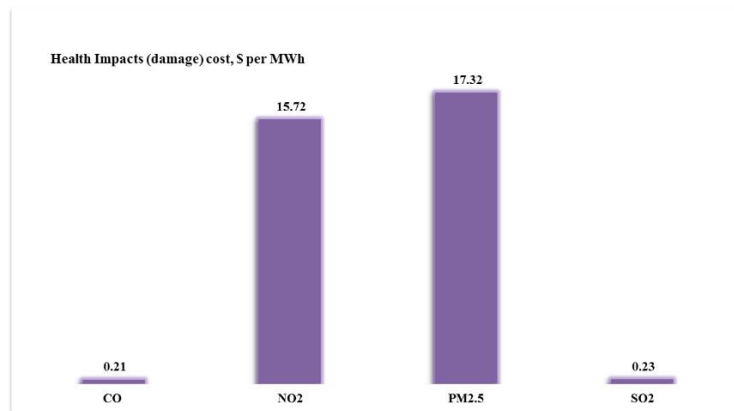
Figure (5.8): The costs of the health impacts associated with using NG fuel

The damage cost of $PM_{2.5}$ is highest as reflected in the wide range of health cases impacted. Although CO has the highest expected annual rate of emission, its damage cost is low due to its limited monetary value. The total impact as expressed as a health cost that can be expected from the proposed CCPP is CAD $33.50 per MWh. This hidden cost represents an additional 30% above the LCOE that should be considered when evaluating the on-peak power generation cost. This means that for every hour the health impact (damage) will cost receptors living in the surrounding area about $7,600 due to the emissions from NG-fueled CCPP. The results of the current study compared to similar studies (Table 5.7), demonstrating that this specific simulation agrees with calculated values of the health impacts of CO, $PM_{2.5}$, and SO_2, while the health impact due to NO_2 is found to be higher in the current study. The deviation in calculated NO_2 health impact according to the cost associated with NG-fired CCPP is due to the wide range of health endpoints assigned by the AQBAT and due to the 2014 dollar value in the current study.

Table (5.7): Comparing current study results to the cited literature for health impacts from NG-fired CCPP

Citations	Criteria of Measuring Health Damage Cost	Health Impacts Cost ($/kg)				Health Impacts Cost ($/MWh)
		CO	NO_2	$PM_{2.5}$	SO_2	
(Friedrich, et al., 2001)	Morbidity (cardio, heart failure, chronic cough, etc.); Mortality (reduction in life, congestive heart failure, etc.); cancers	-	15	13.5	9.5	5.0
(Roth & Ambs, 2004)	Best estimation from literatures	1.10	8.0	5.0	2.0	-
(AEA, 2005)	Chronic effects on: Mortality and Morbidity; Acute effects on: Morbidity	-	53.65	110	23	-
Current study	Acute Exposure Mortality; Acute Respiratory Symptoms Days; Adults Chronic Bronchitis; Asthma Symptoms; Child Acute Bronchitis; and Cardiac & Respiratory Emergency Rooms Visits	0.87	101	114	11	33.50

5.8.2 Scenario 2: Health Impacts associated with NG-fueled vs. HENG-fueled CCPP

This scenario is designed as a techno-economical assessment to evaluate the approach of adding hydrogen into NG when fueling the CCPP in order to reduce emissions. The energy hub cost model mentioned in section 5.5 is used to perform this evaluation. Adding electrolysis-produced hydrogen into NG to form HENG fuel is used to level up the integration of the intermittent sources of wind and solar into the conventional source of NG-fueled CCPP (AlRafea, et al., 2016). The environmental benefits can be achieved when the HENG fuel is utilized in CCPP while meeting demand, and the range of hydrogen concentration in HENG fuel is in the range of 0 - 5%. For this purpose, the reduction in air pollutants' emissions can be acquired from two ways simultaneously: (1) by incorporating wind and solar into the grid while meeting demand through producing electrolysis-hydrogen during off-peak hours; and (2) by using electrolysis-produced hydrogen with NG in fueling CCPP. The emission rates of all expected pollutants when the CCPP is fueled by HENG are calculated by considering hydrogen is generating zero emissions when used as a fuel; the results are presented in Table (5.8).

Table (5.8): The expected emission rates from HENG fuel

Pollutants	Emission Rate (kg/MWh)	
	When H_2 = 1% in HENG fuel	When H_2 = 5% in HENG fuel
CO	0.154	0.148
NO_2	0.240	0.231
$PM_{2.5}$	0.150	0.144
SO_2	0.021	0.020

The pollutant concentrations from the HENG-fired fuel were calculated using the SCREEN3 dispersion model (Fig. 5.9). The highest concentration in µg per m^3 is for NO_2, which is consistent with results of the NG-fired power plant scenario (Fig. 5.7).
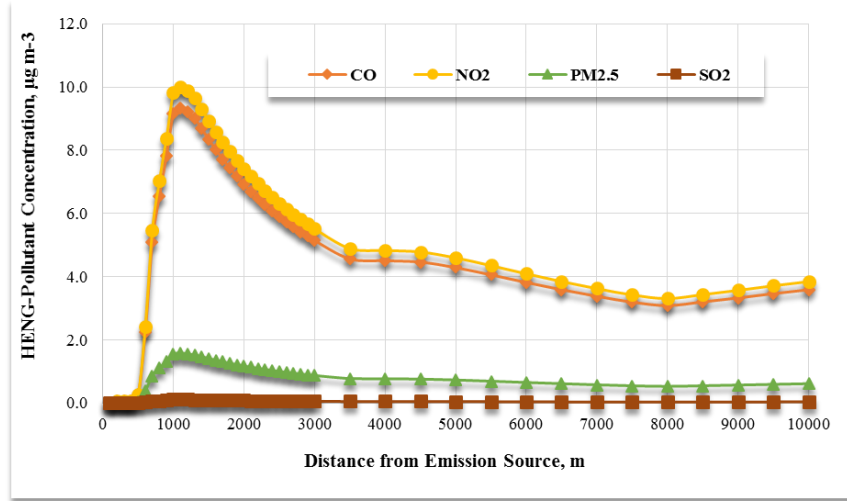
Figure (5.9): SCREEN3 results, HENG-pollutants concentrations vs. distance

The pollutants' concentrations from the NG and HENG fuels are presented and compared in Fig. (5.10). The same pattern is found for all pollutants by graphing their concentration levels against the distance of the emission source in the impacted area.
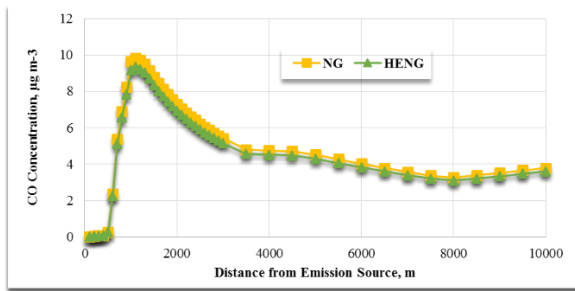
(a)   CO Concentration vs. Distance
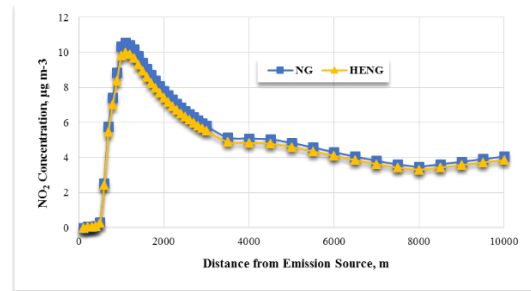
(b) NO_2 Concentration vs, Distance
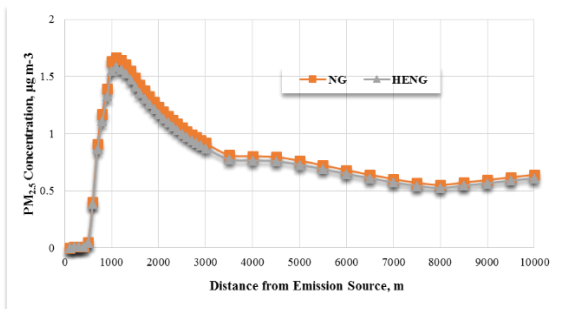
(c) $PM_{2.5}$ Concentration vs. Distance
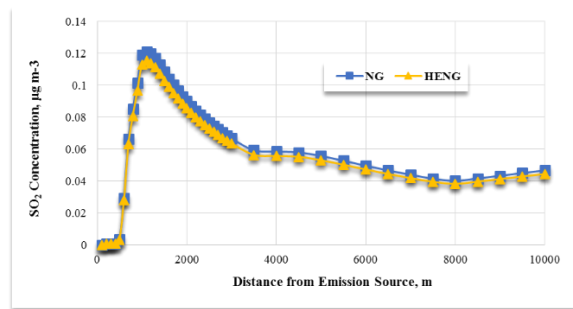
(d) SO_2 Concentration vs. Distance

Figure (5.10): SCREEN3 results, comparing pollutants concentrations of different fuels.

All the pollutants reached the highest concentrations at a distance of 1,000 - 1,200 meters from the CCPP facility. For both fuels, the highest concentration was of NO_2 followed by CO, $PM_{2.5}$, and SO_2; the concentrations of all pollutants emitted from NG had higher values than those from HENG due to hydrogen's presence in HENG. Using the same path as used in scenario 1, the health impacts associated with the pollutants emitted from the HENG-fueled CCPP are monetized and presented in Table (5.9).

Table (5.9): The costs of health impacts associated with using HENG fuel

Pollutants	Health Impacts for HENG-fired fuel ($/MWh)
CO	0.21
NO_2	15.14
$PM_{2.5}$	16.76
SO_2	0.23
Total	32.33

The results suggest that blending hydrogen with NG to fuel CCPP could save CAD $1.14 for every MWh produced. The costs of the health impact resulting from NG-fueled CCPP are compared to the ones from HENG-fueled CCPP and are shown in Fig. (5.11).
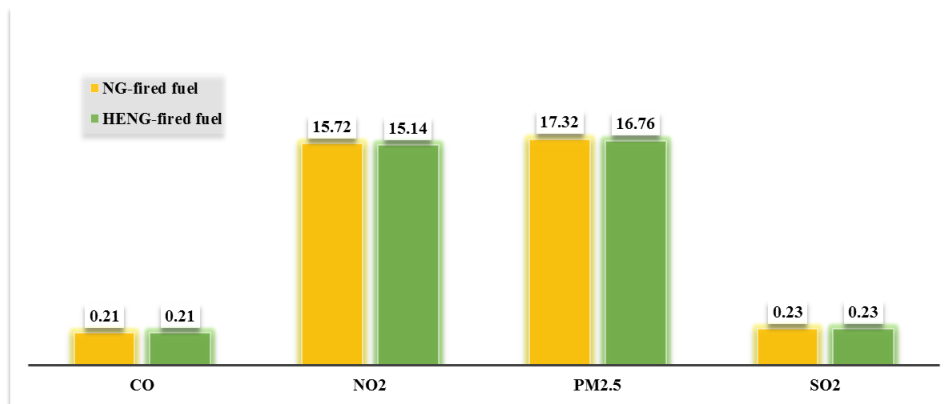
Figure (5.11): Comparing the costs of health Impacts for both fuels, $ per MWh

Neither CO nor SO_2 pollutants' health impact costs were affected by adding hydrogen into NG when fueling CCPP, whereas there is a partial positive saving of NO_2 and $PM_{2.5}$ pollutants in health

impact costs (Figure 5.11). Additionally, a comparison of the monetary value of both fuels is made (Table 5.10). While using HENG to fuel CCPP, the CO health impact cost was reduced by an average of 1.65%, while SO_2 health impact costs were reduced by only 0.5%. The NO_2 health impact cost had the highest reduction at 3.7% followed by the reduction of $PM_{2.5}$'s health impact cost, which averaged 3.3%. Incorporating the HENG fuel with a hydrogen concentration of up to 5% into energy supply system has enhanced the health impact's saving of NO_2 and $PM_{2.5}$ in terms of money saved in Canadian dollars per MWh. The average saving for both pollutants is around CAD $1.14 per MWh, which represents 3.4% of the health impact cost associated with using NG fuel.

Table (5.10): NG fuel vs. HENG fuel in costs of health impacts

Pollutants	Heath Impacts Criteria assigned by AQBAT	Monetary value, ($)		% Reduction in Health Impacts costs when using HENG fuel
		NG-fuel	HENG-fuel	
CO	Acute Exposure Mortality	126,043	124,185	1.5
	Elderly Cardiac Hospital Admissions	3,351	3,290	1.8
NO_2	Acute Exposure Mortality	9,593,637	9,235,759	3.7
$PM_{2.5}$	Acute Respiratory Symptom Days	277,237	269,381	2.8
	Adult Chronic Bronchitis Cases	4,122,748	3,994,400	3.1
	Asthma Symptom Days	32,556	31,470	3.3
	Cardiac Emergency Room Visits	10,570	10,223	3.3
	Child Acute Bronchitis Episodes	25,748	24,781	3.8
	Respiratory Emergency Room Visits	11,729	11,347	3.3
	Chronic Exposure Respiratory Mortality	6,085,237	5,883,704	3.3
SO_2	Acute Exposure Mortality	139,242	138,560	0.5

The cost of electrolysis-produced hydrogen from renewable energy sources in Canadian dollars per MWh was compared to health impact costs that are saved due to using HENG (Table 5.11). The total health impact savings on NO_2 and $PM_{2.5}$ pollutants is CAD \$1.14 per MWh, which is still less than the hydrogen production cost when its concentration in HENG is as high as 5%; therefore, HENG-fired fuel created from hydrogen that is produced from a renewable-electrolysis process is not yet the most economical solution for saving on the health impact from CCPP emissions.

Table (5.11): Comparing health impact costs saved with cost of producing hydrogen

Cost	\$/MWh
NO_2-health impacts cost saved due to using HENG fuel (5% hydrogen)	0.58
$PM_{2.5}$-health impacts cost saved due to using HENG fuel (5% hydrogen)	0.56
Average hydrogen production cost	60 -70

5.8.3 Sensitivity Analysis

A sensitivity analysis is performed in this section to assess the health impact savings while adding hydrogen into NG to fuel CCPPs and then compared to the LCOE as the total cost of electricity when meeting the on-peak power demand. The objective function is controlled by two categories: first is the increase in LCOE due to incorporating the cost of the electrolysis-produced hydrogen; and the second is the decrease in the cost of health impacts due to adding hydrogen into CCPP fuel (Fig. 5.12). Increasing the hydrogen concentration in HENG fuel from 1% to 5% will increase the LCOE from CAD \$100 to CAD \$140 per MWh. This is an increase of about 30%. At the same time, the cost of the health impact will decrease from CAD \$16 to CAD \$1 per MWh, for a decrease of about 94%. While increasing hydrogen concentration in HENG fuel, the LCOE is increasing; whereas the health impacts cost decreasing. The two lines are intersecting at hydrogen concentration of 2.3% (Fig. 5.12) which is considered as an optimum point. At a hydrogen concentration of 2.3%, the LCOE is found to be CAD \$111.4 per MWh while the cost of the health impact was calculated at CAD \$12.7 per MWh.
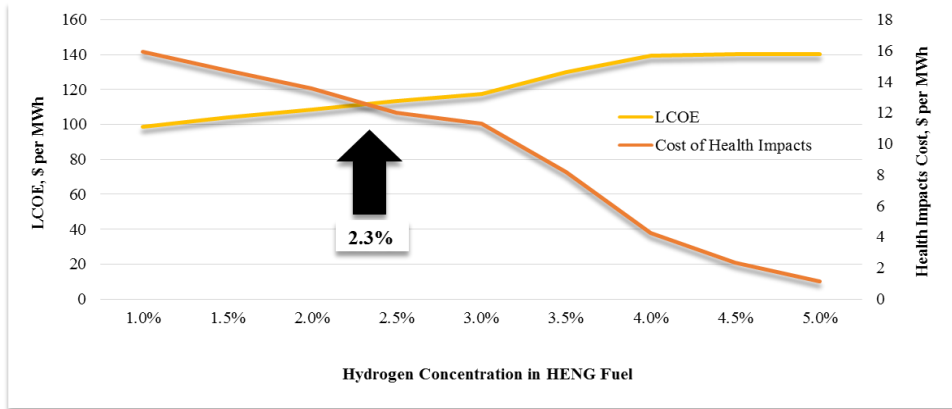
Figure (5.12): Comparing LCOE with cost of health impacts saved while using HENG fuel.

The next step of the sensitivity analysis was to measure the effect of cost components on the LCOE, and is performed at the optimum hydrogen concentration of 2.3%. Four main cost components compose the LCOE: costs associated with capital, cost of operation and maintenance (O&M), cost of fuel, and cost of health impacts. Each cost's component is increased by 20% and then reduced by 20% while calculating the LCOE in each step to assess how sensitive it is to these changes (Figure 5.13). At a LCOE level of CAD $111.4 per MWh, the health impact cost represented 11.4% of the total cost. Capital costs are the component that most impacted the LCOE followed by the fuel's cost, health impact's cost, and O&M's cost. In short, the costs of capital and fuel increased the LCOE significantly when incorporating more hydrogen in a CCPP's fuel due to utilizing more wind and solar power generation technologies and due to utilizing an extra number of electrolyzers.
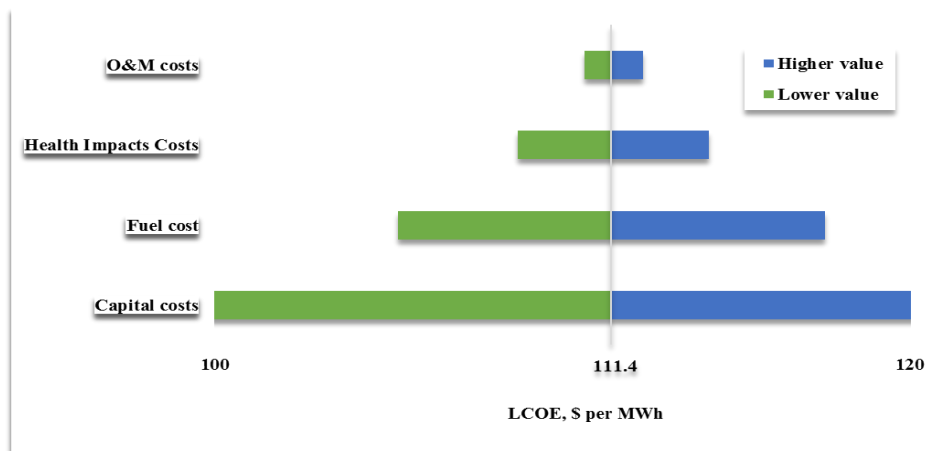
Figure (5.13): Comparing cost's components and assessing their impacts on LCOE

5.9 The Conclusions

This chapter presents a cost analysis of health impacts associated with emissions of air pollution from natural gas fueled combined cycle power plant. The hidden cost of electricity when generated from this facility is found to be CAD$33.5 per MWh due to the cost of health impacts associated with air pollution emission; this cost represents about 30% of the levelized cost of electricity for the on-peak power generation cost. The results show that $PM_{2.5}$'s emission has the most expensive health's cost due to the wide range of health impacts attributed to it, followed by NO_2, SO_2, and CO. Employing hydrogen enriched natural gas in fueling CCPP has reduce the cost of NO_2's health impacts by 3.7%, and reduce the cost of $PM_{2.5}$'s health impacts by 3.3%. For more saving on cost of health impacts, increasing hydrogen concentration in CCPP's fuel is examined. At hydrogen concentration of 2.3% is found to represent an optimum point when the LCOE is CAD$111.4 per MWh and the cost of health impacts is CAD$12.7 per MWh.

The uncertainties due to the morbidity studies that considered in monetizing the health impacts are analyzed and justified. The justification is performed by using real data from an existing power generation facility located on specified area, by using long-term statistical studies when correlating the increased pollutant's concentration to health damages, and by comparing the found results to the most related citations. Despite of the significant enhancement in health when incorporating hydrogen into CCPP's fuel, the electrolysis-renewable produced hydrogen is not yet the most economical solution for saving on health costs.

Chapter Six

6. Integration of Decentralized Energy Systems with Utility-Scale Energy Storage through Underground Hydrogen–Natural Gas Co-Storage Using the Energy Hub Approach

6.1 Introduction

There is a growing concern about the significant negative health and environmental impacts associated with emissions resulting from the increasing production and use of fossil fuel energy sources. The utilization of low carbon intensive fuels such as natural gas has been playing an important role in achieving emission reductions and transitioning to a low-carbon energy future. However, this role is limited as the attained emission reductions are being offset by the considerably increasing energy demands. Electricity demand is increasing at twice the rate of overall energy consumption, which is imposing the requirement of clean electricity production (Environment Canada, 2014).

The use of renewable energy sources in electricity generation as emission-free and sustainable alternatives has been considerably increasing in the energy mix of several markets around the world. Nuclear energy is considered to be the most efficient and reliable source for clean, large-scale, and around-the-clock electricity production. However, investments in nuclear energy are judged critically due to the significant external costs associated with the environmental impacts of radioactive waste storage and water consumption, as well as public and government acceptance and very long construction times (Ramana, 2009). Renewable energy sources such as wind and solar have a high cost per unit of output and are intermittent. However, they are suitable in providing a sustainable marginal clean power source (IRENA, 2015).

Canada is a world leader in the production and use of renewable energy resources, in which they account to approximately 65% of the country's electricity generation. The majority of which is hydroelectric power. Other renewable sources such as wind and solar have a relatively small market share, collectively accounting to 3 per cent of total electricity production and is expected to increase to 12 per cent by 2035 (CEA, 2014). The integration of these renewable sources is

typically done at building or residential level and contribute to a small share of total energy requirements.

There is significant dependence on large centralized energy systems that are mainly based on fossil fuels despite the negative impacts they impose on national security, global climate, and economy. Moreover, the limited capacity of primary fossil fuel resources will eventually hit a peak and decline. Current centralized energy systems (e.g. nuclear, coal, natural gas, etc.) are vulnerable to supply chain disturbances and failures (e.g. ageing, natural disasters). On the other hand, decentralized energy systems can improve reliability, accessibility, security of supply, and efficiency, and can reduce overall energy losses. Producing energy locally reduces imports of energy, which reduces transmission requirements and transportation losses. Community power is considered to be an important framework that can be utilized to provide communities with decentralized sources of renewable energy, and it is also considered to be a significant step towards a sustainable energy future. The potential benefits of this approach in harvesting clean renewable energy sources is increasingly receiving attention from policy makers and community groups. Community power are projects that locally sited, decentralized, and based on renewable energy technologies, which can either be grid-connected or stand-alone. The community power approach has received increasing attention in Canada, particularly Ontario since the adoption of the Green Energy and Green Economy Act, which includes a Feed-In-Tariff policy.

The reliable integration of sustainable decentralized energy systems such as solar photovoltaics and wind energy is a challenging task that requires proper demand side management in order to facilitate the efficient utilization of the produced energy. Thereby the intermittent generation of wind and solar units can be balanced to match peaks in electricity demand, in which, for example, energy storage can be utilized to store excess energy during off-peak hours and discharge stored energy during on-peak hours (Denholm, et al., 2010).

Forecasting renewable intermittent sources of energy and varying their output is a challenging task. The power generated from these resources must be sent to the grid as it is, which does not provide enough flexibility to vary production in order for it to match the market supply and demand. This hinders the viability of developing renewable energy projects, particularly when government subsidies are eliminated. However, the use of energy storage technologies can allow for an improvement in the profitability of these projects, which is achieved by making the power

output more predictable and dis-patchable. The utilization of storage technologies becomes more important as the penetration of renewable energy sources in the supply mix increases. This is because of the increase in the unpredictability of the power output (IRENA, 2015).

The application of an energy storage technology depends on its storage capacity, response time, and rate of storage and retrieval of energy. Technologies typically used in for grid energy storage include batteries, compressed air, capacitors, pumped hydro, flywheel, superconducting magnetic, and hydrogen. Among these options, energy storage through hydrogen offers a lot of advantages (Carnegie, et al., 2013). Hydrogen is characterized by having higher energy density compared to other common fluids (e.g. compressed air and pumped water). In addition, unlike other storage options the energy from hydrogen can be recovered and utilized at a different location from that of the storage facility. Moreover, hydrogen as an energy carrier has off-site applications as a valuable industrial feedstock and transportation fuel (Lipman, 2011).

There is still a lack of adequate energy carrier alternatives to fossil fuels. Over the recent years there has been an increasing interest in the concept of hydrogen economy, in which energy is stored and transported in the form of hydrogen. Delivering energy in the form of hydrogen provides a mitigation option to the environmental impacts of energy use and reduces concerns about the security of fossil-fuel supplies. As a final form of energy, hydrogen burns without producing harmful emissions. Moreover, if hydrogen is produced through a pathway that does not generate greenhouse gas emissions (e.g. renewables), it can form the basis of a highly sustainable energy system.

There are various methods for the storage of hydrogen, which are categorized based on its phase. Hydrogen can be stored as a compressed gas in above or underground storage facilities, as a cryogenic liquid, or as a solid hydride. The selection of a suitable storage method for hydrogen depends on its final application. At the utility scale and for the application of grid energy storage, hydrogen will be most commonly used in gaseous form when it is recovered (e.g. gas turbines) (Lipman, 2011) and (Burke & Gardiner, 2005). Therefore, for grid energy storage underground large scale storage of hydrogen is an attractive alternative. This is particularly true when considering the co-storage of hydrogen with natural gas in underground geologic formations as a mixture (Crotogino, et al., 2010).

The storage of natural gas underground is successful worldwide, and the co-storage of hydrogen in the existing storage infrastructure for natural gas is economically attractive due to the reduced capital investment requirement for the establishment of new hydrogen storage facilities (Melaina, et al., 2013). The hydrogen to be stored underground is produced through water electrolysis, which utilizes the excess power from decentralized energy systems (e.g. wind and solar) during off-peak demand hours. The hydrogen-enriched natural gas (HENG) mixture can then be recovered to be utilized in combine cycle gas turbines for the production of power, or the delivery of pure hydrogen or HENG to end users (e.g. transportation fuel or heating applications).

Recently the energy hub concept has emerged as a modeling framework that can be customized for analyzing and planning of future energy systems. The concept is used as a tool to determine the optimal configurations and operations of future energy systems, and develop the transition paths from the current aging energy systems to the future's optimum. The energy hub system allows for the distribution, conversion and storage of multiple energy carriers. There are various nodes that comprise an energy hub, which are multiple energy sources, different alternatives of energy conversion and storage technologies, distribution networks, and consumers. In addition to the various configurations of the nodes of the energy hub network, there are numerous alternatives for the energy flows among them, which provides an opportunity for the optimization of the multi-energy system (Geidl, et al., 2007).

The design and optimization of multi-energy systems incorporating decentralized energy systems has been addressed in several studies in the literature (Erdinc & Uzunoglu, 2012). Petruschke et al. (Petruschke, et al., 2014) developed a hybrid synthesis method for the design of renewable energy systems that is based on heuristic equipment preselection and superstructure-based optimization. Sharafi and ElMekkawy (Sharafi & ElMekkawy, 2014) proposed a hybrid multi-objective optimization-simulation approach for sizing renewable energy systems. Different multi-energy systems at the neighborhood level are designed and addressed in the literature, in which mathematical programming techniques were used to optimize their design and operations (Krajacic, et al., 2011), (Petruschke, et al., 2014), (Ren, et al., 2010), (Mehleri, et al., 2012), (Weber & Shah, 2011), and (Omu, et al., 2013).

However, these studies did not consider the use of energy storage technologies to facilitate the system's operations, or their design is limited only to a few operating days. Mehleri et al. (Mehleri,

et al., 2012) developed a mixed integer linear programming (MILP) model to determine the optimal configuration of distributed energy systems on a neighborhood level. Yang et al. (Yang, et al., 2015) and Wouters at al. (Wouters, et al., 2015) also proposed MILP models to design decentralized energy systems for residential neighborhoods, from which they determined that optimal configurations can result in annual cost reductions of up to 25%, and that combined heat and power units are essential for the efficient operations of residential micro-grids.

Another modeling approach that is used to integrate multiple energy systems and manage energy flows among them is based on the energy hub concept. The energy hub modeling approach is based on optimization techniques to determine the optimal configuration of energy hub designs, as well as optimal operating schedules for existing energy hubs. The application of this approach to the design of decentralized energy systems have been addressed in several studies in the literature. Maroufmashat et al. (Maroufmashat, et al., 2015) developed an optimization model to improve the economic and environmental performance of a complex network of energy hubs, for which it was determined that distributed energy provides significant advantages.

Orehouing et al. (Orehouing, et al., 2015) proposed a method for the integration of decentralized energy systems, such as biomass and photovoltaics, at a neighborhood scale based on the energy hub concept. Their method can be used to evaluate and size energy production and storage systems based on their economic and environmental performance, and allows for lowering peaks of energy demand and overall energy consumption.

Wasilewski (Wasilewski, 2015) addressed several limitation and operational constraints in the original energy hub model by reformulating the problem using the graph and network theory, which was verified by steady-state calculations. Several studies in the literature have also addressed the problem of determining optimal energy flows and schedules of multicarrier energy hub networks (La Scala, et al., 2014), (Brahman, et al., 2015), (Orehouing, K.; Evins, R.; Dorer, V.; Carmeliet, J., 2014), (Ramirez-Elizondo & Paap, 2015), and (Moghaddam, et al., 2016).

6.2 The Approach

In this study the energy hub concept is deployed (Geidl, et al., 2007), considering the integration of intermittent wind and solar renewable power generation with a set of dis-patch-able natural gas fueled CCPP to service a set community, to be referred to as the community energy hub. The integration of these power generation technologies is facilitated with the use of hydrogen generation for energy storage within the natural gas distribution system, which can be later retrieved to be utilized for power-to-gas-to-users or power-to-gas-to-power applications. In this manner, the community becomes an energy hub with power generation and energy storage within the hub. The community energy hub represented in Figure (6.1) is a delimited system, which balances energy flows within its boundaries, but it is also connected to the local natural gas distribution network to store or extract energy.
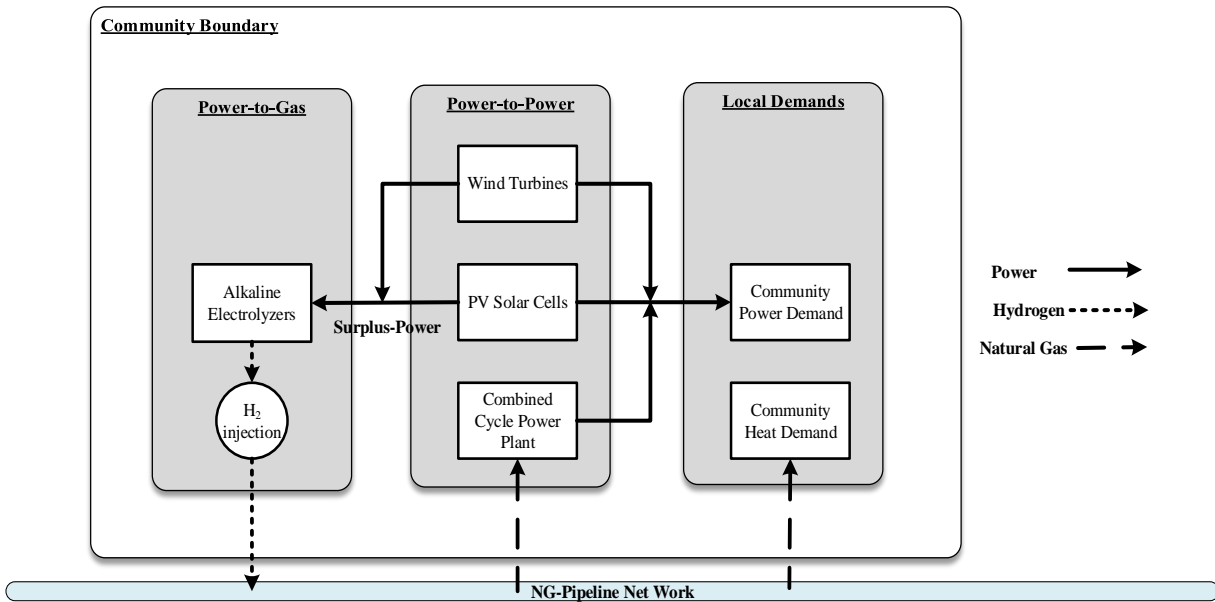
Figure (6.1): The superstructure of the energy hub system

A mathematical optimization model is formulated for an energy hub to represent energy systems, demand and supply at the community level. Energy systems for distribution, conversion and storage are integrated within the energy hub concept. The model is formulated based on the logic presented in Figure (6.2). The model is designed to use surplus-power from wind and solar whenever they are available and during off-peak demand hours to supply a set of electrolyzers for producing hydrogen. Electrolytic hydrogen will mixed with natural gas and stored in UHNG.

The HENG can be recovered and utilized in two different ways, which are to fuel CCPP for power production, or distributed through the NG-pipeline to the community's end users. Available energy flows from potential energy sources is used as an input into the energy hub model. Energy sources include decentralized energy systems, which are distributed solar photovoltaic panels and wind turbine generators. In addition, dis-patchable NG-fueled CCPP can also supply electricity in the energy hub. Moreover, input data including hourly electricity load profiles of the community, as well as the natural gas demand requirements for end-users (e.g. heating applications) are considered. The amount of hydrogen demanded depends on the total amount of natural gas requirements, as well as the optimal concentration of hydrogen in the HENG fuel. The model allows for the assessment of the synergy between natural gas based dis-patch-able power generation and wind and solar energy sources, as well as the synergy between the use of natural gas and hydrogen.
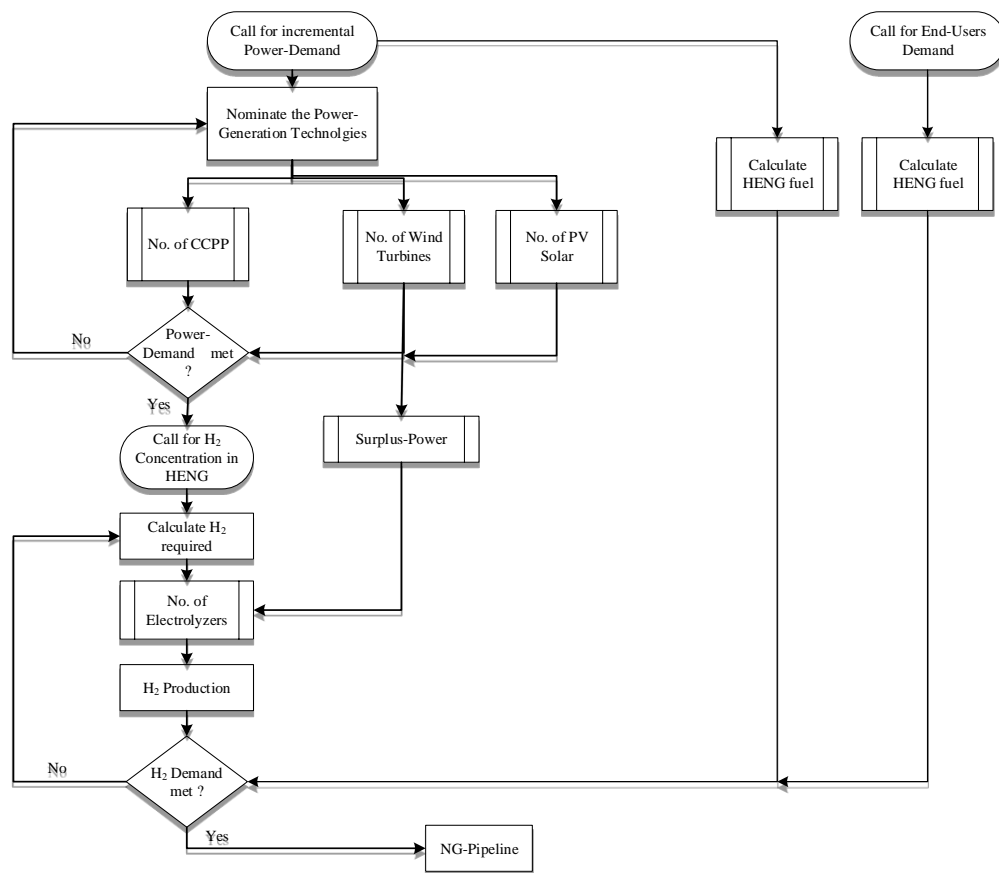
Figure (6.2): Energy flow in the energy hub system

The mathematical model of the energy hub is combined with optimization techniques with an objective function geared towards cost minimization. The cost objective includes the investment and operating costs of power and hydrogen producers, fuel costs, and the health impact costs associated with the generated emissions. The input data for the optimization model include the power demand of the community, capital and operating costs of power and hydrogen production technologies, fuel emission factors (CO_2, CO, NO_2, $PM_{2.5}$ and SO_2) and their associated health impacts costs, and the performance characteristics of all the technologies considered in the system. The model is subject to a set of design constraints that balances the energy supply and demand within the system boundaries, as well as capacity constraints for the energy systems for distribution, conversion and storage.

The proposed model is used to determine the optimal combination of renewable energy sources (i.e. solar photovoltaic and wind generators) and dis-patch-able NG-fueled CCPP, and the optimal configuration of the UHNG storage system required to achieve energy autonomy and curtail peaks in energy demand. The decisions variables include the number of power generation units, amount of power produced from wind generators, solar panels and CCPP, flowrate of hydrogen produced from electrolyzers, flowrate of HENG to CCPP and end users, flowrate of hydrogen to end users, and the concentration of hydrogen in the HENG. The resulting model is a Mixed Integer Program (MIP) representing the energy hub system. The proposed mathematical model is solved using the General Algebraic Modeling Software (GAMS). The solver used for the MIP model is CPLEX.

In order to illustrate its applicability, the model is applied to a case study of an existing community in southern Ontario, in which the local-electrical demand is constituted by residential, commercial and industrial facilities. The average on-peak power demand is 200 MWh. This region is selected because of its wind and solar potential, location to major electrical and natural gas distribution system assets, and the diversity of power demand (i.e. industrial and residential).

6.3 The Mathematical-Optimization Model

The proposed problem is formulated as a multi-objective MILP optimization model with the following notations:

6.3.1 Model's Indices

c capacity level of electrolyzer;

e pollutant (CO, NO_2, $PM_{2.5}$, SO_2, and CO_2);

f fuel (NG and hydrogen);

h time period (8760 hours per year); and,

t power generation technology (t1: CCPP, t2: wind turbines, and t3: solar PV);

6.3.2 Model's Sets

C: set of capacity levels of electrolyzers;

E: set of pollutants (CO, NO_2, $PM_{2.5}$, SO_2, and CO_2);

F: set of fuels (NG and hydrogen);

H: set of time periods (8760 hours per year); and,

T: set of power generation technologies (CCPP, wind turbines, and solar PV);

6.3.3 Model's Parameters

AF: Amortization factor of capital cost;

$AELz^{constant}$: Power constant of electrolyzer (MW per kmol H_2);

$AELz^{Efficiency}$: Efficiency of electrolyzer (%);

$AELz_c^{Max}$: Maximum capacity of electrolyzer "*c*" (MW);

$AELz_c^{Min}$: Minimum capacity of electrolyzer "*c*" (MW);

BI_h : Binary parameter, "1" when hour "*h*" is an on-peak demand (>30 MW), "0" otherwise;

$CAPS^{max}$: Maximum capacity of hydrogen storage tank (kg);

$C_t^{capital}$: Capital cost of power generation technology "t" ($ per MW);

$CC_c^{capital}$: Capital cost of electrolyzer capacity level "c" ($ per MW);

$CS^{capital}$: Capital cost of hydrogen storage tanks ($ per kg);

$C_t^{O\&M}$: Operating and maintenance cost of power generation technology "t" ($ per MWh);

$CC^{O\&M}$: Operating and maintenance cost of electrolyzers ($ per MWh);

$CS^{O\&M}$: Operating and maintenance cost of hydrogen storage tanks ($ per kg.hour);

C_f: Cost of fuel "f" ($ per kmol);

$C_{e,f}$: Cost of health impacts associated with emissions of pollutant "e" from fuel "f" ($ per kmol);

$Demand_h^{Power}$: Hourly power-demand (MWh);

$Demand_h^{End-Users}$: Hourly incremental heat-demand (MJ per hour);

Eff_t : Efficiency of power generation technology "t" (%);

$ER_{e,f}$: Emissions rate of pollutant "e" from fuel "f" (kmol pollutant per kmol fuel);

ET_t^{max}: Maximum capacity of existing power technology "t" (MW);

EC^{max}: Maximum capacity of existing electrolyzers (MW);

ES^{max}; Maximum capacity of existing hydrogen storage (kmol);

FIT_t: Feed in tariff associated with power production technology "t" ($ per MWh);

H_2^{MAX}: Maximum allowable hydrogen concentration in NG-pipeline and in the HENG fuel (%);

HHv_f: High heating value of fuel "f" (MJ per kmol);

$P_t^{nominal}$: Nominal power of power generation technology "t" (MW); and,

W: Weight set on the emission objective function ($0 - 1$).

6.3.4 Model's Continuous Variables

$Cost_{capt.}$: Capital cost of power generation technologies ($ per year);

$Cost_{O\&M}$: O&M's costs of power generation technologies ($ per year);

$Cost_{fuel}$: Fuel cost ($ per year);

$Cost_{emissions}$: Cost of health impact associated with emissions ($ per year);

$TCost$: Total annual cost ($ per year);

$Fuelin_{f,h}$: Flow rate of fuel entering NG-pipeline (kmol per hour);

$FuelOut1_{f,h}$: Flow rate of fuel-fired in CCPP for meeting power demand (kmol per hour);

$FuelOut2_{f,h}$: Flow rate of fuel-fired for meeting end-users demand (kmol per hour);

$FuelInventory_{f,h}$: Fuel inventory inside NG-pipeline (kmol per hour);

$H_{2h}^{produced}$: Hydrogen produced at hour "h" (kmol per hour);

$H_{2h}^{storein}$: Hydrogen sent to storage tanks at hour "h" (kmol per hour);

$H_{2h}^{storeout}$: Hydrogen retrieved from storage tanks at hour "h" (kmol per hour);

$H_{2h}^{invertory}$: Hydrogen remaining in inventory at hour "h" (kmol per hour);

PCU_h: Power curtailed at hour "h" (MWh);

P_h^{AELZ}: Power supplied to the electrolyzers at hour "h" (MWh);

$P_{c,h}^{AELZ}$: Power supplied to electrolyzers of capacity level "c" at hour "h" (MWh);

$P_{t,h}^{Total}$: Total power produced from technology "t" at hour "h" (MWh);

$P_{t,h}^{AElz}$: Power sent from technology "t" to electrolyzers at hour "h" (MWh); and,

$P_{t,h}^{Demand}$: Power used by technology "t" to satisfy power demand at hour "h" (MWh).

6.3.5   Model's Integer Variables

N_c^{AElz}: Number of electrolyzers selected of each capacity level "c";

N^{CCPP}: Number of CCPP units;

N^{PV}: Number of solar PV units;

N^{WT}: Number of wind turbines; and

N^S: Number of hydrogen storage tanks.

6.3.6   Model's Binary Variables

YET_t: "1" indicates the existing power production capacity of technology "t" is operational, "0" otherwise;

YC : "1" indicates the existing electrolyzer capacity is operational, "0" otherwise;

$YElz_c$: "1" indicates the electrolyzer of capacity level "c" is selected, "0" otherwise; and,

YS : "1" indicates the existing hydrogen storage capacity is operational, "0" otherwise.

6.3.7   Model's Constraints

The hourly power generated by CCPP units in MWh ($\mathbf{P_{t1,h}}$) is calculated as shown in presented Eqn. (6.1), where $\mathbf{FuelOut1_{f,h}}$ is the fuel consumption rate in kmol h⁻¹, HHv_f is the high heating value of the fuel consumed (MJ kmol⁻¹), and $\mathbf{Eff_{t1}}$ is the efficiency of CCPP unit.

$$P_{t1,h} = \sum_f HHv_f * FuelOut1_{f,h} * Eff_{t1} / 3{,}600 \qquad (6.1)$$

The power generation by a wind turbine unit is calculated as shown in Eqn. (6.2):

$$P_{t2,h} = 0.5 * \rho_{air} * A_{rotor} * V_h^3 * Eff_{t2} / 1{,}000{,}000 \qquad (6.2)$$

Where: $\boldsymbol{\rho_{air}}$ is the air density in kg m⁻³, $\mathbf{A_{rotor}}$ is the wind turbine rotor area in m², $\mathbf{V_h}$ is the hourly wind speed at 80 m altitude in m s⁻¹, and $\mathbf{Eff_{t2}}$ is the efficiency of the considered wind turbine.

The power generation by solar PV panels is calculated as shown in Eqn. (6.3); where: W_h is the hourly insolation in MJ m^{-2}, A_{cell} is the solar cell area in m^2, and Eff_{t3} is the efficiency of solar panels.

$$P_{t3,h} = W_h * A_{cell} * Eff_{t3}/3,600 \tag{6.3}$$

The power production technologies are constrained by their maximum capacities. The power generated from each technology in every hour $P_{t,h}$ should not exceed the maximum capacity ($P_t^{nominal}$) of all the available newly established units (N_t) and the existing generating capacity (ET_t^{Max}). This is presented as follows:

$$P_{t,h}^{Total} \leq N_t * P_t^{nominal} + YET_t * ET_t^{Max} \tag{6.4}$$

Two possible scenarios are considered in the proposed model. The first one involves a least cost scenario, in which the power demand can be satisfied by CCPPs and renewables during all operational hours; whereas second scenario considers a revaluation of the renewable base load demand, in which the CCPP units are constrained to provide power only during on-peak demand hours. The first scenario is modeled by the following constraint in which the power generated from all power production technologies is used to satisfy the total demand during all operational hours.

$$\sum_{t=1}^{3} P_{t,h}^{Demand} \geq Demand_h^{Power} \tag{6.5}$$

The second scenario is modeled by the Eqns. (6.6) and (6.7), in which the power generated by all production technologies can be used to satisfy demand during on-peak demand hours (Eqn. 6.6). The binary parameter BI_h is used to indicate whether or not hour "h" is an on-peak demand hour (e.g. Off-peak demand assumed to be < 30 MW). The demand during off-peak can be satisfied only by wind and solar power (Eqn. 6.7):

$$\sum_{t=1}^{3} P_{t,h}^{Demand} \geq Demand_h^{Power} * BI_h \tag{6.6}$$

$$P_{t2,h}^{Demand} + P_{t3,h}^{Demand} \geq Demand_h^{Power} * (1 - BI_h) \tag{6.7}$$

To ensure that the power demand is satisfied during on-peak hours the CCPP units are incorporated due to their availability and dis-patch-ability. Normally, the wind power availability varies

between 30 – 40%, and the solar power availability can hardly reach 20%; whereas the availability of CCPP is above 90%. The power generated from wind and solar power can be used to satisfy part of the demand, and the surplus of their power is sent to electrolyzers. Surplus power might also be sold to the grid or curtailed. One of the objectives of the proposed model is to minimize power losses from all the power production technologies. The total power produced from each technology can generally be expressed as shown in Eqn. (6.8):

$$P_{t,h}^{Total} = P_{t,h}^{Demand} + P_{t,h}^{AElz} + P_{t,h}^{loss} + P_{t,h}^{Grid} \tag{6.8}$$

The surplus power available from wind and solar during off-peak periods is sent to satisfy the power requirements of electrolyzers as shown in Eqn. (6.9):

$$P_h^{AELz} = P_{t2,\ h}^{Elz} + P_{t3,\ h}^{Elz} \tag{6.9}$$

The hourly energy required for end-users demand is satisfied by HENG fuel as shown from Eqn. (6.10):

$$\sum_f HHv_f * FeulOut2_{f,h} \geq Demand_h^{End-Users} \tag{6.10}$$

The hydrogen produced in kmol h^{-1} from electrolyzers ($H_{2h}^{produced}$) is calculated by using Eqn. (6.11), which is obtained by diving the power sent to electrolyzers (P_h^{AELz}) in MWh by the power constant ($AELz^{constant}$) in MW per kmol.

$$H_{2h}^{produced} = P_h^{AELz} * AELz^{Efficiency} / AELz^{constant} \tag{6.11}$$

In order to maximize the capacity factor of electrolyzers when they are operational, it is important to size the electrolyzer units and the capacity of the electrolyzer farm. The different sizes of electrolyzer units are discretized, and the total power sent to electrolyzers can be expressed as shown in Eqn. (6.12):

$$P_h^{AELz} = \sum_c P_{c,h}^{AELZ} \tag{6.12}$$

Where: $P_{c,h}^{AELZ}$ is the power sent to each capacity level of electrolyzers considered. The capacity constraint of electrolyzers is presented in Eqn. (6.13) in which the total number of electrolyzers (N_c^{AElz}) selected must satisfy the total required hydrogen production ($H_{2h}^{produced}$).

The $\mathbf{AELz_c^{Max}}$ is the maximum capacity of an electrolyzer in kmol h^{-1} and $\mathbf{AElz_c^{Min}}$ is the minimum capacity of each capacity level. $\mathbf{EC^{max}}$ is the maximum capacity available from existing electrolyzers. Satisfying this constraint ensures that the capacity factor of the electrolyzers is within an adequate range when they are operational.

$$\sum_c N_c^{AElz} * AElz_c^{Min} \leq H_{2_h}^{produced} \leq \sum_c N_c^{AElz} * AElz_c^{Max} + EC^{max} * YC \tag{6.13}$$

Two scenarios are considered for the storage of hydrogen produced by electrolyzers. Hydrogen can be either held in inventory in natural gas distribution pipelines or stored in hydrogen tanks. Pipeline hydrogen storage can be presented as a material balance performed on hydrogen through the NG-pipeline. The hydrogen produced by the electrolyzers is assumed to be injected directly into the NG-pipeline, therefore, the amount of hydrogen produced is equal to the amount of hydrogen that enters the NG-pipeline as shown in Eqn. (6.14). Hydrogen is blended with NG to create HENG fuel with a concentration that does not exceed 5%, and the inventory of hydrogen in the NG-pipeline can be presented as shown in Eqn. (6.15):

$$H_{2_h}^{produced} = Fuelin_{f2,h} \tag{6.14}$$

$$Fuelinventory_{f,h} = Fuelinventory_{f,h-1} + Fuelin_{f,h} - FuelOut1_{f,h} - FuelOut2_{f,h} \tag{6.15}$$

The HENG fuel that exit from the NG-pipeline is equal to HENG fuel that feeds CCPP units plus the HENG fuel that used for meeting end-users demand. The concentration of hydrogen in molar percentage that is injected in the natural gas pipeline to produce HENG for fueling CCPP units or distributed among end-users should not exceed the maximum allowable hydrogen concentration, which for the base case is assumed to be 5%. This is presented by Eqn. (6.16) and (6.17):

$$FuelOut1_{f,h} + FuelOut2_{f,h} = FuelOut_{f,h} \tag{6.16}$$

$$FuelOut_{f2,h} \leq H_2^{MAX} * \sum_{f=1}^{2} FuelOut_{f,h} \tag{6.17}$$

The other option for hydrogen storage is to utilize hydrogen storage tanks. In this case the hydrogen produced from electrolyzers is either injected directly into the pipeline to be utilize in CCPP units or for end-user demand, or sent to the storage tanks to be held in inventory. The purpose of incorporating hydrogen storage tanks is to provide adequate capacity to manage surplus energy produced from wind and solar, which is important due to the limited capacity of hydrogen that can

be injected into the NG-pipeline (i.e. 5%). The material balance on hydrogen for this scenario can be presented as follows in the Eqns. (6.18), (6.19) and (6.20):

$$H_{2h}^{produced} = H_{2h}^{to\ pipe} + H_{2h}^{storein} \tag{6.18}$$

$$H_{2h}^{inventory} = H_{2h-1}^{inventory} + H_{2h}^{storein} - H_{2h}^{storeout} \tag{6.19}$$

$$FuelOut_{f2,h} = H_{2h}^{to\ pipe} + H_{2h}^{storeout} \tag{6.20}$$

Similarly, the constraint presented in Eqn. (6.17) will apply to this scenario to limit the concentration of hydrogen in the HENG sent to the CCPP units and end-user demand. The number of new hydrogen storage tanks installed and the capacity of existing storage must accommodate the inventory levels during all hours, which is presented by the following constraint.

$$H_{2h}^{inventory} \leq N^S * CAPS^{max} + ES^{max} * YS \tag{6.21}$$

6.3.8   The Model's Objective Function

In this model, three objective functions are taken into account:

Z1: total cost of electricity production and storage, including capital and operating cost of power production plants (CCPP units, wind turbines and solar PV), capital and operating cost of electrolyzers and hydrogen storage tanks.

Z2: total costs of emissions, which takes into account various pollutants (i.e. CO_2, CO, NO_2, SO_2, and $PM_{2.5}$).

Z3: energy losses, which is the total power curtailment.

The total cost of electricity produced and stored including capital costs, operating costs and fuel costs (i.e. natural gas) are calculated. The capital cost of power production technologies, electrolyzers and hydrogen storage tanks is calculated by multiplying the number of new units installed by the unit capital cost, maximum capacity, and the amortization factor. This is presented as follows:

$$Cost_{capital} = \sum_t N_t * P_t^{nominal} * C_t^{capital} * AF + \sum_c N_c^{AELz} * AELz_c^{Max} * CC_c^{capital} * AF + N^S$$
$$* CAPS^{Max} * CS^{capital} * AF \tag{6.22}$$

The amortization factor is calculated as presented in Eqn. (6.23); where: r is the interest rate that is assumed to be 8%, and n is the lifetime of the power generation technology that is assumed to be 25 years.

$$AF = (1 + {}^r/_{12})^n ({}^r/_{12})/(1 + {}^r/_{12})^{n-1} \tag{6.23}$$

The operation and maintenance cost is calculated by multiplying the production rate or inventory level at every operational hour "h" by the unit cost, which is presented as shown in Eqn. (6.24). The annual cost of operation is calculated by summing the cost over all time periods. For the scenarios in which interactions with the gird are considered, the revenue obtained from selling excess power from wind and solar energy to the grid (according to the feed in tariff in Ontario) is subtracted from the annual operational cost.

$$Cost_{O\&M} = \sum_h \left(\sum_t P_{t,h} * C_t^{O\&M} + \sum_c PC_{c,h}^{AElz} * CC^{O\&M} + H_{2h}^{inventory} * CS^{O\&M} - \sum_t P_{t,h}^{Grid} * FIT_t \right) \tag{6.24}$$

The cost of fuel utilized is the cost of natural gas consumed in CCPP units and by end-users. Hydrogen cost has already been considered as the cost of installing and operating electrolyzers. The natural gas cost can be calculated as follows by multiplying the total natural gas consumption in each hour by the fuel unit cost as in Eqn. (6.25):

$$Cost_{fuel} = \sum_h FuelOut_{f1,h} * C_{f1} \tag{6.25}$$

The total cost of electricity production and storage can then be calculated as the sum of capital, operating and fuel costs as represented by Eqn. (6.26):

$$Cost^{Total} = Cost_{capt.} + Cost_{O\&M} + Cost_{fuel} \tag{6.26}$$

The total cost of emissions includes the cost of emitting global warming gases and the health impact costs associated with air pollutants. The emission of these pollutants is associated with the consumption of natural gas. The cost of emissions can be calculated as presented in Eqn. (6.27), where $FuelOut_{f1,h}$ is the flowrate of natural gas in the HENG fuel in kmol h^{-1}; $ER_{f1, e}$ is the emission rate of each pollutant produced from the consumption of natural gas expressed as kmol of pollutant "e" per kmol of NG; and $C_{f,e}$ is the emission cost factor associated with each

pollutant in dollars per kmol of the pollutant, which were obtained from a previous study (AlRafea, et al., 2016).

$$\text{Cost}_{\text{emissions}} = \sum_{h} \sum_{e} C_{f1,e} * \text{FuelOut}_{f1,h} / ER_{f1\ e} \qquad (6.27)$$

The total power losses is the surplus power generated by wind and solar sources that is not utilized to satisfy the demand, sent to electrolyzers to produce hydrogen, or sold to the grid. It is presented as the summation of power losses over all time periods as calculated in Eqn. (6.28):

$$\text{Powercurtailed} = \sum_{h} \sum_{t \in t2 \cup t3} P_{t,h}^{loss} \qquad (6.28)$$

The proposed multi-objective MILP formulation takes Eqns. (6.26), (6.27) and (6.28) as the objective functions labelled **Z1**, **Z2** and **Z3**. The multi-objective optimization problem can then be presented as follows:

$$\min_{x \in F} \{z_1(x), z_2(x), z_3(x)\} \qquad (6.29)$$

Where: **X** is the vector of decision variables in the space of feasible region **F**. The solution approach of the proposed multi-objective mathematical model is the ε-constraint method adopted from Liu and Papageorgiou (Liu & Papageorgiou, 2013). The objective functions can, therefore, be presented as follows:

$$\begin{aligned} \min_{x \in F} & \ z_1(x) \\ \text{s.t.} \ & z_2(x) \le \varepsilon_2 \\ & z_3(x) \le \varepsilon_3 \end{aligned} \qquad (6.30)$$

Where: the value of ε_3 can be obtained as follows:

$$\varepsilon_3 = \varphi \sum_{h} \sum_{t} P_{t,h} \qquad (6.31)$$

Where: $\varphi \in [0, 1]$ indicates the maximum percentage of total power losses to the total power production level. Two sub-problems are solved in order to obtain the value of ε_2. The maximum and minimum values of ε_2 are obtained by solving the following two sub-problems individually,

$$\underset{\mathbf{x} \in F}{\min} \mathbf{z_1(x)}$$
$$\text{s.t. } \mathbf{z_3(x)} \le \varepsilon_3 \tag{6.32}$$

As well as:

$$\underset{\mathbf{x} \in F}{\min} \mathbf{z_2(x)}$$
$$\text{s.t. } \mathbf{z_3(x)} \le \varepsilon_3 \tag{6.33}$$

In both of these sub-problems the objective **Z3** is constrained by $\boldsymbol{\varepsilon_3}$. In the problem defined in Eqn. (6.32), **Z1** is the objective, while **Z2** is eliminated, from which the maximum possible value of **Z2** is obtained. In the problem defined in Eqn. (6.33), **Z2** is the objective, while **Z1** is eliminated, from which the minimum possible value of **Z2** is obtained. The problem defined in Eqn. (6.30) can then be solved by defining $\boldsymbol{\varepsilon_2}$ as follows:

$$\varepsilon_2 = \omega z_2^{max} + (1 - \omega)z_2^{min} \tag{6.34}$$

Where: $\boldsymbol{\omega} \in [\mathbf{0, 1}]$ indicates the weight set on the emissions cost objective function.

6.3.9   The Model's Assumptions

The following assumptions are considered while running the model:

(1) There is no leak of hydrogen from NG-pipeline;

(2) For model simplicity it is assumed that there is no need for compression or pressure release when injected hydrogen inside NG-pipeline; and

(3) It is assumed that the hydrogen concentration in HENG fuel is controlled while leaving the NG-pipeline.

6.4 Demand Analysis

There are two scenarios investigated in this case study, which are based on the recovery pathways for the stored HENG fuel. The first scenario is power-to-gas-to-power pathway is incorporated, in which the HENG is used to produce electricity through CCPP units; the second scenario is power-to-gas-to-end user in which the HENG is sent for meeting end-users demand of heating and other

appliances. The proposed scenarios and their analysis are used to illustrate the benefits of storing surplus-power from wind generators and solar panels during off-peak demand hours in the form of hydrogen in the underground natural gas network.

In order to explore the potential of the energy hub system model proposed in this study, it is applied to a case study based on a community in southern Ontario. The power demand in this community is diverse, including demand by residential, commercial and industrial entities. This region is selected because of its wind and solar energy potential, location to major electrical and natural gas distribution system assets, and the diversity of power demand. The hourly demand profile for a winter and summer day in this region is show in Figure (6.3). The average on-peak power demand is 200 MWh.
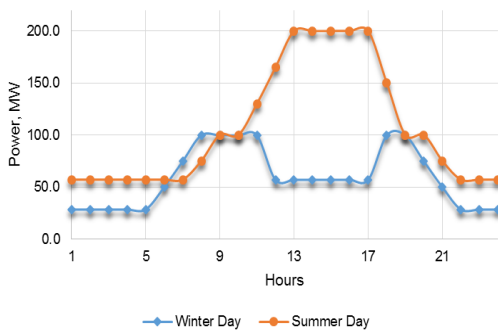
a. Power demand in winter day vs. summer day	b. Power demand vs. heat demand in full year
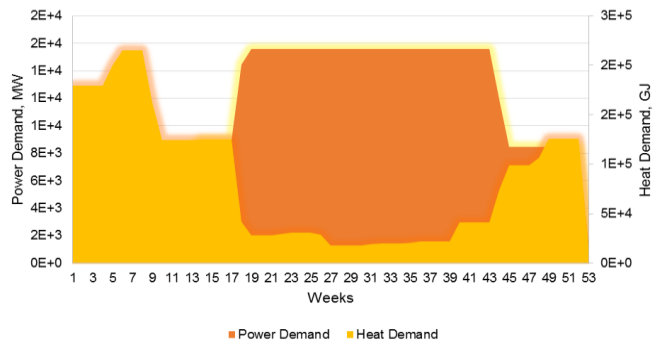
Figure (6.3): Power and end-users demands profile

The proposed power demand as shown in Figure (6.3), is considered to be enough for one community that has the size of a small city or town. As the average power consumption in Canada per person for the residential sector is approximately 5 MWh per year, the proposed power demand will be suitable to address a town that has a population of 200,000 – 300,000 people accompanied with commercial and industrial infrastructures.

An estimation of the average consumption of natural gas by the community's end users was conducted. Natural gas can be used for home and water heating, as well as fuel for other appliances such as stoves, dryers and barbecues. A recent study indicates that the natural gas consumption by Ontario's residents averaged approximately 2,500 m^3 per person per year (NAVIGANT, 2014).

Canadian households used a total of 639,203 TJ worth of natural gas in their homes in 2011, up 9% from 2007 (Statistics Canada, 2015). Households using natural gas consumed an average of 92 GJ of this fuel per household (Statistics Canada, 2015). Based on the size of the community assumed in this study the natural gas demand profile was estimated (Figure 6.4).
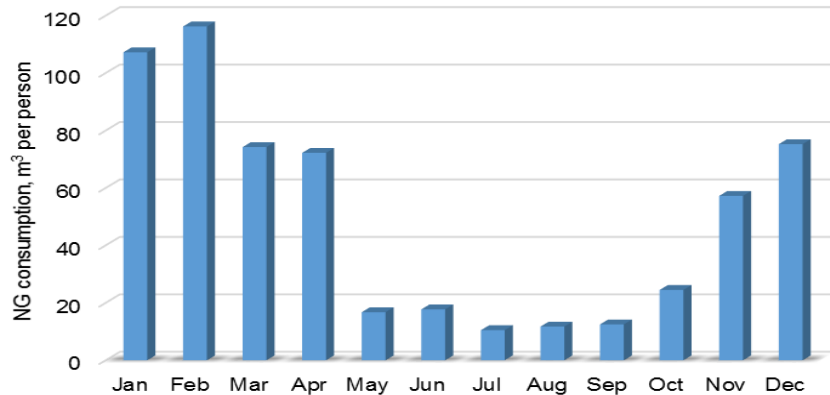
Figure (6.4) Natural gas demand for community's end users

6.5 Energy Production Technologies

The proposed energy production technologies considered in the optimization model include NG-fired CCPP, on-shore wind turbines, and PV-solar panels for power production, as well as alkaline electrolyzers for hydrogen production. The mixed integer linear model allows for design of a system through the incremental discrete addition of each of the key technologies, in order to optimize the energy hub system design based on net cost of electricity provision to the community.

6.5.1 Natural Gas Combined Cycle Power Plant

The NG-fired CCPP is used as the dis-patch-able power generation facility in the proposed model with a maximum capacity of 100 MW (Siemens , 2008) . The power plant consists of a gas turbine generator fueled by NG, a heat recovery steam generator, and a triple pressure, reheat and full condensing steam turbine generator. The thermal efficiency of the plant is assumed to be 52.6%. The capital and operating costs of NG-CCPP units with the required capacity are cited in multiple sources in the literature. The Environmental Protection Agency, National Renewable Energy

Laboratory, and Energy Information Administration, stated the capital and operating cost of NG-CCPP units to be $903,000 per MW and $1.95 per MWh (EPA, 2010), $742,000 per MW and $2.86 per MWh (Tidball, et al., 2010), and $1,023,000 per MW and $3.27 per MWh (US EIA, 2013), respectively. The averages of these values are assumed as the input for capital and operating costs in the proposed model.

The natural gas required for operating the CCPP is purchased from the NG-pipeline network that is available in the community energy hub region. The average price of NG is assumed to be $4.4 per GJ (Natural Resources Canada, 2014), and the high heating value is assumed to be 52 MJ per kg (Boundy, et al., 2011). The atmospheric emissions from the proposed CCPP during operations include: CO_2, CO, NO_2 resulting from incomplete combustion, and $PM_{2.5}$ resulting from mercaptan odorant additive. All of these pollutants are produced from processes utilizing natural gas as a burning fuel (Siemens , 2008). The emission factors of NG-fueled CCPP and the associated health impact costs have been cited in various literature sources (Skone & James, 2012) , (Black, 2013), and (Spath & Mann, 2000).

6.5.2   On-Shore Wind Turbines

The considered on-shore wind turbines have an average capacity of 1.91 MW, which is the average nameplate capacity installed in 2013 in Ontario (Mone, et al., 2015). The capital and operating costs are provided by Lawrence Berkeley National (LBN), EIA and NREL as $2,120,000 per MW and $8 per MWh (Wiser & Bolinger, 2009), $2,213,000 per MW and $11 per MWh (US EIA, 2013), (NAVIGANT, 2014), and $1,728,000 per MW and $13 per MWh (Mone, et al., 2015), respectively. The location of Chatham-Kent, Ontario is selected to install the wind turbines used in the energy hub system due to the high wind speed potential and its close proximity to nearby on-shore wind farms. The expected wind speed in this location varies from 5.35 m s^{-1} during the summer to 8.16 m s^{-1} during the winter. The average annual wind speed is estimated to be approximately 7 m s^{-1} (Environment Canada, 2008).

6.5.3　Photovoltaic Solar

The solar photovoltaic module considered in the proposed energy hub system has a maximum capacity of 117.5 kW, dimensions of 1.2 m by 0.6 m, and power rate of 163.2 W per m^2 (First Solar, 2015). Solar PV systems are typically characterized by having high investment cost and low operation cost. The PV capital cost includes equipment, site preparation, land, permitting & commissioning, labor, and material costs. The capital and operating costs of solar PV panels have been listed by NREL, LBNL, and International Renewable Energy Agency as $4M per MW and $2.3 per MWh (Goodrich, et al., 2011), $4.7M per MW and $3.2 per MWh (Feldman, et al., 2012), and $3.5M per MW and $1.0 per MWh (IRENA, 2015), respectively. The location of Chatham-Kent, Ontario has significant potential for photovoltaic insolation. The expected mean daily insolation varies from 9 – 12 MJ per m^2 during the winter time to 21 – 24 MJ per m^2 during the summer (Natural Resources Canada, 2013).

6.5.4　Alkaline Electrolyzers

One of the key advantages of electrolyzers among other methods for producing hydrogen is the suitability of the technology to adjust to different energy inputs, which is beneficial when integrated with intermittent wind and solar energy. On the smaller end of the scale, distributed electrolyzers can be used to produce hydrogen for use in the same location. The electrolyzers play a significant role in the proposed de-centralized energy hub system as they increase the availability and reliability of wind and solar energy sources. Due to their wide operational range, eletrolyzers can respond very quickly to changes in input-power (FuelCellToday, 2013). The electrolytic hydrogen is assumed to be produced by commercial alkaline electrolyzers, due to their high efficiency that could reach above 70% (Hydrogenics, 2015). This type of electrolyzer is assumed to have a power constant of 0.052 MWh per kg of hydrogen, and a nominal hydrogen flow of 60 Nm^3 per hour. The delivery pressure is 10 barg, and the ambient temperature range is -20°C to +40°C. The hydrogen produced by this electrolyzer has a purity >99% (Hydrogenics, 2015). The maximum capacity of the selected electrolyzer for producing hydrogen is approximately 5.3 kg per hour. For this capacity, the hydrogen production cost can be divided into three main categories, which are the cost of supplied electricity, capital cost, and the operation and maintenance cost (Saur, 2008). The cost of hydrogen production from alkaline electrolyzers ranges from $4.0 – 5.7 per kg for a capacity of 42 – 63 kg per hour (Steward, et al., 2009) , (Levene, et al., 2005) and

(Genovese, et al., 2009). The techno-economic parameters of the proposed energy producers are summarized in Table (6.1). These include the production capacities, operating efficiencies, and the capital and operating costs of natural gas fired turbines, wind generators, solar panels and electrolyzers.

Table (6.1): Techno-economic parameters of power production technologies

	Capacity (MW)	Capital Cost ($/MW)	O&M Cost ($/MWh)	Efficiency (%)
NG-CCPP	100	800,000	2.8	52.6
Wind turbine	1.91	2,000,000	10	-
Solar PV	0.117	4,100,000	2.2	-

Natural gas is the only fossil-fuel considered in the proposed case study, and its emission factors, and unit cost of emissions that are considered as an inputs for the optimization model are summarized in Table (6.2). The emission pollutants considered in this case study include CO_2, CO, NO_2, $PM_{2.5}$, and SO_2. Health impacts cost are estimated using the Air Quality Benefits Assessment Tool (AQBAT), and the estimation method is presented in a previous work (AlRafea, et al., 2016).

Table (6.2): Emission factors and their costs

Pollutant	Emission factor, kg $(MWh)^{-1}$	Emission cost, $ kg^{-1}
CO_2	365	0.013
CO	0.24	0.87
NO_2	0.16	101
$PM_{2.5}$	0.15	114
SO_2	0.021	11

6.6 Feed-In-Tariff Policy in Ontario

The FIT program in Ontario was enabled by the Green Energy Green Economy Act to provide a comprehensive and guaranteed pricing structure for renewable electricity production in Ontario. The FIT price schedule includes provisions for projects that have different levels of equity for community ownership. This indicates that the level ownership will determine the maximum level of price adder in addition to the FIT contract price.

The maximum community price adder that could be received for wind and solar PV is 1.0 cent per kWh. A project with a community share greater than 50% will receive the maximum possible price adder (Martin, n.d.), (Ontario Power Authority, 2010), (Alizamir, et al., 2016) and (Christianson, et al., 2011).

6.7 Results and Discussions

In this section the results obtained from applying the proposed optimization model to a case study based on a community in Southern Ontario are presented. Several scenarios have been generated and investigated in this study including the use of the HENG for power production only, or for power and heat production.

Moreover, the benefits of including hydrogen storage tanks from which hydrogen is retrieved to be injected into the natural gas pipeline versus hydrogen and natural gas pipeline co-storage are also investigated. The consideration of multiple objectives (i.e. cost, emissions and power curtailment) in the optimization model generates different results at different weight factors, which is also presented.

The results presented include the distribution of power production from wind, solar and natural gas, consumption of power by electrolyzers, hydrogen injection levels in the natural gas pipeline, the capacity of energy production and storage technologies installed, total system cost, and emissions mitigated.

The first set of results presented show the stepwise capacity expansion for the power system that has been carried out over a 15-year time frame starting from the year 2015. For each planning step (i.e. 2015, 2020, 2025 and 2030) the capacity expansion was optimized. The input data assumed for each planning period is shown in Table (6.3).

Table (6.3): Summary of Input data used in current model

Characteristics		2015	2020	2025	2030
Power	Total Demand, MW per year	630,855	757,025	870,579	957,637
	On-peak %	74.9	74.9	74.9	74.9
	Off-peak %	25.1	25.1	25.1	25.1
End-Users heat	Total Demand, MJ per year	2.15E10	2.57E10	3.1E10	3.7E10
	On-peak %	84.0	84.0	84.0	84.0
NG average price, $ per GJ		4.4	6.9	9.3	10.8
Weights on emissions		0.5	0.6	0.7	0.8

These include the capital and operating costs of power production technologies, fuel prices, and emission costs. It is assumed that the capacity expansion decisions of energy production and storage technologies are not restricted to a certain limit. The maximum allowable power curtailment was assumed to be five percent of the total power production during each hour.

The least cost results obtained considering the incorporated constraints are summarized in Figures (6.5 to 6.7).

Figure (6.5) shows the capacity expansion of wind turbines, solar photovoltaics, natural gas combined cycle, electrolyzers, and hydrogen storage tanks installed during each planning period, as well as the total annual system cost.

In 2015, a capacity of utility-scale PV of 95 MW and a capacity of onshore wind turbines of 56 MW was integrated into the community's power plant portfolio.

Moreover, in order to achieve the power demand requirements of the community, conventional NG-CCPPs with a capacity of 200 MW are also added to the portfolio. In 2015, no electrolyzers or hydrogen tanks are incorporated in the energy infrastructure. In other words, all the power produced from wind and solar energy is used to satisfy the power requirements, in which no surplus power is available to be used by electrolyzers to produce hydrogen.

From 2020 onwards, utility-scale PV and wind turbines are more competitive in which their total available capacity reaches 815 MW and 430 MW, respectively; by 2030, which provides a substantial and flexible renewable energy capacity. The significant increase in the capacity of solar PV and wind turbines for the year 2030 is attributed to the high emission costs and weight on the emission objective assumed for this planning period.

In order to improve the dis-patch-ability of the energy system, while satisfying the maximum allowable power curtailment level, a significant hydrogen storage capacity is required by the planning period 2030.

A lower renewable production and hydrogen storage capacity is expected if a lower weight on the emission objective is assumed. This translates to the significant increase in the total system cost, which is mainly contributed to by the increase in hydrogen storage capacity.
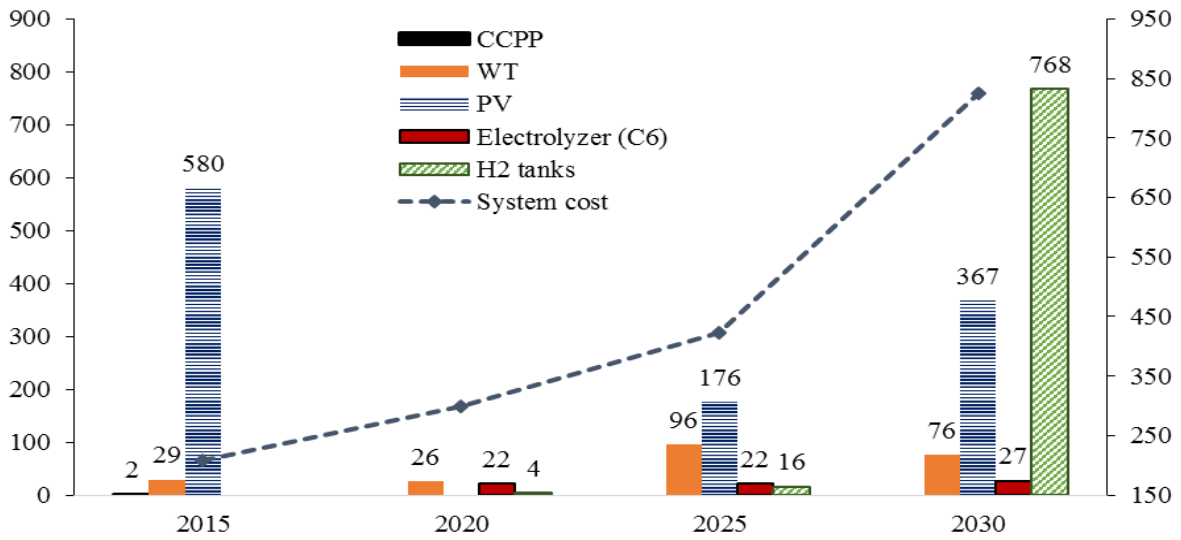
Figure (6.5): Number of power production technologies, electrolyzers and hydrogen tanks installed at each planning period, and the total annual system cost

Figure (6.6) shows the weekly average distribution of power production for each year investigated in the planning period. For the year 2015, no surplus power is available to be utilized by electrolyzers. The power available from wind and solar capacity installed is well below the energy demand during all operating hours, and the majority of the demand is satisfied by power from conventional CCPP. From 2020 onwards, as the cost of emissions and the cost of fuel (i.e. natural gas) increased, and the capital and operating costs of wind turbines and PV solar panels become more competitive, the production from wind and solar energy increases. Moreover, the reliance on power production from CCPP decreases, in which production from CCPP diminishes by the year 2030. This results in a surplus of power production from wind and solar energy, which is utilized by electrolyzers in order to minimize power curtailment. The hydrogen produced mixed with natural gas and is mostly utilized for heat production.
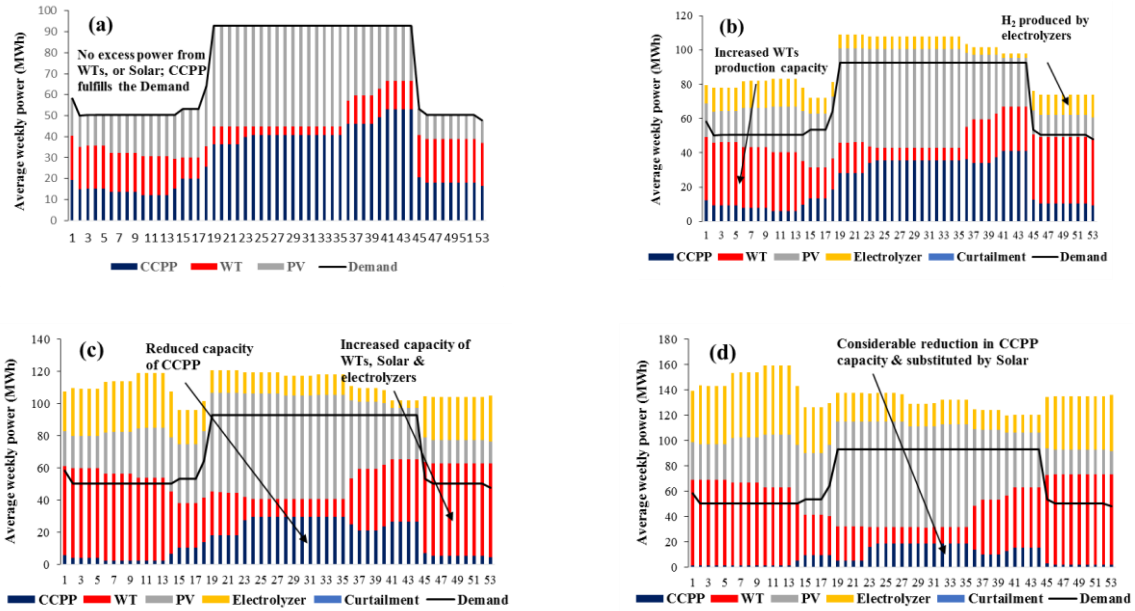
Figure (6.6): The distribution of power production from CCPP, WTs and Solar, the consumption of power by electrolyzers, power curtailed, and the required demand for the planning periods: (a) 2015, (b) 2020, (c) 2025 and (d) 2030

Figure (6.7) shows the weekly average injection of hydrogen in the HENG for all the planning periods. For the year 2015, there is no hydrogen injection due to unavailability of surplus wind and solar power. The trend of hydrogen injection increases during the winter months, which is attributed to the higher requirement for heating. Hydrogen injection then diminishes during the summer months, during which the hydrogen storage capacity is mostly utilized. The increase in hydrogen injection levels from one planning period to the next is associated with the higher heat and power demands. The increase is also attributed to the increase in emission costs, the weight of the emission objective, and the price of natural gas. Moreover, the availability of hydrogen storage contributes to the increase in the hydrogen injection levels into the distribution lines. This is because the model provides flexibility for the power system, in which the more of surplus power can be used to produce hydrogen, and the excess hydrogen that is not injected can then be stored in the available tanks.
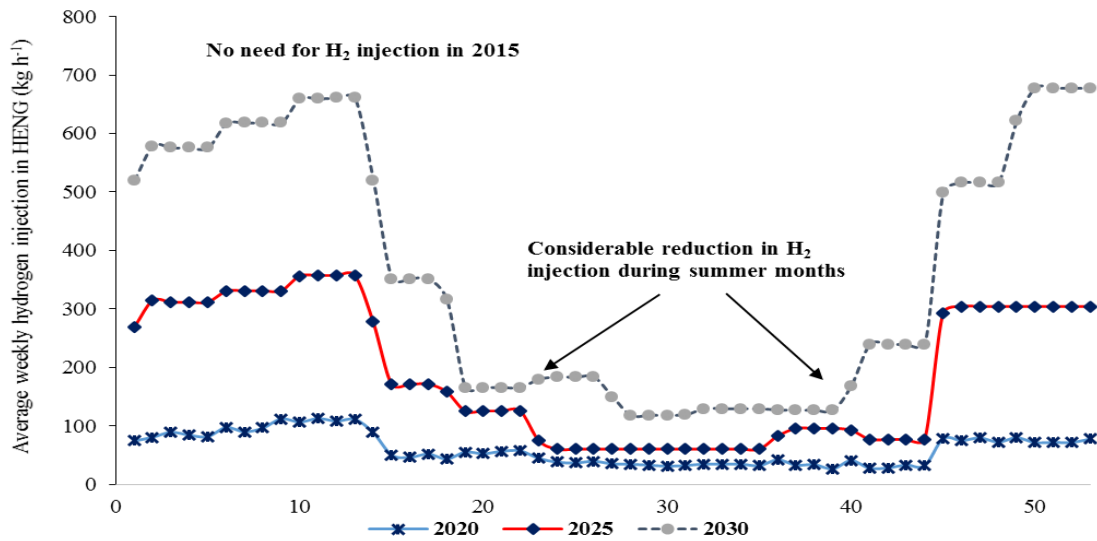
Figure (6.7): Average weekly injection of hydrogen into the natural gas pipeline for each planning period

Natural gas is considered to be a relatively clean fuel; however, the utilization of HENG provides additional potential in reducing total emissions (i.e. CO_2, CO, NO_x, $PM_{2.5}$, SO_x, etc.). The utilization of hydrogen reduces the total amount of natural gas consumed, which is necessary for Ontario to meet its required greenhouse-gas emission targets. The incorporation of hydrogen storage allows for higher injection levels of hydrogen in the natural gas distribution pipeline, which allows for the achievement of higher emission reductions. Figure (6.8) shows the total emission reductions achieved for each planning period investigated. It can be observed that the amount of reductions achieved progressively increases for each planning period. This is due to the higher production capacity of wind and solar energy, and the higher injection levels of hydrogen into the natural gas distribution system. For example, the CO_2 emission reductions achieved in 2020 is 2,685 tons and in 2030 is 16,291 tons. The emission reductions achieved by replacing an amount of the natural gas consumed by clean hydrogen is calculated based on the assumption that the HENG is sent to end users to be used in furnaces for heat generation or used in the CCPP unit for power generation, which would otherwise be pure natural gas. This reduces the total generation of CO_2, as well as other pollutants (i.e. CO_2, CO, NO_x, $PM_{2.5}$, SO_x, etc.). Incentivizing technologies that reduce greenhouse-gas emissions can be achieved, for example, by developing carbon exchange markets. Currently there are no carbon exchange markets existing in Ontario.

The emission costs mitigated are calculated based on the emission cost factors estimated in a previous work.
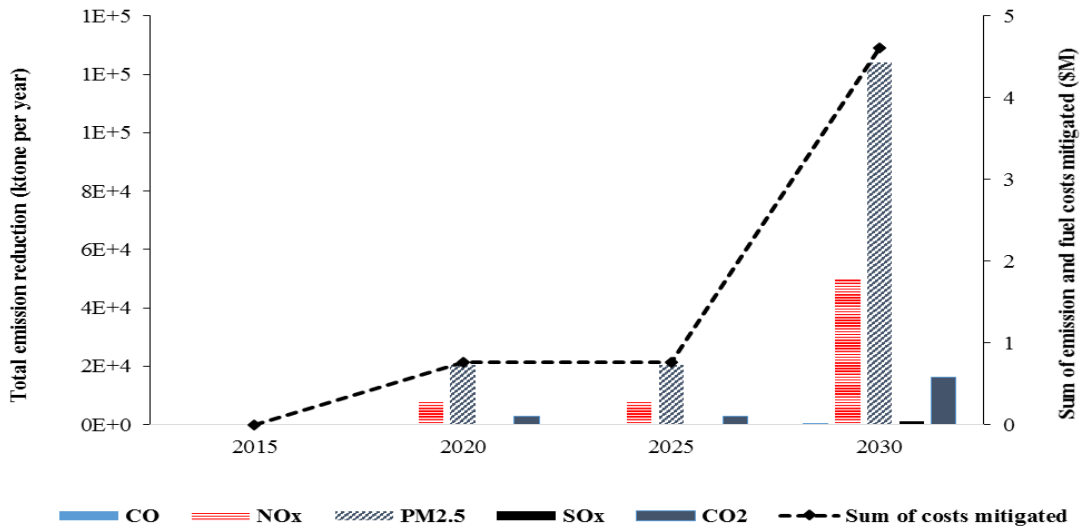
Figure (6.8): Total emissions reduced and cost of emissions mitigated for each planning period due to utilizing hydrogen as fuel

The results presented so far assume a least-cost scenario, in which the integration of renewable technologies into the energy production portfolio is flexible. As a result, the capacity of renewable energy integrated can provide energy well below the demand even during off-peak hours. This will not require the incorporation of energy storage technologies, as was observed from some of the results obtained, particularly for the planning period 2015. However, it is possible that the capacity of renewable energy required to be integrated into the power production portfolio is significant, during which there will be times of high renewable energy (i.e. wind and solar) potential during off-peak hours when base load generation is at a minimum resulting in surplus energy that must be utilized in a productive manner. Realizing the available wind and solar potential for the investigated case study, the revaluation of baseload renewables may well provide a suitable path for power generation while addressing the threat of climate change and social impacts of air pollution. The base case scenario for the planning period 2015 was revisited, and the renewable production capacity was assumed to provide at least the off-peak power demand by enforcing the constraint in Eqns. (6.6 and 6.7). This scenario was first investigated by applying different weights to the emissions objective function. Figure (6.9) shows the capacities of CCPP, wind and solar, and electrolyzer and hydrogen storage farms installed. It can be observed that the total capacity of

wind and solar installed are higher due to the constraint of renewable energy satisfying at least the off-peak power demand. In this case, the CCPP power production units can only operate during on-peak demand hours to satisfy the remaining electricity demand. It can be observed that at a low emission weight factor (0.1) the minimum capacities of wind and solar that are required to be installed to satisfy at least the off-peak demand hours are 183 MW and 70 MW, respectively. The maximum capacity of CCPP power production (200 MW), which is only utilized during on-peak demand hours, is high due to the low weight set on the required reduction in total emissions.
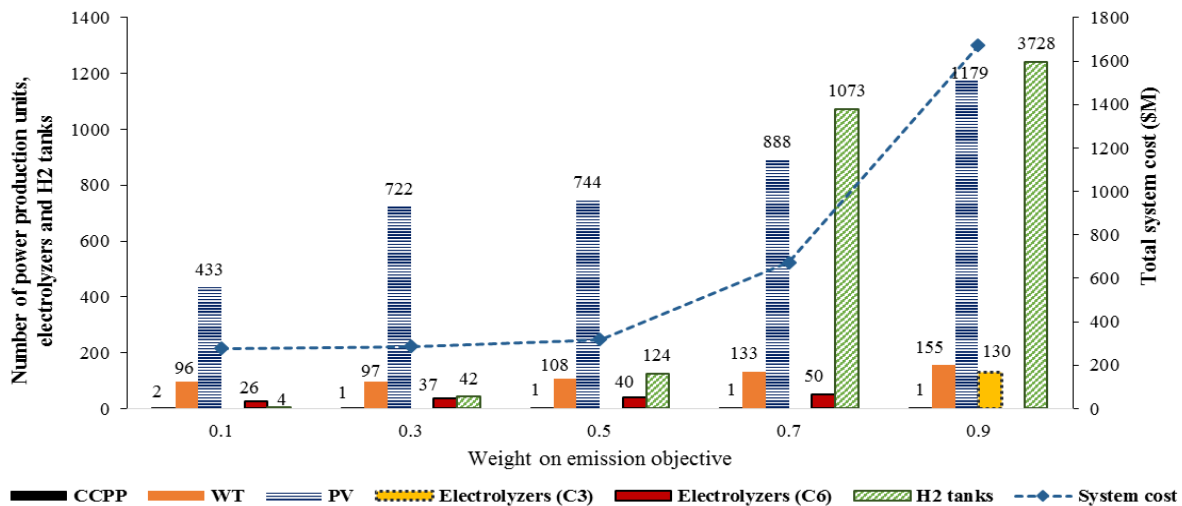
Figure (6.9): Number of power production units, electrolyzers, H$_2$ tanks, and total system cost for the base case of 2015 at different weights on the emission objective function

Electrolyzer and hydrogen storage capacities of 95 MW and 18 MW, respectively, are required in order to utilize the excess power generated during off-peak hours, which is required to minimize power curtailment that is set to an allowable maximum of 5% during all operational hours (Figure 6.10). An increase in the emission weight factor results in an increase in the production capacity of wind and solar power in order to replace the production capacity of CCPP units during on-peak hours and to generate surplus power that can be utilized by electrolyzers to produce hydrogen.

The hydrogen produced is injected into the natural gas distribution system, which reduces emissions generated by CCPP units and from using HENG fuel to satisfy heat demand. It can be observed that at very high weight on the emission objective (0.9), the hydrogen storage capacity considerably increases. This is mainly due to the considerable increase in wind and solar energy

capacity required to satisfy power demand during on-peak and off-peak demand hours. This generates considerable excess surplus power during off-peak hours that must be managed by being sent to electrolyzers for hydrogen production as the power curtailments is constrained to an allowable maximum of 5%. Moreover, the only available route for hydrogen consumption is to be injected into the natural gas pipeline distribution system, which has a maximum allowable injection limit of 5%. This as a result will increase the capacity of hydrogen storage required. Moreover, it can be observed that the increase in total system cost is significantly contributed to by the hydrogen storage cost.
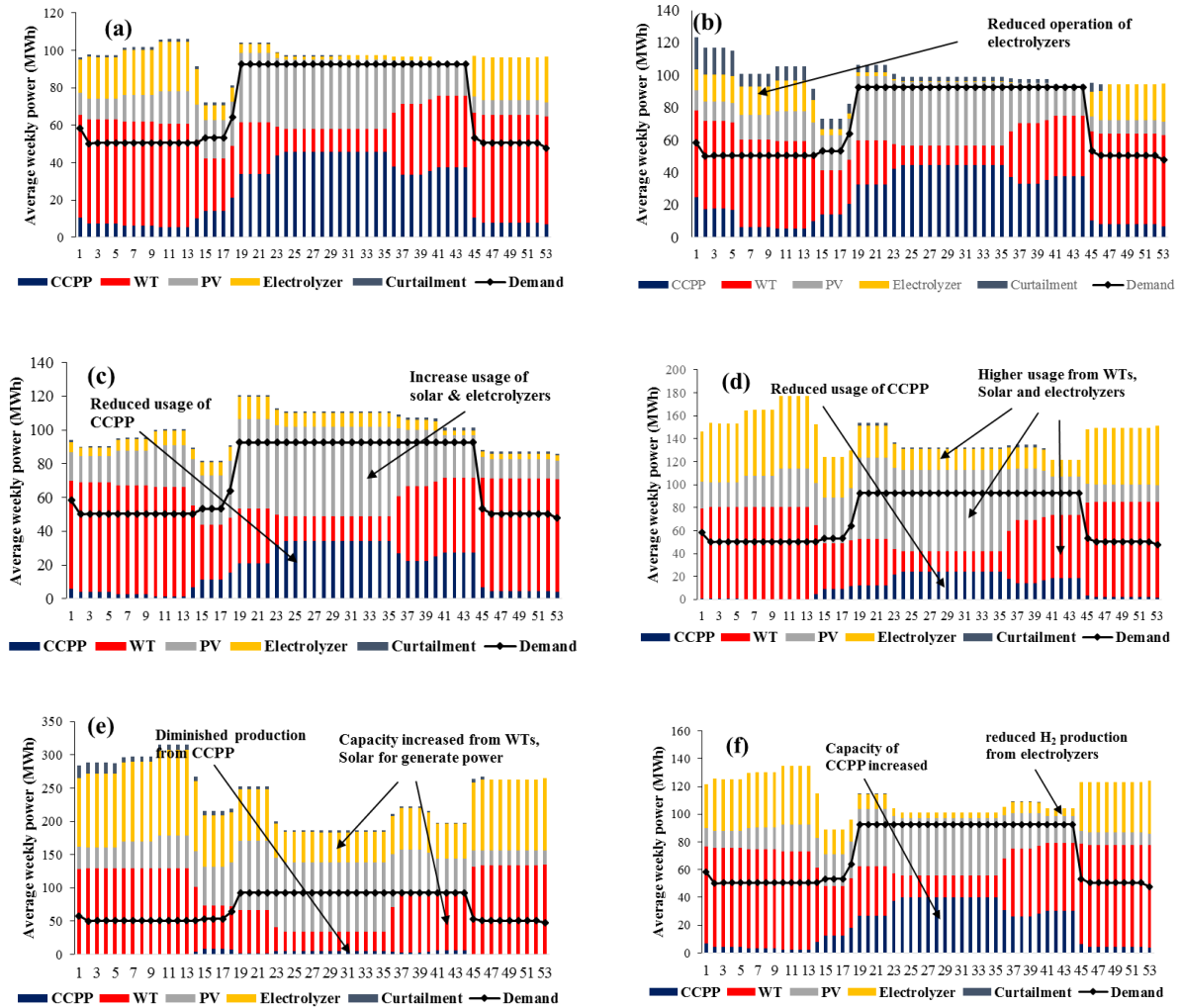
Figure (6.10): Distribution of power production and consumption for (a) P2G2P at a weight of w=0.5 and maximum allowable power curtailment of 5%; (b) P2G2P at maximum allowable power curtailment of 25%; (c) P2G2P and grid-connected at FIT 1.0 cents per kWh; (d)P2G2P/H at an emission weight factor w=0.3; (e) P2G2P/H at a maximum allowable H_2 concentration of 20%; and (f) P2G2P/H at an emission weight factor of w=0.1

Figure (6.11) shows the average weekly content of hydrogen in the HENG existing in the natural gas distribution system for different weight factors of the emissions objective function. It can be observed that the content of hydrogen in the HENG increases with the increasing emissions weight factor. A similar trend can be observed for all the emission weight factors; however, at a high emission weight, the hydrogen content increases to its maximum allowable value of 5%. This is necessary in order to lower the emissions generated from the utilization of natural gas in CCPP units and as a fuel for heat production. The high weight on emissions necessitates the utilization of a higher capacity of wind and solar for power production. This results in the generation of a

high surplus of energy during off-peak hours which is managed by the production of hydrogen. Even though the hydrogen injection is at its allowable maximum, there is still significant amounts of hydrogen that are sent to storage facilities. Increasing the allowable injection limit of hydrogen is expected to reduce the hydrogen storage capacity required, and reduce the total system cost.
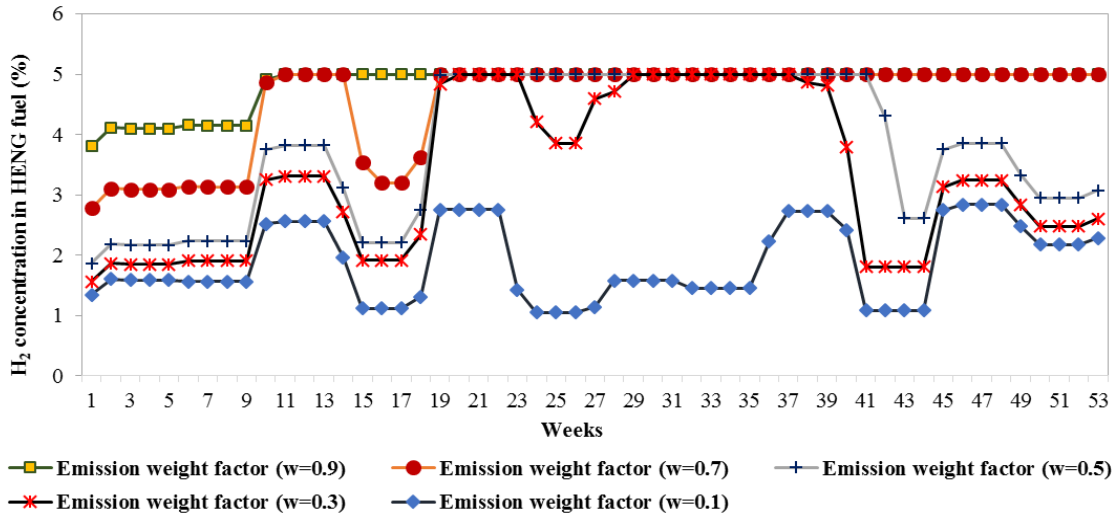
Figure (6.11): Average H_2 concentration in HENG fuel in NG-Pipelines at different weights set on the emissions objective function for P2G2P/H scenario

Figure (6.12) shows the emission reductions achieved at different emission weights from the injection of hydrogen into the natural gas distribution system. The utilization of renewable energy sources (i.e. wind and solar) for the generation of base load demand results in a higher availability of surplus power from wind and solar energy during off-peak demand hours due to their non-dis-patch-able nature. This surplus power can be utilized by electrolyzers for clean hydrogen production, which reduces natural gas consumption when injected into the natural gas distribution system. At low weight factors set on the emission objective (0.1 – 0.3), an adequate amount of hydrogen is produced and utilized as fuel in the HENG, which allows for the achievement of significant emission reductions of up to 4296 tons per year for CO_2. Significant reductions in the generation of other pollutants (i.e. SO_x, NO_x, and $PM_{2.5}$) have similarly been achieved. Even though higher emission reductions and costs mitigated due to emissions are achieved at high emission weight factors (0.7 – 0.9), the costs mitigated are highly offset by the significant increase

in the total system cost associated with the considerable increase in the required hydrogen storage capacity.
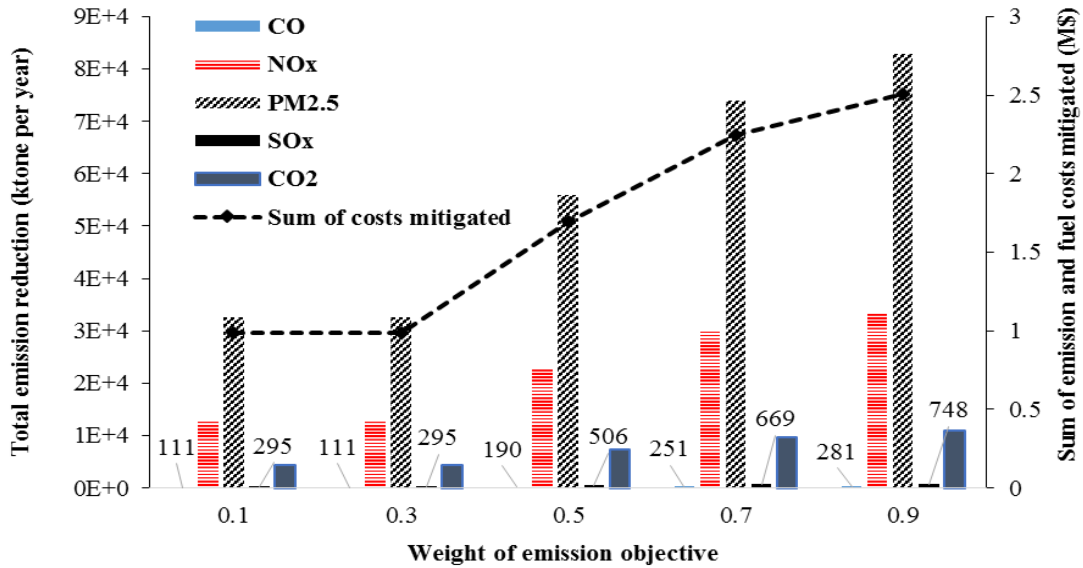
Figure (6.12): Total emissions and their associated costs at various weights factor for the P2G2P/H scenario

As can be observed from the previous results the injection limit of hydrogen into the natural gas pipeline can potentially have a significant impact on optimizing the energy production and storage portfolio. According to Melaina et al. (Melaina, et al., 2013), the maximum allowable hydrogen concentration in the HENG in the existing natural gas pipeline network can range from 5% - 20% by volume. These concentrations can be maintained without significantly increasing the risks associated with utilizing HENG in end user devices, safety, or the durability of the gas distribution system. The selection of the appropriate hydrogen concentration within this range varies significantly among various pipeline networks and must be evaluated on a case-by-case basis. However, to illustrate the effect of its variability on the results of the proposed optimization model, the maximum allowable hydrogen concentration in the pipeline is varied in the range of 5% - 20%, and the results obtained are illustrated in the following figures.

It can be observed from Figure (6.13) that increasing the maximum allowable hydrogen concentration in the natural gas distribution pipeline results in an increase in the capacity of wind and solar energy production for all the investigated allowable limits. It can be observed that as

the hydrogen injection limit is increased from 5% to 10% there is a noticeable increase in the solar PV and wind production capacity, and a reduction in the hydrogen storage capacity. The reduction in hydrogen tank storage contributes significantly to the reduction in the total system cost observed. It is important to note that the maximum and minimum value of the emission objective function used in the ε-constraint are different at different injection levels. For example, at 10% and 15% maximum allowable hydrogen injection limits the minimum total emissions costs that could possibly be achieved are $101.2 M and $99.5 M, respectively. Moreover, the maximum emissions costs (i.e. minimizing only the energy production and storage objective) for both injection limits are $111.4 M and $108.2 M, respectively. At a weight of 0.5 for the emission objective function, the optimal emissions costs obtained for the two injection limits were $106.3 M and $103.8 M, respectively.
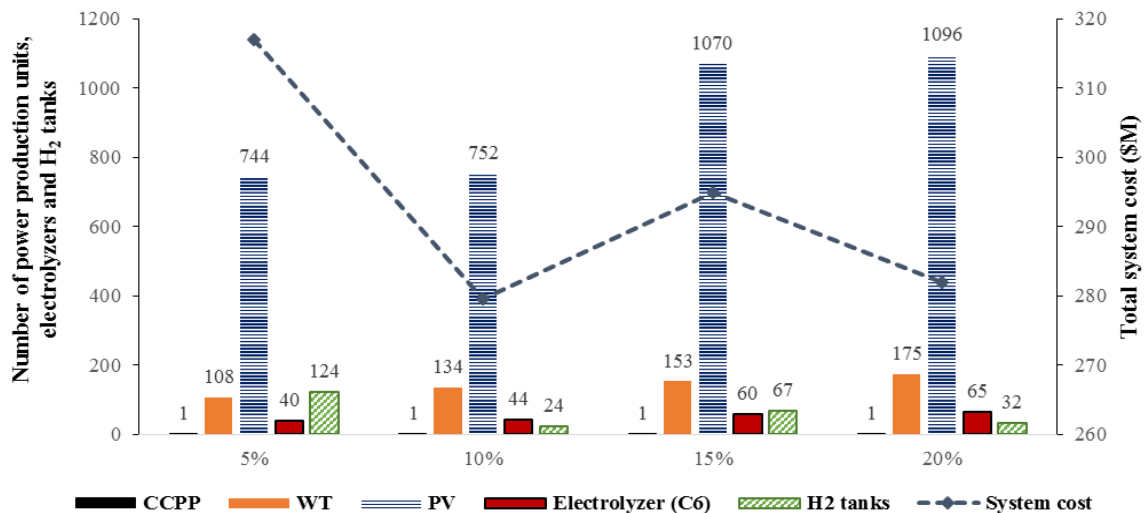
Figure (6.13): Number of power production units, electrolyzers and H_2 tanks at various H_2 concentration for P2G2P/H scenario

Therefore, it can observed that the higher injection limit resulted in a decrease in the total cost of emissions. However, to achieve a lower cost of emissions a corresponding increase in the cost of electricity production and storage, which translates to the increase in the total system cost. The increase in the hydrogen injection limit from 10% to 15% justified the considerable increase in wind and solar energy production capacities, as the surplus power generated by these sources can

be managed more effectively by generating hydrogen and injecting it into the natural gas pipeline. However, this also results in an increase in the hydrogen storage capacity in order to manage periods of low total natural gas fuel demand (e.g. summer months). This is illustrated in Figure (6.14), which shows the weekly average injection of hydrogen into the natural gas distribution system for various maximum allowable injection limits. It can be observed that generally the amount of hydrogen injection is higher when the constraint on the amount of hydrogen injection is relaxed (i.e. higher maximum allowable hydrogen concentration). This is particularly evident during the winter months when the demand for natural gas is highest. However, during the summer months the amount of hydrogen injected reaches similar levels, due to the lower demand of natural gas. If the amount of hydrogen injected is abundantly increased, such as between the 10% and 15% scenarios, this would necessitate a higher requirement of hydrogen storage to be utilized during the summer months.

So far the results presented focused on the scenario in which hydrogen is injected into the natural gas distribution pipeline, and the HENG is utilized for both electricity production and as a fuel for heat production. The utilization of HENG for the production of heat presents a significant sink for the hydrogen generated, which facilities an effective management route for the excess energy generated. However, a possible scenario that must be considered is the utilization of hydrogen at the end-user, particularly in CCPP units for power production only. In all the previously investigated scenarios the maximum allowable power curtailment was assumed to be 5%. The following results are generated for the scenario of power-to-gas-to-power only, and investigated at different power curtailment constraints. Moreover, interactions with the power grid were also considered, in which the surplus power generated from wind and solar can be sold to the grid considering the feed in tariff policy that is currently applied in Ontario.
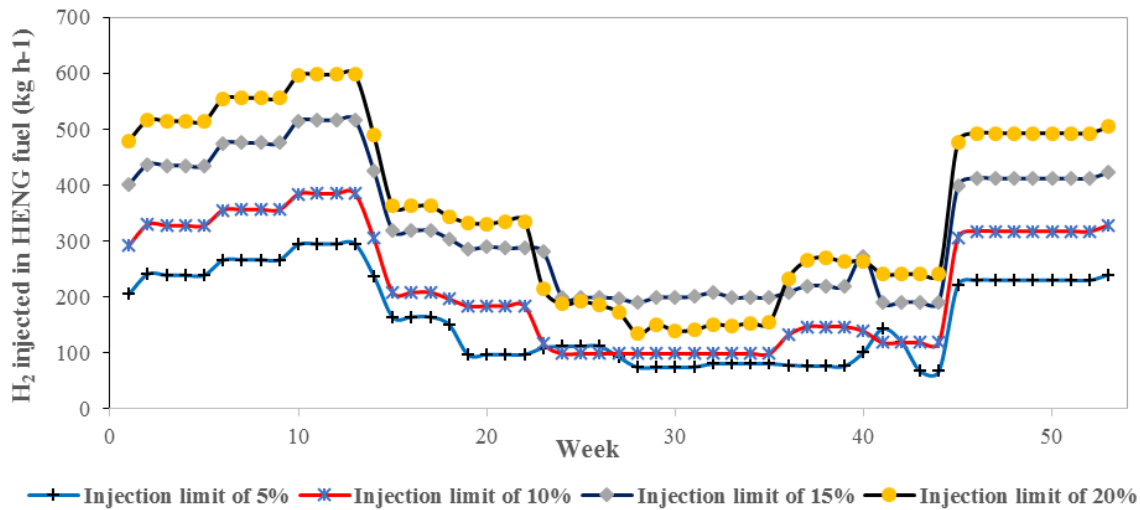
Figure (6.14): Average weekly H_2 injected into NG-Pipelines for P2G2P/H scenario at various H_2 concentration

It can be observed from Figure (6.15) that the maximum allowable power curtailment has a significant effect on the total system cost. Increasing the maximum allowable curtailment results in a considerable decrease in the total cost, which is mostly attributed to the reduction in hydrogen production and storage costs. It can be observed from Figure (10b) the increasing the amount of power curtailment results in a reduction in the operation of electrolyzers. This in return decreases the capacity of electrolyzers required. As can be observed from Figure (6.15), lower unit capacity levels of electrolyzers (i.e. C2 and C3) are preferred at higher power curtailment. Selecting smaller units of electrolyzers in this case maximizes the electrolyzers' capacity factor when they are operating. Moreover, it can be observed that the required hydrogen storage capacity decreases with an increase in the allowable amount of power curtailment. This is due to the lower operational levels of electrolyzers, which results in lower levels of hydrogen production. It is important to note that there is a slight increase in the renewable production capacity, which is a result of the reduced requirement to manage the surplus power generated through the expensive hydrogen storage.
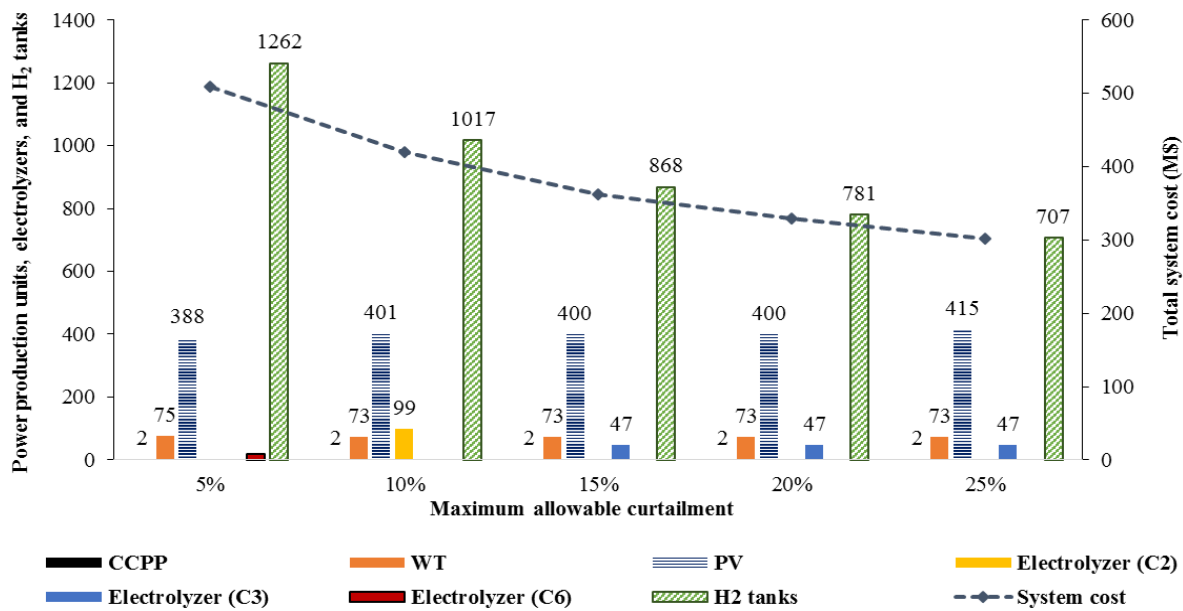
Figure (6.15): Number of power production units, electrolyzers and H2 tanks for the P2G2P scenario at max. power curtailment

From Figure (6.16) it can be observed that the hydrogen injection into the natural gas distribution pipeline for the P2G2P scenario follows an opposite trend to that observed for the P2G2P/H scenario. Moreover, the amount of hydrogen injected for the P2G2P scenario is considerably lower. All the hydrogen produced in the P2G2P scenario is utilized in the HENG fuel injected into CCPP units for power production. The operation of CCPP units is highest during the summer months to satisfy the considerably higher power demands compared to the winter months. This explains the increase in hydrogen injection during the summer months and the following decrease when approaching the winter months. However, for the P2G2P/H scenario the majority of hydrogen is used in HENG fuel sent to satisfy the heat demand of the community, which is higher during the winter months. This translates to the higher injection levels during the first few months (weeks 0 – 15) followed by a depreciation in hydrogen levels during the summer (weeks 20 – 35).
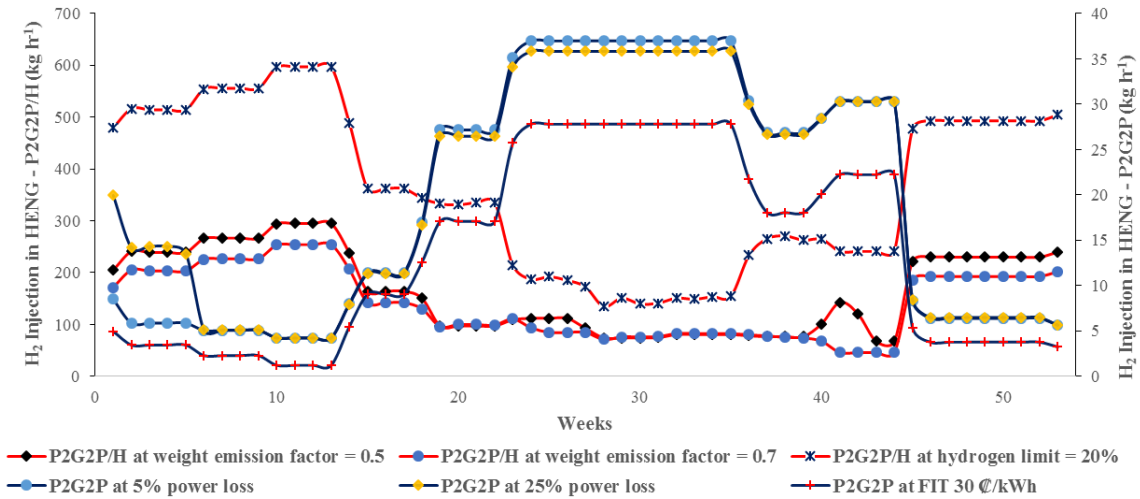
Figure (6.16): Average H_2 injection in NG-Pipelines for P2G2P scenario as well as P2G2P/H scenario at 5% and 25% power curtailments; and interactions with FIT price of 1¢ per kWh

As can be observed from Figure (6.17), the higher maximum allowable power curtailment results in lower levels of hydrogen injection, which is due to the lower levels of hydrogen production from electrolyzers. A similar trend is observed when interaction with the grid are considered and surplus power from wind and solar can possibly be sold to the grid according to the feed in tariff policy. Selling surplus power to the grid reduces the available surplus power that can be utilized by electrolyzers for hydrogen production.

All the previously investigated scenarios considered hydrogen storage tanks for storing excess hydrogen that is not injected into the natural gas distribution pipeline. Another potentially suitable storage options is the utilization of the existing natural gas network as a permanent storage of a fixed mass of hydrogen. The storage capacity of the natural gas network is sufficient to hold the energy requirements that is enough for several months. Pipeline storage of hydrogen is based on increasing the pressure in order to facilitate the line to hold more gas in inventory. In this scenario, the operation of CCPP units and electrolyzers is allowed to be flexible. In other words, the operation of CCPP units is not limited to providing power only during on-peak demand hours. This is important to consider since the capacity for hydrogen inventory in the pipeline is limited (i.e. maximum allowable concentration of hydrogen in the pipeline is 5%). Adding flexibility for its operations allows for an extra route to eliminate hydrogen from inventory in addition to the HENG used to satisfy the heat demand of the community. It is important to note that if this

flexibility is not considered, then the optimization model reaches an infeasible result due to the limited capacity of hydrogen inventory.

It can be observed from Figure (6.18) that the capacity of wind and solar power production increases with the increase in the weight of the emission objective. Similarly the capacity of the electrolyzer farm increases in order to produce clean hydrogen, which reduces reliance on natural gas and production of emissions. It can also be observed that the capacity of CCPP units decreases with the increase on emphasis on the objective of reducing the cost of emissions. Reducing the cost of emissions results in a reduction in the total system cost, for which it can be observed that the lowest cost obtained was associated with the emission weight factor of 0.7. As the capacity of renewables increases, the reduction in the cost of emissions and natural gas utilized is offset by the increase in the cost of power production. It can be concluded that utilizing the existing natural gas distribution pipeline for the storage of hydrogen is more economically attractive than utilizing hydrogen storage tanks. However, this storage technology provides a limited capacity of hydrogen storage. Moreover, there are issues that were not considered in the development of the proposed optimization model, such as costs associated with pipeline materials problems that might arise due to increasing the pressure of hydrogen (e.g. hydrogen embrittlement, hydrogen leakage, etc.).
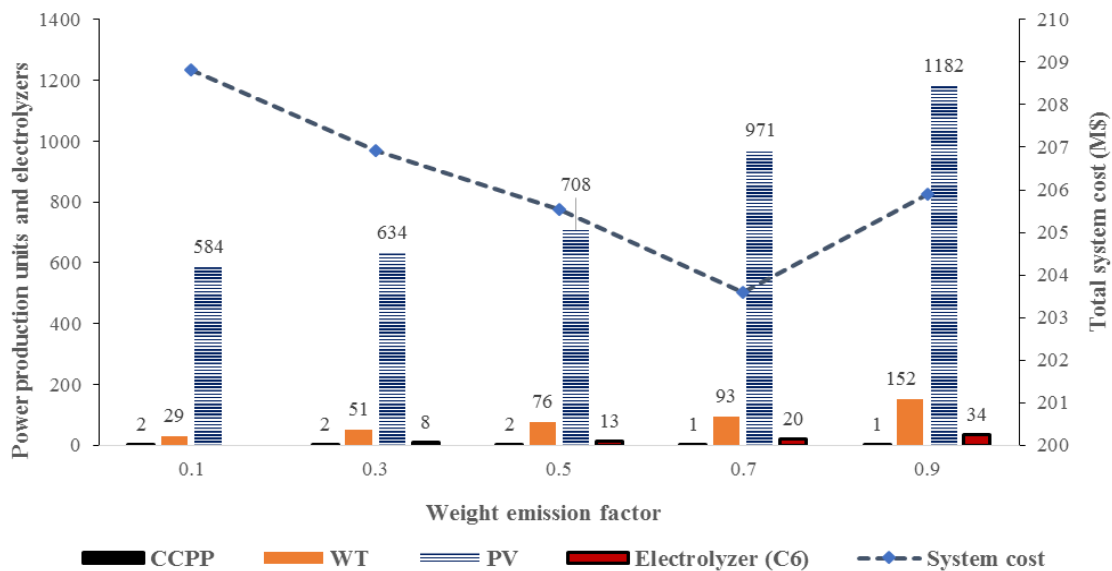
Figure (6.17): Number of power production units and electrolyzers used for P2G2P/H scenario while considering H_2 injection in NG-Pipelines only at different emission weight factors

Figure (6.19) shows the distribution of power production and consumption by electrolyzers for different emission weight factors. It can be observed that at low emission weight factors the production of CCPP units contribute significantly to the power production portfolio. Moreover, no surplus power from wind and solar is available, which eliminates the requirement of electrolyzers. However, the share of production of CCPP units decreases with an increase in the weight of the emission objective, and the production of hydrogen from electrolyzers increases. At very high emission weight factors, production of power from CCPP units diminishes, and hydrogen produced from electrolyzers is mostly utilized in HENG used as a fuel for heat production.
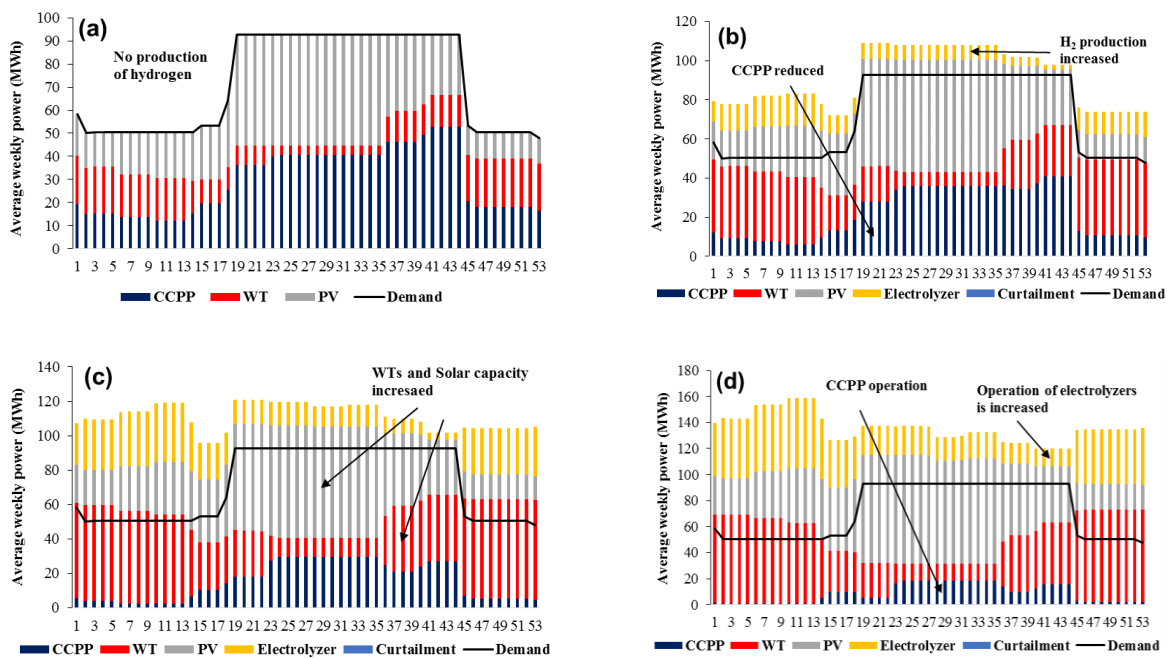
Figure (6.18): Distribution of power production and consumption for the P2G2P/H scenario while considering H_2 injection in NG-Pipeline only at different emission weight factors (a) w=0.1; (b) w=0.3; (c) w=0.7 and (d) w=0.9

It can be observed from Figure (6.19) that the amount of hydrogen injected into the natural gas pipeline and utilized as HENG fuel in CCPP units and in heat-demand increases with the increase of weight on emissions. A trend similar to that observed for the scenario in which hydrogen tanks were utilized for storage is also observed in this scenario.

The amount of hydrogen utilized decreases during the summer months due to a reduction in the heat demand, which has the largest share in the consumption of HENG.

For this scenario, the amount of hydrogen utilized decreased during summer periods as can be observed from Figure (6.19). Since the hydrogen injection is lowered during summer time, there is need for more hydrogen to be held in storage facility. Therefore the inventory is slightly higher during this time of the year.
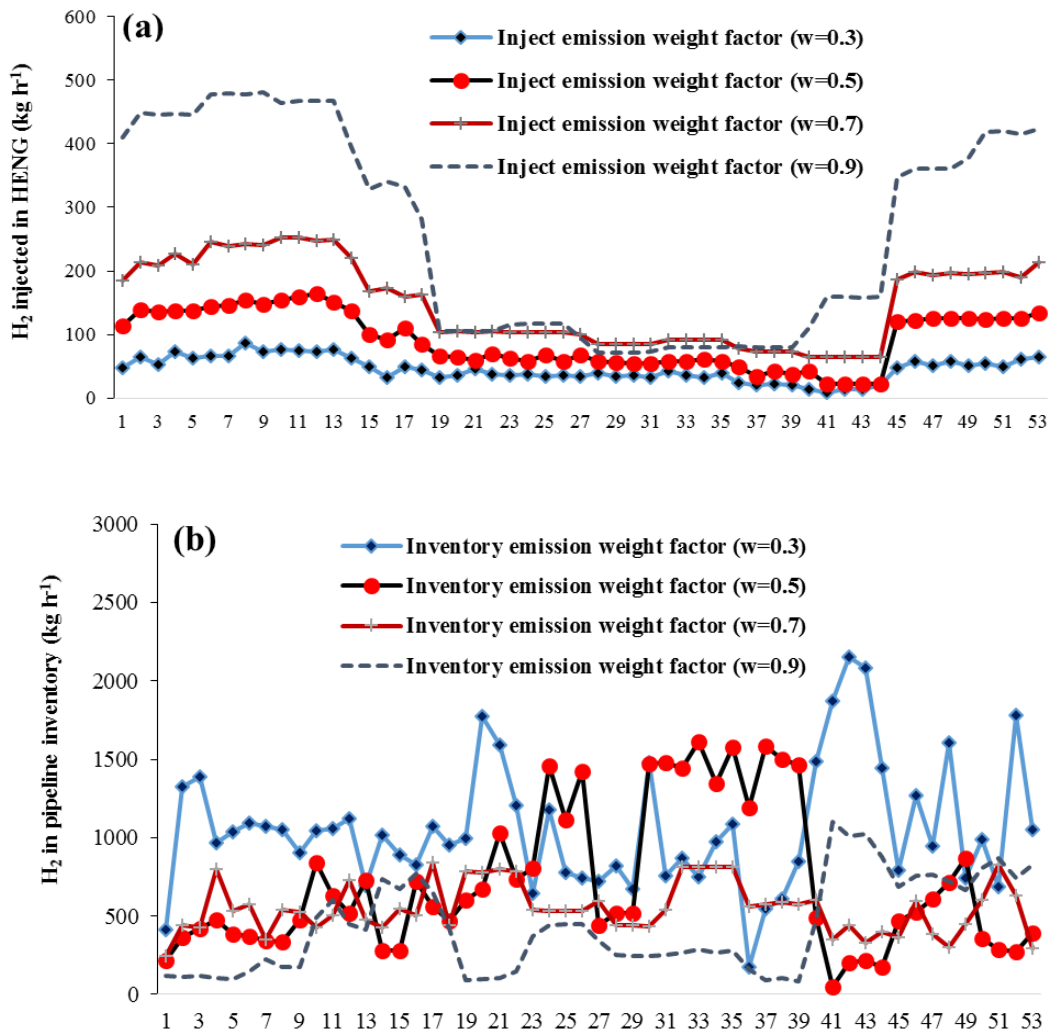
Figure (6.19): (a) Average H_2 injected in NG-Pipeline at various emission weight factors; (b) Average H_2 inventory in NG-Pipeline at various emission weight factors

As can be observed from Figure (6.20), at higher emission weight factors significant emission reductions are achievable by introducing more hydrogen into HENG fuel.

The emission costs mitigated are also high enough to contribute to a noticeable reduction in the total system cost. However, these mitigated costs are offset at very high emission weight factors due to the considerable increase in the power production cost associated with the very high capacity of renewables installed.
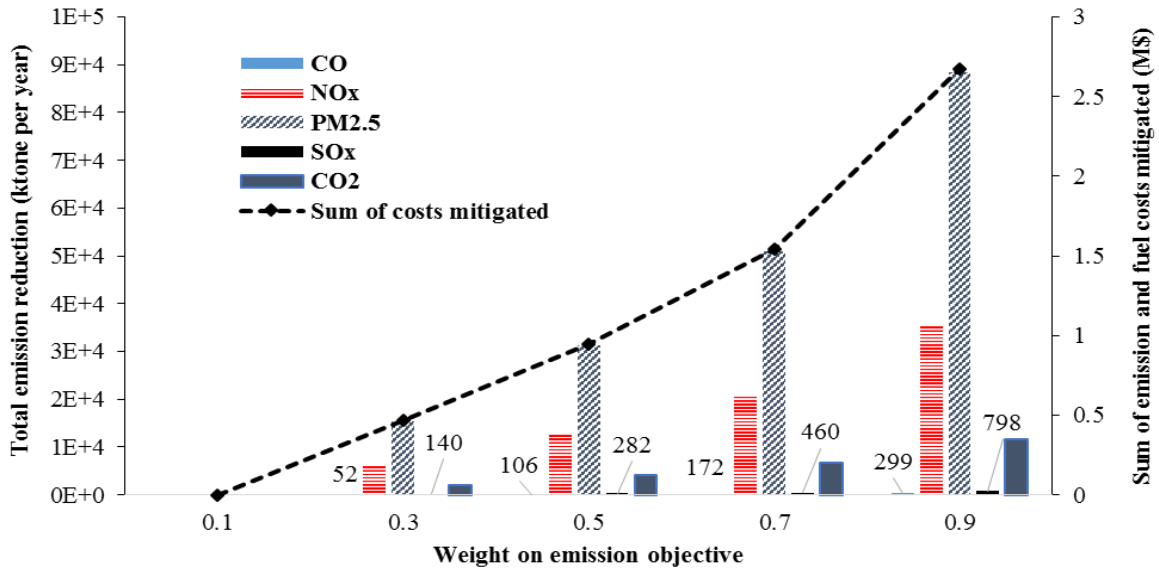
Figure (6.20): Total emissions and their associated costs that mitigated at different weights for the P2G2P/H scenario that considered for H2 injected in NG-Pipeline only

6.8 The Conclusions

Decentralized energy hub system offers energy independence, reliability in energy-management, and flexibility in power supply, while optimizing its techno-economic performance offers optimum costs, sizing and operation. Wind generators reduced reliance on CCPP in meeting power demand by about 40% during winter; whereas during summer time the solar power reduced the reliance on CCPP by about 11% only. The system stored energy as hydrogen for short time only; i.e. the system stored hydrogen during off-periods of a day and retrieved it during on-peak periods of the next day. Integrating wind and solar into the designed energy hub for meeting power demand has saved on costs of social and health associated with emissions of about $17 per MWh; whereas storing the surplus power from wind and solar during off-peak periods as hydrogen inside NG-pipeline network saved 10% of the LCOE of the power generated to meet the demand. The criteria air pollutants of CO, NO_2, $PM_{2.5}$ and SO_2 have the most significant impacts on most of the model's outputs such as number of solar units, number of electrolyzers, energy stored and the total costs other than the CO_2 has. Increasing the cost-weight of social and health impacts has impacted the number of solar units, the number of electrolyzers, energy stored and the total costs significantly. The LCOE is more sensitive to the costs of health impacts than does to the social cost, and the number of solar units as well as the number of electrolyzers are sensitive to the hydrogen percentage in HENG fuel.

Chapter Seven

7   Conclusions and Recommendations for future work

7.1 Conclusions from Comparing the Results of four Studies

In this chapter the results and conclusions of the four studies are compared, reviewed and presented in order to summarize the most important findings.

In the first part of the research, the NG-fueled CCPP is used to meet the proposed demand at all levels, i.e. from base-load to the on-peak load, i.e. high operating hours per year, therefore the calculated COE found relatively low ($0.092/kWh) which is close to the results found in the second study. The proposed energy hub in the first study utilized 97% of CCPP-power and 3% of WTs & Solar for meeting the power demand; whereas the proposed energy hub in the second study utilized HENG-fueled CCPP for meeting the power demand while WTs & Solar were used in generating hydrogen during their available time; therefore more hydrogen was generated. In the third study, the HENG-fueled CCPP is proposed to meet the on-peak power demand, therefore its COE was relatively high at $0.11/kWh.

In the second part of the research, the best concentration of hydrogen to be injected into NG-pipelines was investigated from economic perspective. Annual revenue could be achieved when the selling price of electricity was at $0.12/kWh and when hydrogen concentration of 3.7% in HENG-fueled CCPP is used. Emissions reduction credits for both pollutants CO_2 and NO_x were assessed and balanced within the COE while meeting the power demand.

The hidden costs of generating electricity were estimated, assessed and included within the COE while meeting power demand by monetizing the health impacts associated with specified CCPP-emissions. It is found that the cost of health impacts associated with air pollution emission from NG-fueled CCPP represents about 30% of the COE for the on-peak power generation cost. Blending hydrogen with NG to fuel CCPP could save CAD $1.15 for every MWh produced, at hydrogen concentration of 2.3% in HENG fuel, the COE was $0.11/kWh while 11% of this cost is the health impacts cost.

The main contributions of last part of the research were extended investigations to include further parameters such as assessing the cost-weight, emissions-weight and the time for storing energy. Generating power close to the demand area enables the energy system to operate through interactions with the local grid, through feeding the surplus power, or as a stand-alone isolated energy system. It is found that during winter time, incorporating WTs into the energy system reduces the reliance on CCPP in meeting power demand by about 40%; whereas during summer time the solar power reduced the reliance on CCPP by about 11% only. Storing the surplus power from WTs and solar during off-peak periods as hydrogen within the NG-pipeline network saved 10% of the COE of the power generated to meet the demand. Within this study, it is proved that the system could store hydrogen during off-periods of a day and retrieved it during on-peak periods of the next day. Increasing the cost-weight of health impacts has impacted the number of solar units, the number of electrolyzers, energy stored and the total costs significantly.

Utilizing electrolytic produced hydrogen as a fuel in combustion process for generating power and in fuel cell vehicle will enable the 'Power to-gas' technology to bridge between the current and future markets.

7.2 Recommendations for future work

- Future work should explore the best economic location for the eletcrolyzers within the 'power-to-gas' energy system, a comparison between locate them beside the renewable sources versus locating them close to the consumers will support the optimization of the cost-emissions model,

- Extend the time at which the hydrogen can be stored inside NG-pipelines should be explored in future research since it will add further flexibility into the power-grid,

- Extend the research for assessing the technical limitations/challenges of utilizing HENG as fuel for end-users,

- Further research is needed to investigate/assess the choices for sustainable power supply that can balance the environment regulations versus the economical requirements,

- Other impacts associated with utilizing NG-fueled CCPP should be explored such as social impacts and climate change in order to give thorough idea of the hidden cost of generating electricity from CCPP.

References

1. Abbey, D. et al., 1995. Long-Term Ambient Concentrations of Particulates and Oxidants and Development of Chronic Disease in a Cohort of Nonsmoking California Residents. *Inhalation Toxicology ,* pp. 19-34.

2. Abdelwaheb, A., Moncef, Z. & Hamed, B. D., 2014. Quantification of air pollutant emissions from the Jebel Chakir landfill site (Tunis City). *Arabian Journal of Geosciences,* pp. 3335 - 3341.

3. AEA, 2005. *Damages per tonne emission of PM2.5, NH3, SO2, NOx and VOCs from each EU25 Member State (excluding Cyprus) and surrounding seas,* United Kingdom: AEA Technology Environment.

4. Akansu, S., Dulger, Z., Kahraman, N. & Veziroglu, N., 2004. Internal combustion engines fueled by natural gas-hydrogen mixtures. *Int. Journal of Hydrogen Energy,* Volume 29, pp. 1527-1539.

5. Alberta Environment, 2010. *Air Quality Dispersion Models,* Alberta, Canada: Fort Air Partnership.

6. Alizamir, S., Véricourt, F. & Sun, P., 2016. Efficient Feed-In-Tariff Policies for Renewable Energy Technologies. *Operations Research,* 64(1), p. 52–66.

7. AlRafea, K., Elkamel, A. & Al-Sulaiman, S., 2016. Cost-Analysis of Emission's Health Impacts from Combined Cycle Power Plant Fueled with Natural Gas and with Hydrogen Enriched Natural Gas Fuels. *Atmospheric Environment Journal,* pp. 1408-1424.

8. AlRafea, K., Fowler, M., Elkamel, A. & Hajimiragha, A., 2016. Integration of Rnewable Energy Sources into Combined Cycle Power Plants Through Electrolysis Generated Hydrogen in a New Designed Energy Hub. *International Journal of Hydrogen Energy,* p. 16718–16728.

9. Altfeld, K. & Pinchbeck, D., 2014. *Admissible Hydrogen Concentrations in Natural Gas Systems,* s.l.: The European Gas Research Group.

10. Atlantic Hydrogen, 2009. *Hydrogen-Enriched Natural Gas Bridge to an Ultra-Low Carbon World,* Fredericton, NB: National Grid and Atlantic Hydrogen Inc..

11. Attala, L., Facchini, B. & Ferrara, G., 2001. Thermodynamic Optimization Method as Design Tool in Gas-Steam Combined Plant Realization. *Energy Conversion and Management,* 42(18), pp. 2163 - 2172.

12. Ayoub, J., Dignard-Bailey, L. & Poissant, Y., 2010. *National survey report of PV power applications in Canada. ,* Québec: Canmet Energy.

13. Bahrami, N., Huang, M., Huang, A. & Tsai, Y., 2013. *An Investigation into Waste Heat Recovery Methods for the UBC Microbrewery,* s.l.: University of British Columbia.

14. Bakken, B. H. & Holen, A. T., 2004. *Energy Service Systems: Integrated planning case studies.* Denver, CO, IEEE, pp. 2068-2073.

15. Ball, M. & Kennett, J., 2012. *Argus Air Daily, US Emissions Market Prices,* London: Argus Media Inc..

16. Barn, P. et al., 2011. *Air quality assessment tools: A guide for public health practitioners. National Collaborating Centre for,* s.l.: National Collaborating Centre for Environmental Health.

17. Bentein, J., 2014. *Power-to-gas technology enables utility-scale storage of renewable energy ,* Canada: CleanTech Canada.

18. Bickel, P. & Friedrich, R., 2005. *ExternE: Externalities of energy, methodology 2005 update,* Shtuttgart, Germany: IER Univeritat.

19. Biegler, T., 2009. *The hidden costs of electricity: Externalities of power generation in Australia,* Parkville, Victoria: The Australian Academy of Technological Sciences and Engineering (ATSE).

20. Bing, J. M., 2007. *A Simplified Cost Model for Photovoltaic Energy,* Littleton, MA: New Energy Options, Inc..

21. Birol, F., 2013. *World Energy Outlook Special Report,* Cedex, France: International Energy Agency.

22. Black, J., 2013. *Cost and Performance Baseline for Fossil Energy Plants,* s.l.: National Energy Technology Laboratory.

23. Blanco, M. I., 2009. The economics of wind energy.. *Renewable and Sustainable Energy Reviews,* 13(6-7), pp. 1372-1382.

24. Boundy, B., Diegel, S. W., Wright, L. & Davis, S. C., 2011. *Biomass Energy Data Book, 4th Edition.* Oak Ridge, Tennessee: Oak Ridge National Laboratory .

25. Brahman, F., Honarmand, M. & Jadid, S., 2015. Optimal electrical and thermal energy management of a residential energy hub, integrating demand response and energy storage system. *Energy and Buildings,* Volume 90, pp. 65-75.

26. Bucher, M., Haring, T. & Andersson, G., 2015. *Modeling and economic evaluation of Power2Gas technology using energy hub concept.* Denver, CO, s.n.

27. Buhler, R., 2010. *Integration of Renewable Energy Sources Using Microgrids, Virtual Power Plants and the Energy Hub Approach,* Zurich: Swiss Federal Institute of Technology (ETH) .

28. Burgherr, P., Eckle, P. & Hirschberg, S., 2012. Comparative Assessment of Severe Accident Risks in the Coal, Oil and Natural Gas Chains. *Reliability Engineering and System Safety,* Volume 105, pp. 97-103.

29. Burgherr, P. & Hirschberg, S., 2008. Severe Accident Risks in Fossil Energy Chains: A Comparative Analysis. *Energy,* Volume 33, pp. 538-553.

30. Burke, A. & Gardiner, M., 2005. *Hydrogen Storage Options: Technologies and Comparisons for Light-duty Vehicle Applications,* s.l.: s.n.

31. Burnett, R. et al., 1997. Association between ambient carbon monoxide levels and hospitalizations for congestive heart failure in the elderly in 10 Canadian cities. *Epidemiology,* pp. 162-167.

32. Burnett, R. et al., 1995. Association between ambient particulate sulfate and admissions to Ontario hospitals for cardiac and respiratory diseases. *American Jnl of Epidemiology ,* pp. 15-22.

33. Burnett, R. et al., 2004. Associations between Short-Term Changes in Nitrogen Dioxide and Mortality in Canadian Cities. *Archives of Environmental Health: An International Journal,* 59(5), pp. 228-236.

34. Burtraw, D. & Krupnick, A., 2012. *The True Cost of Electric Power ,* s.l.: Center for Energy Economics and Policy, Resources for the Future.

35. Burtraw, D., Krupnick, A. & Sampson, G., 2012. *The true cost of electric power: An inventory of methodologies to support future decision-making in comparing the cost and competitiveness of electricity generation technologies,* s.l.: Center for Energy Economics and Policy, Resources for the Future.

36. Buzz Solar, 2012. *Retail Prices.* [Online]
Available at: http://www.solarbuzz.com/facts-and-figures/retail-price-environment/module-prices
[Accessed 15 12 2015].

37. C2ES, 2013. *Leveraging Natural Gas to Reduce Greenhouse Gas Emissions,* Arlington, VA: Center For Climate and Energy Solutions.

38. California Environmental Protection Agency, 2012. *Health Effects of Air Pollution.* [Online]
Available at: http://www.arb.ca.gov/research/health/health.htm
[Accessed 07 2015].

39. California Hydrogen Business Council, 2015. *Power-to-Gas: The Case for Hydrogen White Paper,* Los Angeles, CA: California Hydrogen Business Council.

40. CanadaStatistics, 2011. *Income of Canadians 2011.* [Online]
Available at: http://www.statcan.gc.ca
[Accessed 27 11 2015].

41. CanadianSolar, 2013. *CS6P-Module.* [Online]
Available at: http://www.canadiansolar.com/product_pro_detail.aspx
[Accessed 10 12 2015].

42. Capital Power, 2015. *PORT DOVER & NANTICOKE WIND FACT SHEET,* Ontario, Canada: Capital Power.

43. Carnegie, R., Gotham, D., Nderitu, D. & Preckel, P., 2013. *Utility Scale Energy Storage Systems Benefits, Applications, and Technologies,* s.l.: s.n.

44. CEA, 2014. *Vision 2050 - The Future of Canada's Electricity System,* s.l.: Canadian Electricity Association.

45. Cetin, B., Erdem, H. & Sevilgen, S., 2008. Electricity Production Cost Analysis of a Combined Cycle Power Plant. *Energy Sources, Part B,* 3(3), p. 224–232.

46. Changik, J., 2014. Cost-of-illness studies: concepts, scopes, and methods. *Clinical and Molecular Hepatology,* 20(4), pp. 327-337.

47. Chen, H. et al., 2009. Progress in electrical energy storage system: a critical review. *Progress in Natural Science,* 19(3), pp. 291-312.

48. Chen, X., Shao, S., Tian, Z. & Yin, P., 2016. Impacts of air pollution and its spatial spillover effect on public health based on China's big data sample. *Journal of Cleaner Production,* pp. 1-11.

49. CHFCA, 2008. *Analysis of a Potential Clean Energy Hub in the Nanticoke Region,* Vancouver , BC: Canadian Hydrogen and Fuel Cell Association.

50. CHFCA, 2014. *WHERE DOES HYDROGEN COME FROM?.* [Online]
Available at: http://www.chfca.ca/education-centre/where-hydrogen-comes-from/
[Accessed 07 01 2015].

51. Christianson, R., Lohmueller, J. & French, H., 2011. *Initiating Your Co-operative Solar PV Community Power Project,* Ontario: Ontario Sustainable Energy Association.

52. Committee on Health and Environmental, 2010. *Hidden Costs of Energy.* Washington, DC: The National Academies Press.

53. Crotogino, F., Donadei, S., Bunger, U. & Landinger, H., 2010. *Large-Scale Hydrogen Underground Storage for Securing Future Energy Supplies.* Essen, s.n.

54. De Vries, H., Florisson, O. & Tiekstra, G. C., 2007. *Safe operation of natural gas appliances.* San Sebastian, Spain, s.n.

55. DEFRA, 2015a. *Air quality: economic analysis. Air Quality and Environmental Management,* UK: Department for Environment, Food & Rural Affairs.

56. DEFRA, 2015b. *Damage costs by location and source, Air Quality and Environmental Management,* UK: Department for Environment, Food & Rural Affairs.

57. Denholm, P., Ela, E., Kirby, B. & Milligan, M., 2010. *The Role of Energy Storage with Renewable Electricity Generation,* s.l.: National Renewable Energy Laboratory.

58. Dockery, D. et al., 1996. Health effects of acid aerosols on North American children: respiratory symptoms. *Environmental Health Perspectives,* pp. 500-505.

59. Dodge, E., 2014. *Power-to-Gas Enables Massive Energy Storage,* s.l.: Breaking Energy.

60. Earth Observation System, 2012. *Atmospheric Science Data Center.* [Online]
Available at: https://eosweb.larc.nasa.gov
[Accessed 20 12 2015].

61. Eastern Power Limited, 2012. *Air quality impact study: Green electron power project (East site),* Township of St. Clair, Ontario: Eastern Power Limited.

62. EIA, 2012. *Annual Energy Review 2011,* Washington, DC: U.S. Energy Information Administration.

63. Eichman, J., 2015. *Hydrogen Energy Storage (HES) and Power-to-Gas Economic Analysis,* s.l.: NREL.

64. El-Guindy, R., 2013. *Environmental Externalities from Electric Power Generation,* s.l.: Regional Centre for Renewable for Energy and Energy Efficiency.

65. Environment and Climate Change Canada, 2015. *Air Quality Health Index,* Canada: Environment and Climate Change Canada.

66. Environment Canada, 2008. *Canadian Wind Energy Atlas,* s.l.: Environment Canada.

67. Environment Canada, 2013. *Human Health Costs.* [Online]
Available at: https://www.ec.gc.ca/Air/default.asp?lang=En&n=085A22B0-1
[Accessed 24 03 2015].

68. Environment Canada, 2014. *Canada's Emissions Trends,* s.l.: Environment Canada.

69. EPA, 2010. *Updates to EPA Base Case v3.02 EISA Using the Integrated Planning Model ,* s.l.: U.S. Environmental Protection Agency .

70. EPA, 2015a. *Dispersion modeling.,* s.l.: Environmetal Protection Agency.

71. EPA, 2015b. *What are the six common air pollutants?,* s.l.: Environmental Protection Agency.

72. Erdinc, O. & Uzunoglu, M., 2012. Optimum design of hybrid renewable energy systems: Overview of different approaches. *Renewable and Sustainable Energy Reviews,* 16(3), pp. 1412-1425.

73. European Commission, 2016. *Large Combustion Plants,* s.l.: Institute for Prospective Technological Studies .

74. Favre-Perrod, P., Geidl, M., Klockl, B. & Koeppel, G., 2005. *A vision of future energy networks. Paper presented at the Power Engineering Society Inaugural Conference and Exposition in Africa.* Durban, South Africa, IEEE.

75. Feldman, D. et al., 2012. *Photovoltaic (PV) Pricing Trends: Historical, Recent, and Near-Term Projections,* s.l.: NREL and LBNL.

76. Fingersh, L., Hand, M. & Laxson, A., 2006. *Wind Turbine Design Cost and Scaling Model,* Golden, Colorado: National Renewable Energy Laboratory.

77. First Solar, 2015. *First Solar PV Modules: The Industry Benchmark for Utility-Scale PV Power Plants,* Tempe, Arizona: First Solar.

78. Friedrich, R., Rabl, A. & Spadaro, J., 2001. Quantifying the Costs of Air Pollution: the ExternE Project of the EC. *Pollution Atmosphérique,* pp. 77-104.

79. FuelCellToday, 2013. *Water Electrolysis & Renewable Energy Systems,* s.l.: Fuel Cell Today.

80. Garmsiri, S., Rosen, M. & Smith, G., 2014. Integration of Wind Energy, Hydrogen and Natural Gas Pipeline Systems to Meet Community and Transportation Energy Needs: A Parametric Study. *Sustainability,* 6(5), pp. 2506 - 2526.

81. Geidl, M. & Andersson, G., 2005. A modeling and optimization approach for multiple energy carrier power flow. *IEEE Russia,* pp. 1-7.

82. Geidl, M. et al., 2007. Energy hubs for the future. *IEEE Power & Energy Magazine,* Volume 5, pp. 24-30.

83. Geidl, M. et al., 2007. *The Energy Hub, A Powerful Concept for Future Energy Systems.* s.l., s.n.

84. Genovese, J., Harg, K., Paster, M. & Turner, J., 2009. *Current (2009) State-of-the-Art Hydrogen Production Cost Estimate Using Water Electrolysis,* Golden, CO: NREL.

85. Giannakoudis, G., Papadopoulos, A., Seferlis, P. & Voutetakis, S., 2010. Optimum design and operation under uncertainty of power systems using renewable energy sources and hydrogen storage. *International Journal of Hydrogen Energy,* 35(3), pp. 872-891.

86. Goldstein, R. & MacDougall, W., 2012. *Green Hydrogen and Power-to-Gas Technology,* Berlin: Germany Trade and Invest.

87. Goodrich, A., James, T. & Woodhouse, M., 2011. *Solar PV Manufacturing Cost Model Group: Installed Solar PV System Prices,* Golden, CO: Stanford University: Precourt Institute for Energy.

88. Gotz, M. et al., 2016. Renewable Power-to-Gas: A technological and economic review. *Renewable Energy ,* Volume 85 , pp. 1371-1390.

89. Goverment of Canada, 2010. *Canada's action on climate change.* [Online]
Available at: http://www.climatechange.gc.ca/default.asp?lang=En&n=72F16A84-1
[Accessed 03 04 2013].

90. Greenfield South Power Corporation, 2012. *Electron power project: Executive summary,* Toronto, Ontario: s.n.

91. Gunatilake, H., Ganesan, K. & Bacani, E., 2014. *Valuation of Health Impacts of Air Pollution from Power Plants in Asia: A Practical Guide,* s.l.: ASIAN DEVELOPMENT BANK.

92. Gwartney, T., 2015. *Estimating Land Values.* [Online]
Available at: http://www.henrygeorge.org/ted.htm
[Accessed 28 11 2015].

93. Haeseldonckx, D. & D'haeseleer, W., 2008. *The Use Of The Natural-Gas Pipeline Infrastructure For Hydrogen Transport In A Changing Market Structure,* s.l.: KULeuven Energy Institute .

94. Haines, M., Polman, W. & de Laat, J., 2003. *Reduction of CO2 Emissions by Adding Hydrogen to Natural Gas,* Apeldoorn, The Natherlands: Gastech.

95. Hainoun, A., Almoustafa, A. & Seif Aldin, M., 2010. Estimating the health damage costs of syrian electricity generation system using impact pathway approach. *Energy ,* p. 628–638.

96. Hajimiragha, A. et al., 2007. *Optimum Energy Flow of integrated energy systems with hydrogen economy considerations.* South Carolina, USA, s.n.

97. Harrison, K. & Miller, E., 2012. *Renewable Electrolysis Integrated Systems Development and Testing,* Golden, CO: National Renewable Energy Laboratory .

98. HCWH Europe and HEAL, 2010. *Acting now for better health: A 30% reduction target for eu climate policy. ,* s.l.: Health Care Without Harm Europe and Health and Environment Alliance.

99. Hydrogenics , 2013. *Hydrogenics Selected References: Grid Balancing, Power to Gas (PtG) ,* s.l.: Hydrogenics Corporation.

100. Hydrogenics Corporation, 2009. *HySTAT Alkaline Electrolyzer ,* Mississauga, Ontario:: Hydrogenics Corporation.

101. Hydrogenics, 2011. *HySTAT® HYDROGEN GENERATORS.* [Online]
Available at: http://www.hydrogenics.com/docs/default-source/pdf/211-industrial-brochure-english.pdf
[Accessed 25 12 2015].

102. Hydrogenics, 2012. *Hydrogenics Shift Power Energize your World.* [Online]
Available at: http://www.hydrogenics.com/about-the-company/news-updates/2012/04/20/hydrogenics-announces-agreement-with-enbridge-to-develop-utility-scale-energy-storage-in-north-america
[Accessed 30 11 2015].

103. Hydrogenics, 2015. *Hystat Hydrogen Generators,* Oevel, Belgium: Hydrogenics Incorporation.

104. Ibrahim, H., Ilinca, A. & Perron, J., 2008. Energy storage systems—Characteristics and Comparisons. *Renewable and Sustainable Energy Reviews,* Volume 12, pp. 1221-1250.

105. IEA, 2012. *Key World Energy Statistics,* s.l.: International Energy Agency.

106. IEA, 2014. *Technology Roadmap: Energy Storage,* Paris, France: International Energy Agency .

107. IEC, 2011. *Electrical Energy Storage,* Geneva, Switzerland: International Electrotechnical Commission.

108. IESO, 2009. *Ontario's Smart Grid Forum, Enabling tomorrow's electricity system: Report of the Ontario Smart Grid Forum,* Toronto, Ontario: Independent Electricity System Operator.

109. IESO, 2014. *Green Electron Power Project ,* St. Clair Township: s.n.

110. IESO, 2015. *Progress Report on Contracted Electricity Supply,* s.l.: Independent Electricity System Operator.

111. IESO, 2016. *IESO Report: Energy Storage,* Toronto, Ontario: Independent Electricity System Operator.

112. Ilbas, M., Yilmaz, I., V. T. & Kaplan, Y., 2005. Hydrogen as burner fuel: modelling of hydrogen-hydrocarbon composite fuel combustion and NOx formation in a small burner. *International Journal of Energy Research,* Volume 29, pp. 973-990.

113. IRENA, 2015. *Renewable Energy Target Setting,* s.l.: International Renewable Energy Agency.

114. IRENA, 2015. *Renewable Power Generation Costs,* s.l.: International Renewable Energy Agency.

115. IRENA, 2015. *Renewables and Electricity Storage A Technology Roadmap for REmap 2030,* s.l.: International Renewable Energy Agency.

116. Itliong, F., Holbien, B. & Vogt, H., 2012. *Air Quality Impact Study, Green Electron Power Project (East Side) ,* St. Clair, Ontario: Eastern Power Limitted.

117. Jacobs, J., Salhany, K., Fox, K. & Aziz, K., 1996. Steady-State Gas Flow in Pipes. *Journal of Petroleum Science and Engineering,* 14(3).

118.   Jentsch, M., Trost, T. & Sterner, M., 2014. Optimal Use of Power-to-Gas Energy Storage Systems in an 85% Renewable Energy Scenario. *Energy Procedia,* Volume 46, pp. 254-261.

119.   Jesse, L., Cristiane, L. & Michael, A., 2007. *Screening Air Dispersion Model (SCREEN3) User Guide,* Waterloo, Ontario : Lakes Environmental Software.

120.   Judek, S., Stieb, D., Jovic, B. & Edwards, B., 2012. *Air Quality Benefits Assessment Tool (AQBAT) user guide: Version 2 ,* Ottawa, Ontario: Health Canada.

121.   Kehlhofer, R., Rukes, B., Hannemann, F. & Stirnimann, F., 2009. *Combined cycle gas and steam turbine power plants, 3rd edition.* Oklahoma, USA: Pennwell Corporation.

122.   Kotowicz, J. & Bartela, L., 2010. The influence of economic parameters on the optimal values of the design variables of a combined cycle plant. *Energy,* 35(2), p. 911.

123.   Krajacic, G., Zmijarevic, Z. M. B., Vucinic, A. & Carvalho, A. G., 2011. Planning for a 100% independent energy system based on smart energy storage for integration of renewables and CO2 emissions reduction. *Applied Thermal Engineering,* 31(13), pp. 2073-2083.

124.   Krupnick, A. & Harrington, W., 1990. Ambient ozone and acute health effects: Evidence from daily data. *Journal of Environmental Economics and Management,* pp. 1-18.

125.   Kurtulan, S. & Sevgi, L., 2009. A village house energy supply system: Fundamentals of energy conversion.. *Antennas and Propagation Magazine, IEEE,* 51(4), pp. 233-237.

126.   La Scala, M., Vaccaro, A. & Zobaa, A., 2014. A goal programming methodology for multiobjective optimization of distributed energy hubs operation. *Applied Thermal Engineering,* 71(2), pp. 658-666.

127.   Lazzaretto, A. & Toffolo, A., 2004. Energy, Economy and Environment as Objectives in Multi-Criterion Optimization of Thermal Systems Design. *Energy,* 29(8), pp. 1139-1157.

128.   Levene, J. I., Mann, M. K., Margolis, R. & Milbrandt, A., 2005. *An Analysis of Hydrogen Production from Renewable Electricity Sources,* Golden, CO: NREL.

129.   Li, C. & Yu, W., 2016. Techno-economic comparative analysis of off-grid hybrid photovoltaic/diesel/battery and photovoltaic/battery power systems for a household in Urumqi, China. *Journal of Cleaner Production,* pp. 258-265.

130.   Li, C. et al., 2009. Dynamic modeling and sizing optimization of stand-alone photovoltaic power systems using hybrid energy storage technology. *Renewable Energy ,* Volume 34, pp. 815-826.

131.   Lipman, T., 2011. *An Overview of Hydrogen Production and Storage Systems with Renewable Hydrogen Case Studies,* s.l.: s.n.

132.   Liu, C., Li, F. M. L. P. & Cheng, H. M., 2010. Advanced Materials for Energy Storage. *Advanced Energy Materials,* 22(8), pp. 28-62.

133.   Liu, S. & Papageorgiou, L., 2013. Multiobjective optimisation of production, distribution and capacity planning of global supply chains in the process industry. *Omega,* Volume 41, p. 369–382.

134.   Lowesmith, B., 2011. *Vented confined explosions involving Methane/Hydrogen Mixture,* Loughborough, UK: International Association for Hydrogen Energy.

135.   Madrzykowski, D. & Kerber, S., 2009. *Fire Fighting Tactics Under Wind Driven Conditions: Laboratory Experiments,* Gaithersburg, MD: U.S. Department of Commerce-National Institute of Standards and Technology.

136.   Ma, F. et al., 2007. Experimental study on thermal efficiency and emission characteristics of a lean burn hydrogen enriched natural gas engine. *International Journal of Hydrogen Energy,* 32(18), pp. 5067-5075.

137.   Mansouri, M., Ahmadi, P., Ganjeh, A. & Jaafar, M., 2012. Exergetic and economic evaluation of the effect of HRSG configurations on the performance of combined cycle power plants.. *Energy Conversion and Management,,* Volume 58, pp. 47-58.

138.   Maroufmashat, A. et al., 2015. Modeling and optimization of a network of energy hubs to improve economic and emission considerations. *Energy,* 93(2), pp. 2546-2558.

139.   Martin, S., n.d. *The Sustainability case for community power: Empowering Communities Through Renwable Energy,* Toronto, Ontario: York University.

140.   McCarl, B. A., 2012. *McCarl GAMS User Guide.* Texas: GAMS Development Corporation.

141.   McKenzie, L., Witter, R., Newman, L. & Adgate, J., 2012. Human health risk assessment of air emissions from development of unconventional natural gas resources. *Science of The Total Environment,* Volume 424, pp. 79-87.

142.   Mehleri, E., Sarmveis, H., Markatos, N. & LG, P., 2012. A mathematical Programming Approach for Optimal Design of Distributed Energy Systems at The neighbourhood Level. *Energy,* 44(1), pp. 96-104.

143.   Melaina, M. W., Antonia, O. & Penev, M., 2013. *Blending Hydrogen into Natural Gas Pipeline Networks: A Review of Key Issues,* Golden, Colorado: National Renewable Energy Laboratory.

144.   Ministry of Energy, 2011. *Electricity Sector-Renewable Energy Initiatives,* s.l.: office of the Auditor General of Ontario.

145.   Ministry of Energy, 2013. *Ontario's Long-Term Energy Plan,* Toronto, ON: Ministry of Energy.

146.   Ministry of the Environment, 2008. *Air Dispersion Modelling Guideline for Ontario,* Toronto, ON.: Ontario Ministry of Environment.

147.   Mitchell, D., 2010. *Solar Vision 2025: Beyond Market Competitiveness,* s.l.: Canadian Solar Industries Association.

148.   Moghaddam, I., Saniei, M. & Mashhour, E., 2016. A comprehensive model for self-scheduling an energy hub to supply cooling, heating and electrical demands of a building. *Energy,* Volume 94, pp. 157-170.

149.   Molnar, S., Debrecin, N., Kovacevic, T. & Molnar, M., 2008. *Estimation of external costs of electricity generating using ExternE model,* Gödöllő, Hungary: Bulletin of the Szent István University.

150.   Mone, C., Smith, A., Maples, B. & Hand, M., 2015. *2013 Cost of Wind Energy,* Golden, CO: NREL.

151.   Mrris, J., Paltsev, S. & Reilly, J., 2008. *Marginal Abatement Costs and Marginal Welfare Costs for Greenhouse Gas Emissions Reductions: Results from the EPPA Model,* Cambridge, MA: Massachusetts Institute of Technology.

152.   Muneer, W., Bhattacharya, K. & Canizares, C., 2011. Large-Scale Solar PV Investment Models, Tools, and Analysis: The Ontario Case. *IEEE Transactions on Power Systems,* 26(4).

153.   Musial, W. & Ram, B., 2010. *Large-Scale Offshore Wind Power in the United States,* s.l.: National Renewable Energy Laboratory.

154.   National Academy of Sciences, 2009. *Hidden Costs of Energy: Unpriced Consequences of Energy Production and Use,* Washington DC, US: National Research Council of the National Academies.

155.   Natural Resources Canada, 2013. *PV potential and insolation.* [Online]
Available at: http://pv.nrcan.gc.ca/pvmapper.php?MapSize=Map+Size&ViewRegion
[Accessed 08 2015].

156.   Natural Resources Canada, 2014. *EnErgy MarkEts Fact Book for 2014-2015,* s.l.: Natural Resources Canada.

157.   NAVIGANT, 2014. *Analysis Investigating Revenue Decoupling for Electricity and Natural Gas Distributions in Ontario,* Toronto, ON.: Navigant Consulting Ltd..

158.   NAVIGANT, 2014. *Marginal Cost of Wind and Solar PV Electricity Generation,* Toronto, ON: Navigant.

159.   NETL, 2010. *Life Cycle Analysis: Natural Gas Combined Cycle (NGCC) Power Plant,* s.l.: U.S. Department of Energy.

160.   NPI, 2012. *Emission Estimation Technique Manual for Fossil Electric Power Generation,* Australia: Department of Sustainability, Environment, Water, Population and Communities.

161.   NRC, 2009. *Hidden Costs of Energy: Unpriced Consequences of Energy Production and Use,* Washington DC, US: National Research Council of the National Academies.

162.   OMA, 2005. *The Illness Costs of Air Pollution: 2006-2026 Health & Economic Damage Estimates,* Ontario, Canada: Ontario Medical Association.

163.   Omu, A., Choudhary, R. & Boies, A., 2013. Distributed Energy Resources System Optimization using Mixed Integer Linear Programming. *Energy Policy,* Volume 61, pp. 249-266.

164.   Ontario Feed-In Tariff, 2011. *Ontario Feed-In Tariff More jobs, affordable, clean energy, and a brighter future for Ontario,* s.l.: The Pembina Institute.

165.   Ontario Power Authority, 2010. *FEED-IN Tariff (FIT) Program,* Ontario: Ontario Power Authority.

166.   Orehouing, K.; Evins, R.; Dorer, V.; Carmeliet, J., 2014. Assessment of Renewable Energy Integration for a Village Using the Energy Hub Concept. *Energy Procedia,* Volume 57, pp. 940-949.

167.   Orehouing, K., Evins, R. & Dorer, V., 2015. Integration of decentralized energy systems in neighbourhoods using the energy hub approach. *Applied Energy,* Volume 154, pp. 277-289.

168.   Ostro, B., Lipsett, M., Wiener, M. & Selner, J., 1991. Asthmatic responses to airborne acid aerosols.. *American Journal of Public Health,* pp. 694-702.

169.   Petruschke, P. et al., 2014. A Hybrid Approach for the Efficient Synthesis of Renewable Energy Systems. *Applied Energy,* 135(1), pp. 625-633.

170.   Pinchbeck, D. & Huizing, R., 2006. *Preparing for the hydrogen economy by using the existing natural gas system as a catalyst,* s.l.: The European Gas Research Group.

171.   Polman, E. A., Wingerden, A. & Wolters, M., 2003. *Pathways to a hydrogen society.* Orlando, USA, s.n.

172.   Polman, E. & Wolters, M., 2004. *Addition of Hydrogen to Natural Gas.* Vancouver, Canada, s.n.

173.   Pope III, C., Brook, R., Burnett, R. & Dockery, D., 2001. How is cardiovascular disease mortality risk affected by duration and intensity of fine particulate matter exposure? An integration of the epidemiologic evidence. *Air Quality, Atmosphere & Health,* pp. 5-14.

174. Rabel, A., Thach, T., Chau, P. & Wong, C., 2011. How to determine life expectancy change of air pollution mortality: a time series study. *Environmental Health,* 10(25).

175. Rabl, A., 2005. *Health Impacts of Pollutants,* Paris: MAXIMA project of the ExternE series.

176. Ramana, M. V., 2009. *Nuclear Power: Economic, Safety, Health, and Environmental Issues of Near-Term Technologies,* s.l.: Princeton University.

177. Ramirez-Elizondo, L. & Paap, G., 2015. Scheduling and control framework for distribution-level systems containing multiple energy carrier systems: Theoretical approach and illustrative example. *International Journal of Electrical Power & Energy Systems,* Volume 66, pp. 194-215.

178. Region of Waterloo Public Health, 2008. *Air quality and urban health impacts, Waterloo Region: A Premilinary Assessment ,* Waterloo, Ontario: Region of Waterloo Public Health.

179. Remoundou, K. & Koundouri, P., 2009. Environmental Effects on Public Health: An Economic Perspective. *International Journal of Environmental Research and Public Health,* 6(8), pp. 2160-2178.

180. Ren, H. et al., 2010. Multi-objective optimization for the operation of distributed energy systems considering economic and environmental aspects. *Applied Energy,* 87(12), pp. 3642-3651.

181. Rizk, N. K. & Mongia, H. C., 1993. Semianalytical correlations for NOx, CO, and UHC emissions. *Journal of Engineering for Gas Turbines and Power,* 115(3), pp. 612-619.

182. Robinson, L., 2008. *Valuing the Health Impacts of Air Emissions,* s.l.: The Encyclopedia of Environmental Health.

183. Roth, I. & Ambs, L., 2004. Incorporating externalities into a full cost approach to electric power generation life-cycle costing. *Energy,* 29(12-15), p. 2125–2144.

184. Russell, M. C. & Bergman, D. A., 1986. Photovoltaic flat-plate array and insolation measurements.. *Solar Cells,* 18(3-4), pp. 353-362.

185. Rutherford, T. F., 2002. *Mixed Complementarity Programming with GAMS,* s.l.: University of Colorado.

186. Saur, G., 2008. *Wind-To-Hydrogen Project: Electrolyzer Capital Cost Study,* Golden, CO: NREL.

187. Saur, G. & Ramsden, T., 2011. *Wind Electrolysis: Hydrogen Cost Optimization,* Golden, Colorado: National Renewable Energy Laboratory.

188. Schaber, C., Mazza, P. & Hammerschlag, R., 2004. Utility-Scale Storage of Renewable Energy. *The Electricity Journal,* 17(6), pp. 21-29.

189. Schefer, R. & Oefelein, J., 2003. *Reduced Turbine Emissions Using Hydrogen-Enriched Fuels,* Livermore, CA: Sandia National Laboratories.

190. Sctwartz, J. & Morris, R., 1995. Air pollution and hospital admissions for cardiovascular disease in Detroit, Michigan.. *American Journal of Epidemiology,* pp. 23-35.

191. Shaahid, S., Al-Hadhrami, L. & Rahman, M., 2014. Review of economic assessment of hybrid photovoltaic–diesel–battery power systems for residential loads for different provinces of Saudi Arabia. *Renewable and Sustainable Energy Reviews,* pp. 174-181.

192. Sharafi, M. & ElMekkawy, T., 2014. Multi-objective optimal design of hybrid renewable energy systems using PSO-simulation based approach. *Renewable Energy,* Volume 68, pp. 67-79.

193. Sharif, A. et al., 2014. Design of an energy hub based on natural gas and renewable energy sources. *International Journal of Energy Research,* p. 363–373.

194.   Siemens , 2008. *Siemens Combined Cycle Power Plants,* Erlangen, Germany: Siemens AG.

195.   Siemens AG, 2009. *Siemens Wind Turbine SWT 2.3-93,* s.l.: Siemens AG.

196.   Sieniutycz, S. & Jezowski, J., 2013. *Energy Optimization in Process Systems and Fuel Cells.* s.l.:Elsevier.

197.   Sinnott, R. K., 2005. *Chemical Engineering Design, Volume 6.* 4th ed. Oxford, MA: Elsevier Butterworth-Heinemann.

198.   Skone, T. & James, R., 2012. *Life Cycle Analysis: Natural Gas Combined Cycle (NGCC) Power Plant,* s.l.: National Energy Technology Laboratory.

199.   Smith, R., 2005. *Chemical process design and integration.* New York: Wiley Ltd..

200.   Solarbuzz, 2011. *Inverter prices.* [Online]
Available at: http://www.solarbuzz. com/facts-and-figures/retail-price-environment/inverter-prices
[Accessed 09 2011].

201.   Spath, P. L. & Mann, M. K., 2000. *Life Cycle Assessment of a Natural Gas Combined-Cycle Power Generation System,* Golden, Colorado: National Renewable Energy Laboratory.

202.   Statistics Canada, 2015. *Households and the Environment: Energy Use.* [Online]
Available at: http://www.statcan.gc.ca/pub/11-526-s/2013002/part-partie1-eng.htm
[Accessed 10 02 2016].

203.   Steward, D., Saur, G., Penev, M. & Ramsden, T., 2009. *Life Cycle Cost Analysis of Hydrogen Versus Other Technologies for Electrical Energy Storage,* Golden, CO: National Renewable Energy laboratory.

204.   Stieb, D. et al., 2000. Air Pollution, aeroallergens and cardiorespiratory emergency department visits in Saint John, Canada. *Journal of Exposure Analysis and Environmental Epidemiology,* pp. 461-477.

205.   Stockie, J. M., 2011. The Mathematics of Atmospheric Dispersion Modeling. *Society for Industrial and Applied Mathematics,* 53(2), pp. 349-372.

206.   Sunpower Corporation, 2008. *More Power A Better Investment.* [Online]
Available at: https://us.sunpower.com/sites/sunpower/files/media-library/brochures/br-sunpower-solar-panels-are-most-efficient-solar-panels-pv-industry.pdf
[Accessed 07 2013].

207.   Tabkhi, F., Azzaro-Pantel, C., Pibouleau, L. & Domonech, S., 2008. A mathematical framework for modelling and evaluating natural gas pipeline network under hydrogen injection. *International Journal of Hydrogen Energy,* 33(21), pp. 6222-6231.

208.   Taha, M., Pollard, S., Sarkar, U. & Longhurst, P., 2005. Estimating fugitive bioaerosol releases from static compost windrows: Feasibility of a portable wind tunnel approach. *Waste Management,* pp. 445 - 450.

209.   TerMaath, C., Skolnik, E., Schefer, R. & Keeler, J., 2006. Emissions reduction benefits from hydrogen addition to midsize gas turbine feedstocks. *International Journal of Hydrogen Energy,* Volume 31, p. 1147 – 1158.

210.   Thornton, S., Price, R. & Nelson, S., 2007. *The Social Cost of Carbon and the shadow price of carbon: What they are and how to use them in economic appraisal in the UK,* LONDON, UK: Department for Environment, Food and Rural Affairs.

211. Tidball, R., Bluestein, J., Rodriguez, N. & Knoke, S., 2010. *Cost and Performance Assumptions for Modeling Electricity Generation Technologies,* Faifax, Virginia: National Renewable Energy laboratory.

212. Toronto Public Health Department, 2007. *Air pollution burden of illness from traffic in Toronto: Problems and solutions,* Toronto, Canada: s.n.

213. Toronto Public Health, 2004. *Air pollution burden of illness from traffic in Toronto: Problems and solutions,* Toronto, Canada: s.n.

214. US EIA, 2013. *Updated Capital Cost Estimates for Utility Scale Electricity Generating Plants,* Washington DC: US Energy Information Administration.

215. US EPA, 2005. *SCREEN3 Stationary Source Modeling Guidance,* Colarado: Colarado Department of Public Health and Environment.

216. US EPA, 2014. *Ozone and Your Patients' Health Training for Health Care Providers.* [Online]
Available at: http://www.epa.gov/apti/ozonehealth/population.html
[Accessed 25 03 2015].

217. USA-EPA, 2016. *The Sources and Solutions: Fossil Fuels,* s.l.: US Environmental Protection Agency.

218. Vestas, 2004. *General Specification for V90 – 3.0 MW.* [Online]
Available at: http://www.vestas.com/Files/Filer/EN/Brochures/Vestas_V_90-3MW-11-2009-EN.pdf
[Accessed 26 11 2015].

219. Vestas, 2008. *Versatile megawattage, V80-1.8 MW.* [Online]
Available at: http://maritimesenergy.com/flow/uploads/vertas_v80_18
[Accessed 25 11 2015].

220. Vogt, H. & Holbein, B., 2012. *Environmental Screening and Review Report,* St. Clair Township: Oil Springs Line.

221. Walker, S., Mukherjee, U., Fowler, M. & Elkamel, A., 2016. Benchmarking and selection of Power-to-Gas utilizing electrolytic hydrogen as an energy storage alternative. *International Journal of Hydrogen Energy,* Volume 41, pp. 7717-7731.

222. Wasilewski, J., 2015. Integrated modeling of microgrid for steady-state analysis using modified concept of multi-carrier energy hub. *International Journal of Electrical Power & Energy Systems,* Volume 73, pp. 891-898.

223. Weber, C. & Shah, N., 2011. Optimization based Design of a District Energy System for an Eco-Town in the United Kingdom. *Energy,* 36(2), pp. 1292-1308.

224. Weinstein, M., Torrance, G. & McGuire, A., 2009. *QALYs: The Basics,* s.l.: Value in Health.

225. Weis, T., Stensil, S. P. & Harti, J., 2013. *Renewable is Doable: Affordable and flexible options for Ontario's long term energy plan,* s.l.: Greenpeace.

226. Whitehead, S. & Ali, S., 2010. Health outcomes in economic evaluation: the QALY and utilities. *British Medical Bulletin,* 96(1), pp. 5-21.

227. Wiser, R. & Bolinger, M., 2009. *2008 Wind Technologies Report,* Berkeley, CA: Lawrence Berkeley National Laboratory.

228. Wizelius, T., 2007. *Developing Wind Power Projects: Theory and Practice.* s.l.:Routledge.

229.   Wouters, C., Fraga, E. & James, A., 2015. An energy integrated, multi-microgrid, MILP (mixed-integer linear programming) approach for residential distributed energy system planning – A South Australian case-study. *Energy,* Volume 85, pp. 30-44.

230.   Yang, Y., Zhang, S. & Xiao, Y., 2015. Optimal design of distributed energy resource systems coupled with energy distribution networks. *Energy,* Volume 85, pp. 433-448.

231.   Zhou, Z. & Ersoy, D., 2010. *Review Studies of Hydrogen Use in Natural Gas Distribution Systems,* Des Plaines, Illinois, US: Gas Technology Institute.

232.   Zoulias, E. I. & Lymberopoulos, N., 2007. Techno-economic analysis of the integration of hydrogen energy technologies in renewable energy-based stand-alone power systems. *Renewable Energy ,* Volume 32, pp. 680-696.